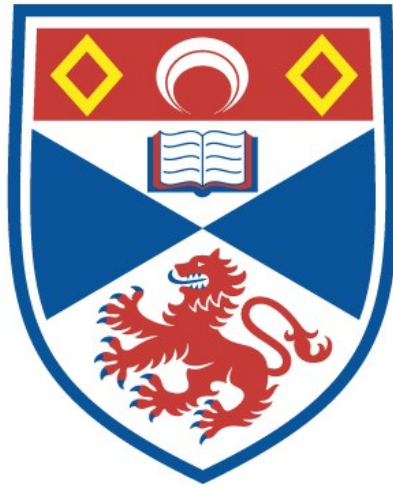


University of St Andrews



Full metadata for this thesis is available in
St Andrews Research Repository
at:

<http://research-repository.st-andrews.ac.uk/>

This thesis is protected by original copyright

E.S.R. AND THEORETICAL STUDIES
OF FREE RADICALS CONTAINING PHOSPHORUS

-

A Thesis
presented for the degree of
Doctor of Philosophy
in the Faculty of Science of the
University of St. Andrews

by

David Kilcast B.Sc.

October 1970

United College of St. Salvator
and St. Leonard,
St. Andrews



Declaration

I declare that this thesis is my own composition, that the work of which it is a record has been carried out by myself, and that it has not been submitted in any previous application for a Higher Degree.

The thesis describes the results of research carried out at the Chemistry Department, United College of St. Salvator and St. Leonard, University of St. Andrews, under the supervision of Dr. C. Thomson, since 1st October 1967, the date of my admission as a research student.

Certification

I hereby certify that David Kilcast has spent twelve terms at research work under my supervision, has fulfilled the conditions of Ordinance No. 16 (St. Andrews), and is qualified to submit the accompanying thesis in application for the degree of Doctor of Philosophy.

Director of Research

Abstract

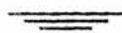
The reactions of a series of phospholes and phosphole oxides with alkali metals have been investigated, and attempts have been made to characterise the radicals so formed. The phosphole oxides were found to give stable monoanions at room temperature. The phospholes gave a series of unusual radicals of uncertain structure at room temperature, whilst at low temperatures the stable monoanions were formed. The radical anions and cations of some phosphorins have also been investigated. The data so obtained has been correlated with the results from McLachlan calculations and some phosphorus spin-polarization parameters have been estimated.

CNDO calculations have been performed on a number of inorganic phosphorus radicals, and the calculated geometries and spin densities compared with those found experimentally. Good agreement was obtained for most radicals, but some larger radicals gave poorer results. Attempts have been made to explain the possible reasons for these poor results, and also the poor results from calculations on some phosphole and phosphorin radical ions.

No direct evidence has been found for d-orbital participation in any of these compounds, although the possibility cannot be ruled out altogether.

CONTENTS

	Page
LIST OF TABLES	i
LIST OF FIGURES	i
ACKNOWLEDGEMENTS	ii
ABBREVIATIONS	iii
CHAPTER I : INTRODUCTION	1
1. General	1
2. Hyperfine Interactions	2
3. Spin Densities and Splitting Constants	6
4. Calculation of Spin Densities	10
5. Calculation of Q Factors	12
6. Programme of Research	18
7. Previous ESR Work on Phosphorus Radicals	20
CHAPTER II : EXPERIMENTAL	34
1. General	35
2. Radical Anions from Phospholes	42
A.: Reactions at Room Temperature with Alkali Metals	42
B.: Reactions at Low Temperature with Alkali Metals	49
3. Radical Anions from Phosphole Oxides	58
4. Attempted Preparations of Cations from Phospholes and Phosphole Oxides	64
5. Radical Ions from Phosphorins	66
A.: Anions	67
B.: Cations	70
CHAPTER III : SPIN DENSITY CALCULATIONS	76
1. π -Electron Calculations	77
2. All-Valence Electron Calculations	100
CHAPTER IV : DISCUSSION	123
1. Radicals from Phospholes and Phosphole Oxides	123
2. Radicals from Phosphorins	142
3. CNDO Calculations	148
4. Q-Values	164
5. CNDO Programme	169
6. Conclusions	174
REFERENCES	177



LIST OF TABLES

<u>Table</u>	<u>Page</u>	<u>Table</u>	<u>Page</u>
I	23	XVIII	112
II	87	XIX	112
III	87	XX	112
IV	91	XXI	112
V	91	XXII	113
VI	92	XXIII	113
VII	93	XXIV	113
VIII	95	XXV	114
IX	97	XXVI	114
X	98	XXVII	125
XI	109	XXVIII	139
XII	109	XXIX	141
XIII	109	XXX	145
XIV	110	XXXI	146
XV	110	XXXII	147
XVI	111	XXXIII	148
XVII	111	XXXIV	164

LIST OF FIGURES

<u>Figure</u>	<u>following page</u>	<u>Figure</u>	<u>following page</u>
1	29	25,26	66
2	35	27,28	67
3,4	38	29	69
5,6,7,8,9,10	41	30	71
11	47	31,32	72
12,13	49	33	73
14,15,16,17,18	50	34	85
19,20	53	35	108
21,22,23,24	58	36	108

ACKNOWLEDGEMENTS

I should like to thank Dr. Colin Thomson for suggesting this topic of research and for his constant help and encouragement throughout this work. My thanks are also due to Professor K. Dimroth and Dr. E.H. Braye for their kind donations of phosphorins and phospholes, without which this work would have been so much more difficult.

I would also like to thank the members of the teaching, technical and secretarial staff in this Department, and particularly the patient and long-suffering members of the Computing Laboratory in the University of St. Andrews.

I am indebted to the Carnegie Trust for the award of a Research Studentship for the period of this work.

D.K.

ABBREVIATIONS

There follows a list of the most common abbreviations used in the course of this thesis.

g, g_N	electron and nuclear g-values, respectively
β, β_N	electron and nuclear Bohr magnetons, respectively
h	Planck's constant
$\delta(r)$	Dirac delta function
\bar{S}, \bar{I}	electron and nuclear spin operators, respectively
\bar{S}_z, \bar{I}_z	z-components of above
hfs	hyperfine splitting
s.d.	spin density
G	gauss
AO	atomic orbital
MO	molecular orbital
LCAO	linear combination of atomic orbitals
SCF	self-consistent field
HF	Hartree-Fock
RHF	Restricted Hartree-Fock
UHF	Unrestricted Hartree-Fock
ZDO	Zero Differential Overlap
CNDO	Complete Neglect of Differential Overlap
TPP	triphenylphosphine
TPPO	triphenylphosphine oxide
PBP	phenylbiphenylenephosphine
DMADPO	dimethylaminodiphenylphosphine oxide
HMPA	hexamethylphosphoramide
DME	1,2-dimethoxyethane
THF	tetrahydrofuran

CHAPTER I
INTRODUCTION

	Page
1. <u>General</u>	1
2. <u>Hyperfine Interactions</u>	2
3. <u>Spin Densities and Splitting Constants</u>	6
4. <u>Calculation of Spin Densities</u>	10
5. <u>Calculation of Q Factors</u>	12
6. <u>Programme of Research</u>	18
7. <u>Previous ESR Work on Phosphorus Radicals</u>	20
(a) Radicals in solids	20
(b) Radicals in solution	24

1. General

ESR spectroscopy is now well established as a technique for investigating the electronic structure of free radicals. Many reviews are available on the subject,¹⁻⁵ and yearly progress is reported in Annual Reviews of Physical Chemistry and Annual Reports of the Chemical Society. This thesis is concerned mainly with studies of organic radicals in solution, and there follows a summary of the relevant theory. The theory behind the anisotropic ESR spectra of radicals in the solid state will not be described in any detail; more comprehensive treatments may be found in references 2-6.

2. Hyperfine Interactions

For a radical in solution, the Zeeman Hamiltonian operator for the interaction of the unpaired electron with a strong magnetic field H is

$$\bar{H}_0 = g\beta H \bar{S}_z \quad . \quad . \quad . \quad . \quad . \quad (1)$$

where \bar{S}_z is the component of the electron spin angular momentum operator \bar{S} in the Z -direction, with values $\pm\frac{1}{2}$; g , the g -value, is the isotropic component of the g -tensor, and β is the Bohr magneton. This Hamiltonian has eigenvalues $E_1 = +\frac{1}{2}g\beta H$, and $E_2 = -\frac{1}{2}g\beta H$; their difference, $E_1 - E_2 = g\beta H$. If microwave radiation is applied perpendicular to the direction of H , transitions between the energy levels will occur provided the microwave frequency, ν , satisfies the condition

$$h\nu = g\beta H \quad . \quad . \quad . \quad . \quad . \quad (2)$$

Although this result predicts a single absorption line, in most free radicals a series of lines are observed. These result from the interaction of the unpaired electron with any magnetic nuclei present in the molecule, and appear at slightly different field values as H is varied through resonance. The Hamiltonian, \bar{H}_1 , for this hyperfine interaction is the sum of the anisotropic dipolar Hamiltonian \bar{H}_1' and the isotropic contact interaction term, \bar{H}_1'' . In the strong field approximation, for interaction with a single magnetic nucleus,

$$\bar{H}_1' = g\beta g_N \beta_N \left(\frac{\bar{S}_z \cdot \bar{I}_z}{R^3} - \frac{3(\bar{S}_z \cdot \mathbf{r})(\bar{I}_z \cdot \mathbf{r})}{R^5} \right) \quad . \quad . \quad (3)$$

where \mathbf{r} is the radius vector from \bar{S} to \bar{I} , and R is the distance between

them. For a radical with more than one magnetic nucleus, (3) is summed over all such nuclei.

In solution, rapid tumbling causes \bar{H}_1' to vanish,⁸ leaving \bar{H}_1''

$$\begin{aligned}\bar{H}_1'' &= (8\pi/3)g\beta g_N\beta_N\delta(r)\bar{I}_z\cdot\bar{S}_z \\ &= a\bar{I}_z\cdot\bar{S}_z\end{aligned}\quad . \quad . \quad . \quad (4)$$

where a is the isotropic hyperfine splitting constant of the nucleus.

An alternative expression for \bar{H}_1'' can be found by integrating over the spatial part of the wave function, giving

$$\bar{H}_1'' = (8\pi/3)g\beta g_N\beta_N|\psi(0)|^2\bar{I}_z\cdot\bar{S}_z \quad . \quad . \quad (5)$$

where $\psi(0)$ is the value of the electronic wave function at the nucleus.

Equations (4) and (5) show that contact interaction can only occur when the electron has finite probability density at the nucleus.

The total effective Hamiltonian is then

$$\begin{aligned}\bar{H} &= \bar{H}_0 + \bar{H}_1'' \\ &= g\beta H\bar{S}_z + a\bar{S}_z\cdot\bar{I}_z\end{aligned}\quad . \quad . \quad . \quad (6)$$

As \bar{H}_1'' is much smaller than H_0 , the hyperfine energy levels can be regarded as small perturbations of E_1 and E_2 , and the eigenvalues of H , found by perturbation theory, are

$$E_{m_S, m_I} = g\beta H m_S + a m_S m_I \quad . \quad . \quad . \quad (7)$$

where the quantum numbers m_S, m_I have the values $m_S = \pm\frac{1}{2}$, $m_I = I, I-1, \dots, -I-1, -I$, and are the eigenvalues of \bar{S}_z, \bar{I}_z . The selection rules for

transitions between these levels are $\Delta m_S = \pm 1$, $\Delta m_I = 0$. Thus, by interaction with a single nucleus of spin I , $(2I + 1)$ hyperfine lines are seen, separated by a .

A radical may contain numbers N_A , N_B , $N_C \dots$ of symmetrically equivalent nuclei of types A, B, C... with nuclear quantum numbers I_A , I_B , $I_C \dots$. If $a_A > a_B > a_C$, each of the $(2N_A I_A + 1)$ hyperfine lines obtained by interaction with type A is further split into $(2N_B I_B + 1)$ lines by interaction with type B etc. Complete analysis of such an ESR spectrum gives all the hyperfine coupling constants a_A , a_B , a_C , etc.

For a radical in the solid state, the complete electronic Hamiltonian may be written, in a general form,

$$\bar{H} = \beta \mathbf{H} \cdot \mathbf{g} \cdot \bar{\mathbf{S}} + \bar{\mathbf{S}} \cdot \mathbf{T} \cdot \bar{\mathbf{I}} \quad . \quad . \quad . \quad . \quad (8)$$

where \mathbf{g} is the anisotropic g -tensor, and \mathbf{T} is the hyperfine tensor. The latter is the sum of two terms: an isotropic term $a \bar{\mathbf{S}} \cdot \bar{\mathbf{I}}$ arising from Fermi contact interaction, and an anisotropic term $\bar{\mathbf{S}} \cdot \mathbf{T}' \cdot \bar{\mathbf{I}}$ arising from electron-nuclear dipolar interaction. \mathbf{T}' can be reduced to diagonal form by choosing as axes the principal axes X , Y , Z , giving the principal values t_1' , t_2' , t_3' . Then

$$\bar{\mathbf{S}} \cdot \mathbf{T} \cdot \bar{\mathbf{I}} = A \bar{\mathbf{S}}_X \bar{\mathbf{I}}_X + B \bar{\mathbf{S}}_Y \bar{\mathbf{I}}_Y + C \bar{\mathbf{S}}_Z \bar{\mathbf{I}}_Z \quad . \quad . \quad . \quad . \quad (9)$$

where

$$\begin{aligned} A &= t_1' + a \\ B &= t_2' + b \\ C &= t_3' + c \end{aligned} \quad . \quad . \quad . \quad . \quad (10)$$

Since the dipolar term has zero trace, a is the average of the principal values A , B , C . Hence the isotropic splitting may easily be calculated from the anisotropic splittings.

In general, free radicals may be broadly classified as σ -radicals or π -radicals.⁹ A σ -radical may be defined as a radical in which one or more atoms has some direct s-orbital spin density; a π -radical may be defined as a radical in which the unpaired electron occupies a π -orbital, and in which the s-orbital spin density responsible for the splitting constants appears only by a spin-polarization mechanism (see Section 3). Most radicals derived from planar unsaturated organic systems in solution are π -radicals, such as the naphthalene anion and the phenazine cation,⁵ but some σ -radicals are known, such as the nitrosobenzene cation and phenyl diazotate.¹⁰ Many examples of both types are known in the solid state; for example, the σ -radicals FCO , HPO_2^- and $\text{S}_2\text{O}_2^{6-}$, and the π -radicals NF_2 , PH_2 and H_2NO^6 .

It is convenient at this stage to give a definition of spin density: the normalized spin density function $\rho(x,y,z)$ at the point (x,y,z) is given by

$$\rho(x,y,z) = \bar{S}^{-1} \langle \Psi | \sum_k \bar{S}_{kz} \delta(r_k) | \Psi \rangle \quad . \quad . \quad . \quad (11)$$

where Ψ is the total molecular wave function, and the other quantities as defined previously. This function, the spin density at the nucleus, is a probability density, and it is more convenient to define an atomic orbital spin density ρ_i^a in orbital a on atom i as

$$\rho_i^a = P_i^a(\alpha) - P_i^a(\beta) \quad . \quad . \quad . \quad (12)$$

where α, β refer to the eigenvalues of \bar{S}_{kz} , having values $+\frac{1}{2}, -\frac{1}{2}$ respectively, and the $P_i^{\alpha}(\alpha), P_i^{\beta}(\beta)$ refer to the probability densities of α spin and β spin respectively.

The relationship between this quantity and the hyperfine splitting constant is discussed in the next section, and its theoretical calculation is discussed in Section 4.

3. Spin Densities and Splitting Constants

As may be seen from equations (4) and (5), hyperfine splitting constants may only be observed if the wave function of the unpaired electron has a finite value at the nucleus. This can only occur if the wave function has some s character; p and d orbitals both have a node at the nucleus. In 1953, however, Weissman¹¹ observed isotropic proton splittings from the naphthalene anion, a π radical. The appearance of a non-zero spin density in the hydrogen 1s orbital was first rationalised by McConnell, in a valence bond calculation,¹² and by Weissman in a molecular orbital calculation.¹³

McConnell considered a C-H fragment, with a $\pi(2p_z)$ orbital on the carbon, a $\sigma(sp^2)$ hybrid on the carbon pointing towards the proton, and a 1s orbital on the proton. The required electron correlation was introduced by mixing in an appropriate excited state, $\psi = \psi_o^{\pi} + \lambda \psi_{ES}^{\pi}$. The use of first-order perturbation theory to solve for λ then gave

$$Q_{CH}^H = - (1 - S_o^4)^{-1} \frac{[\int \pi o | \pi o] - [\int \pi s | \pi s]}{\Delta E_{21}} a_H^H \quad (13)$$

where Q_{CH}^H is the proton hyperfine splitting for unit spin density in π , a_H^H is the proton hyperfine splitting, S_0 is the overlap integral between σ and s , ΔE_{21} is the energy difference between the ground state and the excited state, and the $\int ab|ab \int$ are exchange integrals of the form

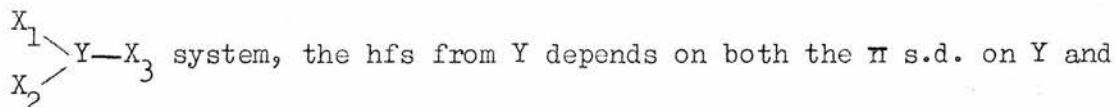
$$\int ab|ab \int = \langle a(1)b(2) | e^2 r_{12}^{-1} | a(2)b(1) \rangle \quad . \quad . \quad (14)$$

(The superscript in the term Q_{AB}^A refers to the nucleus giving rise to the hyperfine splitting; the subscript refers to the σ bond polarized by the π spin density on the atom nearest the Q.) McConnell and McLachlan¹⁴ have shown that the proton hfs a_i^H at carbon i varies linearly with the spin density in π for molecules in which the π spin density is distributed over more than one centre, leading to the McConnell relation,

$$a_i^H = Q_{CH}^H f_i^\pi \quad . \quad . \quad . \quad (15)$$

The problem of evaluating Q_{CH}^H is discussed in Section 5.

The extension of the McConnell relation to isotropic splittings from nuclei other than protons is more complex. Karplus and Fraenkel¹⁵ developed the theory for ^{13}C hfs, and this has been extended to other nuclei, such as ^{14}N , ^{17}O , ^{19}F . These authors showed that, for a



also the π s.d. on X_1 . The former gives rise to two types of interaction: spin polarization of the $1s$ electrons on Y, and spin polarization of the $2s$ electrons in the three $Y-X_i$ bonds. The latter gives

rise to the same type of interactions as in the C—H fragment. These interactions lead to the relationship

$$a^Y = (S^Y + \sum_i Q_{YX_i}^Y) P_Y^\pi + \sum_i Q_{X_i Y}^Y P_{X_i}^\pi \quad . \quad . \quad . \quad (16)$$

where S^Y includes polarization of the 1s electrons on Y, $Q_{YX_i}^Y$ represents the polarization of the 2s electrons in the Y— X_i bonds, $Q_{X_i Y}^Y$ represents the polarization of the 2s electrons by the π electrons on X_i , and P_Y^π , $P_{X_i}^\pi$ are the π s.d.'s on Y, X_i respectively.

In the case of ^{14}N splittings, two common bonding situations are encountered: nitrogen bonded to two carbon atoms, as in pyridine, and nitrogen bonded to two carbons and one hydrogen, as in pyrrole. Equation (16) then takes the respective forms

$$a^N = (P^N + 2Q_{NC}^N) P_N^\pi + Q_{CN}^N \sum_i P_i^\pi \quad . \quad . \quad . \quad (17)$$

$$a^N = (S^N + Q_{NH}^N + 2Q_{NC}^N) P_N^\pi + Q_{CN}^N \sum_i P_i^\pi \quad . \quad . \quad . \quad (18)$$

where P^N includes spin polarization of both the 1s and the lone pair electrons. Although attempts have been made to calculate individual contributions in (17) and (18), the equations are usually written in the simpler form

$$a_N = Q_{NN}^N P_N^\pi + Q_{CN}^N \sum_i P_i^\pi \quad . \quad . \quad . \quad (19)$$

Equation (19) was also obtained by Henning¹⁶ in a molecular orbital treatment of an aromatic CNC fragment. The π electrons were taken to move in π orbitals constructed from linear combinations of 2pz atomic orbitals. The σ orbitals were constructed from linear

combinations of sp^2 hybrid orbitals h_N and h_C , which point along the CN bond axis:

$$\begin{aligned}\sigma_{NC} &= \sqrt{2}(1+S)\sqrt{\frac{1}{2}}[h_N + h_C] \text{ (bonding)} \\ \sigma_{NC}^* &= \sqrt{2}(1+S)\sqrt{\frac{1}{2}}[h_N - h_C] \text{ (antibonding)}\end{aligned} \quad (20)$$

where $S = \langle h_N | h_C \rangle$ is an overlap integral. The lone pair n_N and $(nS)_N$ orbitals were treated as σ orbitals.

Excited configurations were then mixed with the ground state wave function to give a first-order contribution to the spin density $\rho(r_N)$ at the nitrogen nucleus. The relevant excitations were, in general, the one-electron type $\sigma_i \rightarrow \sigma_p^*$. A first-order perturbation treatment then gave the nitrogen splitting as

$$A^N = \sum_r \sum_s Q_{rs}^N \rho_{sr}^\pi \quad (21)$$

where Q_{rs}^N is an element of the hyperfine coupling matrix. Considering only the nitrogen atom and nearest neighbours, the expression for A^N simplifies to

$$A^N = Q_{NN}^N \rho_N^\pi + Q_{CC}^N (\rho_{C_1}^\pi + \rho_{C_2}^\pi) + (Q_{NC}^N + Q_{CN}^N) (\rho_{C_1N}^\pi + \rho_{C_2N}^\pi) \quad (22)$$

(Note: the Q_{CC}^N in this notation is equivalent to Q_{CN}^N in the notation of Fraenkel described previously.) Henning showed that $Q_{NC}^N = -Q_{CN}^N$, and hence the third (off-diagonal) term in (22) vanishes, giving equation (19).

A more recent molecular orbital calculation of ^{13}C , ^{14}N and ^{17}O splitting constants by Kato et al.¹⁷ led to a three-parameter equation,

similar to (22), of the form

$$a^Y = Q_{YY}^Y \rho_Y^\pi + \sum_i Q_{YX_i}^Y \rho_i^\pi + \sum_i R_{YX_i}^Y \rho_{YX_i}^\pi \quad (23)$$

where the last term results from a contribution from the overlap spin densities in the $Y-X_i$ bonds.

The estimation of the various spin polarization parameters is discussed in Section 5.

4. Calculation of Spin Densities

As outlined in Section 2, the normalised spin density function is defined by equation (11), but it is more convenient to consider the atomic orbital spin density ρ_i^a defined by equation (12). The total molecular wave function can be expressed in terms of a set of normalised atomic orbitals ψ_λ which are not, in general, orthogonal. The spin density is then formulated in terms of the elements P of the atomic orbital spin density matrix \bar{P} , defined by

$$P = \sum_{\lambda\mu} P_{\lambda\mu} \psi_\mu^* \psi_\lambda \quad (24)$$

Since the ψ_λ are not orthogonal, \bar{P} will have off-diagonal elements, interpreted as spin density concentrated between the atoms, i.e. in the bonds. The spin density values in these overlap regions are found by multiplying the appropriate off-diagonal element by the corresponding overlap integral. The diagonal elements $P_{\lambda\lambda}$ of the matrix are the atomic orbital spin densities given by equation (12).

The theoretical calculations of spin densities can be grouped broadly into three main classes:-

(a) π electron calculations. These assume the σ - π separability approximation, in which the π electrons are regarded as distinct from the σ electrons, which are assumed to be part of a non-polarizable core.¹⁸ The theory is only applicable to planar π -electron systems, and cannot be used to describe σ electrons. Calculations of spin densities can then give only pz orbital spin densities, and hfs must be calculated using these and the appropriate Q-values. Despite these restrictions and the high degree of empirical or semi-empirical parameterisation that is necessary, various types of calculations based on π electron theory have been very successful in reproducing experimental spin densities in π systems. The Hückel^{19,20} and McLachlan^{21,22} methods are described in Chapter III.

(b) All-valence electron calculations. These calculations remove the restriction of planar π -electron systems and include all valence electrons, the inner shell electrons being regarded as part of the core. The most generally useful at present are Hofmann's extended Hückel method,²³ and Pople's CNDO method; the latter is discussed in Chapter III.

(c) Ab initio calculations. These calculations, of the IBMOL²⁴ and POLYATOM²⁵ type, are all-electron calculations, use a minimum number of fundamental constants as input and evaluate all integrals explicitly. However, the large number of integrals causes extreme

computational difficulties, and the size of the available programmes restricts usage to the largest computers. This problem is magnified if spin density calculations are desired; the SCF part of most available programmes is of the Restricted Hartree-Fock (RHF) type, in which α and β electrons are treated as indistinguishable, and either an Unrestricted Hartree-Fock (UHF) formalism (see Chapter III) or limited configuration interaction must be invoked to calculate s-orbital spin densities and hyperfine coupling constants. This increases the complexity of the programmes still further.

5. Calculation of Q-Factors

The calculation of Q-factors may be approached in two distinct ways: either by direct calculation via evaluation of all the relevant exchange integrals, using equations such as (13), or by comparing experimental hyperfine splittings with calculated π spin densities.

Owing to the great complexity of the problem, most direct calculations have been limited to the carbon-hydrogen systems. Various calculations of Q_{CH}^H have given values in the range -20G to -30G, and Jarrett,²⁶ evaluating equation (13), found $Q_{CH}^H = -28G$. The more accurate calculations of Vincow²⁷ found the value of Q_{CH}^H to be very sensitive to the hydrogen 1s orbital exponent. These calculations, together with those of Malrieu,²⁸ also suggested that Q_{CH}^H could be sensitive to the order of perturbation theory used. A very detailed calculation of the proton and ^{13}C hfs in the CH_3 radical has recently

been reported by Vincow.²⁹ The good agreement with experiment obtained holds promise for accurate calculations on even larger radicals.

From analysis of experimental data on alkyl radicals, Fessenden and Schuler³⁰ found a dependence on the groups attached to the trigonal carbon, Q_{CH}^H varying from -18G to -26G. In the benzene anion³¹ and the neutral methyl radical,³⁰ ρ_i^π may be reliably estimated from the symmetries, giving -22.5G and -23.03G respectively. It can be seen, then, that Q_{CH}^H can vary slightly in different environments.

For even alternant hydrocarbons, the pairing theorem³² predicts that the anions and cations should have the same spin distribution, and hence the same hfs. In general, however, the cations tend to have larger splittings than the anions.²¹ This could arise from either a breakdown of the pairing theorem or from a dependence of Q_{CH}^H on charge. Work by Bolton and Fraenkel³³ on proton and ^{13}C hfs has shown the latter to be the case. For example, for the cation and anion of anthracene, Q_{CH}^H was found to have values -29G, -25G respectively.

Colpa and Bolton³⁴ extended the McConnell relation to account for these "excess charge" effects. Using a molecular orbital treatment based on second order perturbation theory, they derived the equation

$$a_i^H = \int Q_{CH}^H(o) + K_{CH}^H \epsilon_i \int \rho_i \quad . \quad . \quad . \quad (25)$$

where $Q_{CH}^H(o)$ is the value of Q_{CH}^H for the neutral radical, K_{CH}^H is a constant, and ϵ_i is the excess π charge density on the i th carbon atom,

$$\epsilon_i = 1 - q_i \quad . \quad . \quad . \quad (26)$$

where q_i is the total π electron density on i . Theoretical calculations are at variance as to the sign of K_{CH}^H .³⁵ A recent calculation by Bolton including the effect of excess charge on the orbital exponents gave K_{CH}^H a negative value. Analysis of experimental data from a series of hydrocarbon ions suggested a best fit of $Q_{CH}^H(o) = -27G$, $K_{CH}^H = -12G$.

A similar type of expression proposed by Giacometti, Nordio and Pavan³⁶ took the form

$$a_i^H = Q_1 p_{ii}^\pi + Q_2 \sum_j p_{ij}^\pi \quad . \quad . \quad . \quad . \quad (27)$$

where p_{ij} is an element of the π atomic orbital spin density matrix, and Q_1 and Q_2 are constants. However, Bolton has pointed out³⁷ that any departure from equality of splittings in anion and cation for even alternant hydrocarbons would, under the G-N-P scheme, represent a breakdown of both the pairing theorem and the Mulliken integral approximations. A recent analysis by Moss and Fraenkel³⁸ showed the C-B scheme to be superior to the G-N-P scheme and also that, if Hückel orbitals are used, the G-N-P scheme is a subset of the C-B scheme.

Calculations of heteroatom Q -values have been made mainly by comparison with experimental data. The two-parameter equation (19) has been used by several authors to calculate nitrogen Q -values,¹⁷ giving values of Q_{NN}^N ranging from +19G to +31G, and of Q_{CN}^N from +9G to -4G. Henning's analysis¹⁶ of nitrogen heterocyclic anions gave $Q_{NN}^N = +19G$, $Q_{CN}^N = +9G$. A more recent study by Talcott and Myers³⁹ on the anions of pyridine, pyrazine and pyrimidine - all simple, single

ring compounds - gave $Q_{NN}^N = +27.3G$, $Q_{CN}^N = -1.7G$. Experimental evidence, then, suggests that Q_{CN}^N is probably negative and small compared with Q_{NN}^N . A calculation of the relevant excitation energies by Henning⁴⁰ showed this to be the result of two excitations, $\sigma_{NC} \rightarrow \sigma_{NC}^*$ and $n_N \rightarrow \sigma_{nc}^*$, being opposite in sign and almost cancelling out.

Kato,¹⁷ using the three-parameter equation (23), calculated theoretical values which were in good agreement with those found from experimental data for ^{13}C and ^{14}N . For the latter, the calculated values were $Q_{NN}^N = +24.5G$, $Q_{CN}^N = -5.4G$, $R^N = +1.3G$, and least-squares fit to experimental data gave $Q_{NN}^N = +29.0G$, $Q_{CN}^N = -4.3G$, $R^N = +0.9G$. As may be seen, the overlap s.d. contribution is relatively small, and neglect of this term would be justified. For ^{17}O , Q_{CO}^O and R^O values were abnormally high. A recent study of ^{17}O hfs by Broze and Luz⁴¹ showed that a two-parameter equation was sufficient to correlate experimental data, and also give good agreement with calculated values.

Data on ^{19}F hfs indicates that, in general, a two-parameter equation first proposed by Eaton⁴² is satisfactory, although Murrell and Hinchcliffe⁴³ used a three-parameter equation. Thomson and McCulloch⁴⁴ have shown a two-parameter equation to be superior from a study of fluorinated naphthalene cations. Recent work by Schastnyev ⁴⁵ et al. has confirmed this, although they also obtained Q-values close to those of Murrell and Hinchcliffe using a three-parameter equation.

The effect of charge on heteroatom splittings is less well documented than the effect on proton splittings. The situation here

is complicated by the fact that introduction of a heteroatom breaks down the pairing theorem; hence, any variation in heteroatom splittings may be due to either different spin densities in anion and cation, different Q -values in anion and cation or, most likely, a combination of the two.

There are very few cases where both anions and cations of the same nitrogen-containing compound have been prepared. The difficulty appears to lie in the preparation of the cations; for instance, sulphuric acid oxidant protonates the nitrogen. The anion⁴⁶ and cation⁴⁷ of nitrosobenzene have been prepared, but unfortunately the latter is a σ radical. However, the anion and cation of 1,3,6,8-tetraazapyrene have been prepared,⁴⁸ and both are π radicals. The spectra show the proton splittings to be slightly different for each ion, and the nitrogen splitting in the anion (2.39G) to be significantly higher than in the cation (1.87G). Hückel calculations suggest that the carbon s.d.'s differ in the two ions, and that the Q_{CH}^H values are about the same, -24G. They also suggest that the nitrogen s.d. in the cation is greater than in the anion; neglecting adjacent atom terms, this leads to the values $(Q_{NN}^N)^+ = +15G$, $(Q_{NN}^N)^- = +27G$. It is unlikely that adjacent atom terms would affect these values greatly.

The only other data available⁴⁹ is on a series of diazine anions and diprotonated diazine anions, the latter having slightly different structures from the true cations. The nitrogen splittings in the cations are, in general, greater than those in the anions, and lead to

the values $(P^N + 2Q_{NC}^N) = 20-30G$ for the anions, and $(S^N + Q_{NH}^N + 2Q_{NC}^N) = 23-28G$ for the cations.

Work on fluorine radical ions has been similarly hindered by the lack of comparable data. The anion⁵⁰ and cation⁵¹ of 4,4'-difluorobiphenyl have been prepared, the most striking feature being the large fluorine splitting in the latter (19.28G) compared with the former (3.13G), although the proton splittings are similar. McLachlan calculations proved inconclusive, possibly due to a combination of inaccuracies in the very small ρ_F values and also lack of information on the geometries, but it seems certain that there is a large variation of Q_{FF}^F . This is supported in the work on fluorinated naphthalene cations,⁴⁴ where the values $(Q_{FF}^F)^+ = +290G$, $(Q_{CF}^F)^+ = +63G$ were found, compared with the corresponding values for some fluorinated anions,⁵² $(Q_{FF}^F)^- = +146G$, $(Q_{CF}^F)^- = +48G$.

The mechanism of the variation of Q_{YY}^Y with charge is not certain, but is presumably related to the well-known effect of the contraction of atomic orbitals as the formal positive charge on the atom is increased.⁵³ Some evidence for this comes from Vincow's observations on the sensitivity of the value of Q_{CH}^H to the hydrogen 1s exponent.²⁷

6. Programme of Research

Although much work has been done on hydrocarbon radicals and radicals containing the heteroatoms nitrogen, oxygen, sulphur and fluorine (as outlined in the previous section), comparatively little work has been done on radicals containing phosphorus, particularly radicals in which experimental spin densities could be compared with calculated spin densities. The only comparison available was made by Cowley and Hnoosh^{54,55} for a series of anions prepared by potassium reduction of various phosphines, and no attempt was made at interpretation of the phosphorus splittings.

The synthesis of phosphorins, the analogues of pyridines, by Märkl⁵⁶ and, later, by Dimroth⁵⁷ gave an aromatic system which the latter found could be easily reduced to the anion⁵⁸ and oxidised to the cation.^{57,59} This offered an ideal system for comparison of experimental spin distributions with calculated spin distributions. The first estimation of spin polarization parameters for phosphorus would also prove possible.

Some years earlier, substituted phospholes, the analogues of pyrroles, had been prepared.⁶⁰ Although some doubt existed as to the aromatic character of these compounds,⁶¹ it seemed likely that it would prove possible to prepare some radical ions from these compounds. Investigation of the reaction of phospholes with alkali metals would also provide an interesting comparison with the corresponding reaction with phosphines (see Section 7(b)), and possibly provide some information on the aromatic character of the phospholes.

It was hoped at the start of this work that stable, less substituted or unsubstituted phosphorins and phospholes would eventually be available. This would be of great help in correlating observed and calculated spin densities. However, no synthetic route has yet been found to simpler phosphorins, although these should be reasonably stable, and the simplest phosphole prepared⁶² has proved rather reactive.

No theoretical descriptions of phosphorus spin polarization parameters have yet appeared, the difficulty presumably lying in the large number of possible excitations arising from the introduction of the third shell. In view of this, it was decided to use equations analogous to those used for nitrogen, particularly the one- and two-parameter type

$$a_P = Q_{\text{eff}}^P \rho_P^\pi \quad . \quad . \quad . \quad . \quad . \quad (28)$$

$$a_P = Q_{PP}^P \rho_P^\pi + Q_{CP}^P \sum_i \rho_{C_i}^\pi \quad . \quad . \quad . \quad (29)$$

The effect of charge on the spin distributions and the Q-values may also be investigated.

When this work was started, the only well-established s.d. calculations for heteroatom radicals were of the Hückel and McLachlan type. During the period of this work, a larger computer was acquired, and it was found possible to scale down a second-row CNDO programme to fit this machine. In order to test the suitability of the programme before applying it to the relatively large phosphorin and phosphole

molecules, calculations were performed on a wide range of small inorganic radicals. Owing to the sparsity of systematic calculations of any sort on small phosphorus radicals, it was hoped to obtain information not only on hyperfine splittings, but also on their electronic structure and equilibrium geometries.

This thesis is based on the possible investigations outlined above.

7. Previous ESR Work on Phosphorus Radicals

(a) Radicals in solids

Most work in the solid state has been performed on radicals containing 3-5 atoms. In the following section the work on oxygenated radicals is reviewed first, followed by the work on fluorinated and chlorinated radicals. Work on phosphinyl radicals, including the simplest yet studied, PH_2 , is then reviewed.

Much of the early work on the ESR spectra of radicals containing phosphorus was done by irradiation of single crystals of various types of inorganic phosphates. Irradiation of $\text{Na}_2\text{HPO}_3 \cdot 5\text{H}_2\text{O}$ with γ -rays,^{63,64} and of $\text{MgHPO}_3 \cdot 6\text{H}_2\text{O}$ with X-rays,⁶⁵ gave a radical ascribed in each case to PO_3^{2-} , although the phosphorus hfs differed slightly in each case, varying from 578G to 675G. A recent study by Luz *et al.*⁶⁶ using ^{17}O -labelled $\text{Na}_2\text{DPO}_3 \cdot 5\text{D}_2\text{O}$ has confirmed the identity of this radical. Irradiation with γ -rays of $\text{Mg}(\text{H}_2\text{PO}_2)_2$ by Keen⁶⁴ and of $\text{NH}_4\text{H}_2\text{PO}_2$ by Morton⁶⁷ produced a radical identified as HPO_2^- . As well as a

phosphorus hfs of 495G, Morton also reported the unusually large proton hfs of 82.5G. A radical tentatively identified as $O_2\dot{P}HO_2^{2-}$ was also observed in the same work, analysis of the spectrum giving phosphorus splittings of 384.4G and 148.6G, and a proton hfs of 32G. Irradiation of various phosphates and pyrophosphates with δ -rays⁶⁸ has produced a radical identified in each case as the PO_4^{2-} radical. The phosphorus hfs, however, varies from 28.5G to 50G, and Symons⁶ has pointed out that at least one of these radicals may be PO_3 .

Work on halogenated phosphorus radicals has been concerned solely with fluorinated and chlorinated radicals. The radical PF_4 was first observed by Morton⁶⁹ on irradiation of NH_4PF_6 with δ -rays. This species was found to be tumbling at room temperature, and the isotropic splittings found were $a_P = 1345G$, $a_F = 196G$. These high values also allowed observation of second-order splittings. Atkins and Symons⁷⁰ observed the same radical on irradiation of KPF_6 , and obtained a broad envelope spectrum on lowering the temperature. This was interpreted as meaning that the radical deviated significantly from tetrahedral symmetry and that rapid inversion at room temperature rendered all four fluorines equivalent. A different form of the same radical was observed by Fessenden and Schuler⁷¹ on radiolysis of PF_3 in a SF_6 matrix. This radical, with phosphorus splitting 1330G, was found to have two pairs of equivalent fluorines, with splittings 59G, 282G. An analysis⁷² by Atkins showed the inversion mode to involve a regrouping of the pairs of fluorines.

Morton also observed two further radicals in the radiolysis of NH_4PF_6 , which he tentatively identified as F and either PF^+ or PF^- . The former was shown by Fessenden⁷³ to be the PO_3^{2-} radical, with $a_P = 633\text{G}$. The latter, with unassigned doublet splittings of 169G, 699G, was also shown by Fessenden to be the FPO_2^- radical, the phosphorus splitting being the larger.

On δ -irradiation of ND_4PF_6 , Morton et al.⁷⁴ observed a radical not obtained from NH_4PF_6 , and identified this as PF_2 , with $a_P = 36.0\text{G}$, $a_F = 60.5\text{G}$. Although they allowed the possibility of other species, such as FP_2 , F_3 , P_3 , or doubly charged analogues, a recent study by Wei et al.⁷⁵ has supported this assignment. This group generated the radical by passing P_2F_4 over a heated wire, and also by photolysis of PF_2H .

Chlorinated phosphorus radicals have been produced in the photolysis of phosphorus chlorides at 77°K .⁷⁶ Irradiation of PCl_3 gave the PCl_2 radical, $a_P = 71\text{G}$, $a_{\text{Cl}} = 5\text{G}$, and also the PCl_4 radical. The latter had a very similar phosphorus splitting to the PF_4 radical, 1206G, and, like the species observed by Fessenden, had two pairs of equivalent chlorine nuclei, splittings 62G, 7G. A radical thought to be Me_2PCl_2 , with $a_P = 1077\text{G}$, was observed on irradiation of MePCl_2 .

A number of phosphinyl radicals, R_2P , have been observed. Gordy et al.⁷⁷ found the radical PH_2 in the δ -irradiation of PH_3 in an inert matrix, with $a_P = 80\text{G}$, $a_H = 18\text{G}$. The diphenylphosphinyl radical Ph_2P was generated⁷⁸ by gas phase photolysis of Ph_2PH or $(\text{Ph}_2\text{P})_2$, but on

subsequent trapping on a cold finger, only a single broad line was seen. Irradiation of PhPH_2 with γ -rays⁷⁹ at low temperature gave the radical PhPH , with $a_P = 251\text{G}$. The same workers also irradiated a series of organic phosphites and phosphates, and found two distinct types of radical; those with phosphorus hfs 250-300G were assigned the structure $>\text{P}\cdot$, and those with hfs 600-800G were assigned the structure $>\text{P}(\text{O})\text{O}\cdot$.

The splitting constants of some of these radicals are summarised in Table I.

TABLE I: Splitting constants for some simple phosphorus radicals

Radicals	$a_P(\text{G})$	$a_X(\text{G})$	Refs.
PO_3^{2-}	578-675	—	63-66
HPO_2^-	495	82.5	64,67
$\text{PO}_4^{=}$	28.5-50	—	68
$\text{O}_2\dot{\text{P}}_a\text{P}_b\text{HO}_2^{2-}$	$a = 384.4$ $b = 148.6$	32	67
PF_4	1330	59,282	71
FPO_2^-	699	169	73
PF_2	36.0	60.5	74
PCl_2	71	5	76
PCl_4	1206	62,7	76
Me_2PCl_2	1077	—	76
PH_2	80	18	77
PhPH	251	—	79

As may be seen from the above, some doubt exists as to the true structures of many of the radicals, even though most of the assignments

are made after careful study of anisotropic and isotropic splittings and g-values. More recent work of this nature is discussed in Chapter IV.

(b) Radicals in solution

The previous work on phosphorus radicals in solution may, for this study, be classified broadly into two groups: radicals in which the phosphorus atom or grouping is not part of a π system, and radicals in which the phosphorus atom is in the π system. In the first group, phosphorus-substituted phenoxy type radicals are reviewed, together with the work on phosphorane radicals and radicals produced in flow systems. In the second group, the work on phosphine oxides, phosphines and the recent work on phosphorins is reviewed.

The first ESR work on phosphorus-containing radicals in solution was performed by Müller et al.,⁸⁰ who prepared a series of phenoxy radicals derived from diphenyl(4-hydroxy-3,5-ditertiarybutyl)phosphine. As groups attached to the phosphorus were varied, the phosphorus hfs varied from 6.8G to 16.8G. This variation was paralleled by an increase in the electrophilic nature of the phosphorus grouping. However, no definite conclusions could be made as to the mechanism of the transmission of the s.d. to phosphorus. Gulick and Geske,⁸¹ in a study of phosphate-containing nitroaromatic anions, concluded that a hyperconjugation mechanism was important, but that steric effects were also important, as the phosphorus hfs increased as the phosphorus atom was forced out of the plane of the aromatic ring. These conclusions

were supported by the work of Allen and Bond⁸² in a study of radicals produced by the oxidation of quinol phosphates, who found a large phosphorus hfs (ca.18G) only with bulky ortho substituents present. They surmised that the phosphorus s.d. arose not from spin polarization via any s.d. on the oxygen in the C-O-P grouping, but from a hyper-conjugation mechanism, the 3s orbital on the phosphorus overlapping with the 2pz orbital on the carbon. This would occur to a greater extent if the phosphorus was pushed out of the plane of the ring by bulky ortho groups. Although none of the proton splittings could be assigned, it is unlikely that these general conclusions would be affected by slightly different structures.

Further phenoxy radicals substituted at the para carbon by phosphorus-containing groups were prepared by Müller et al.⁸³ and by Rieker and Kessler.⁸⁴ The radical studied by the latter authors, with a $-\text{CH}_2\text{P}(\text{O})(\text{OPr}^i)_2$ grouping, had an unusually large phosphorus hfs of 38.56G, probably indicating a very high degree of overlap.

Much work has been done on the reaction of tertiary phosphines with semiquinones.⁸⁵ Although a number of phosphorus-containing radicals were identified, no evidence was found for the phosphinium radical $\overset{+}{\text{P}}\text{R}_3$.

Studies⁸⁶ of phosphorane radical cations, $\text{>}\overset{+}{\text{P}}-\dot{\text{O}}<$, have shown there to be little delocalisation of the unpaired electron on to the phosphorus grouping, the phosphorus hfs arising from spin-polarization of the C-P bond. These studies also showed the ^{31}P hfs to be positive.

Phosphorus-containing radicals have also been generated in flow systems from phosphite and phosphate esters. Lucken⁸⁷ found the ethyl esters to have a phosphorus hfs 30-40% higher than the methyl esters, and attributed this to a possible combination of electronic and steric effects. In a similar study, Metcalfe and Waters⁸⁸ made the unexpected observation that the phosphorus hfs decreased as the s.d. associated with the phosphorus grouping increased. No explanation was offered for this effect.

Recent studies⁸⁹ on U.V. irradiated aroylphosphonates showed the phosphorus hfs of the radicals produced to be extremely sensitive to the para-substituent on the phenyl ring, the variation being over the range 53G-128G.

The reaction of aryl phosphine oxides and phosphines with alkali metals to give coloured solutions was first noted by Hein et al.⁹⁰ The first ESR study of such a system was made by Hofmann and Tesch,⁹¹ who observed ESR signals in the reaction of TPPO (triphenylphosphine oxide) with alkali metals in DME. Reaction with Li and Na gave a signal attributable to the biphenyl anion, whereas reaction with K gave an 11-line spectrum, spacing 1.75G, which changed to the biphenyl anion spectrum on further reaction with K. (The cleavage of phenyl-phosphorus bonds by reaction with alkali metals had been well-established previously.⁹²) A later investigation by Kabachnik et al.⁹³ of similar reactions in THF showed TPPO to give a 12-line spectrum on reaction with K. This was ascribed to the radical $\text{Ph}_3\text{PO}^\cdot$, with $a_P = 5.25\text{G}$,

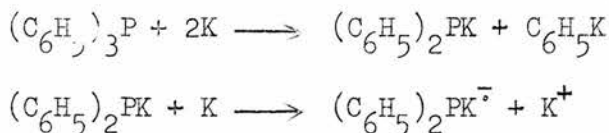
$a_H(\text{ortho}) = 1.75\text{G}$ (7 lines), and $a_H(\text{para}) = 3.5\text{G}$ (4 lines). However, a further study by Cowley and Hnoosh⁵⁴ of the K reaction at -10° in THF gave a blue solution exhibiting a 28-line spectrum. This was also ascribed to $\text{Ph}_3\text{PO}^\cdot$, but with $a_P = 5.25\text{G}$, $a_H = 1.75\text{G}$ (10 lines) and $a_K = 0.875\text{G}$ (4 lines). In contrast, the reaction in DME gave a red-brown solution with a 10-line spectrum analysed as $\text{Ph}_2\text{PO}^\cdot$, with $a_P = 7.7\text{G}$, $a_H = 2.6\text{G}$ (7 lines) and $a_K = 0.4\text{G}$ (4 lines). (No meta-proton splittings were resolved in either case.) The authors supported these assignments by Hückel calculations, which gave spin densities in very good agreement with experiment. The situation was further complicated by an electrolytic preparation⁹⁴ of $\text{Ph}_3\text{PO}^\cdot$, which had a phosphorus splitting of 6.4G and proton splittings of less than 1G . The authors ascribed the differences from Kabachnik's results to the effect of the Et_4N^+ gegenion, but it seems unlikely that this would affect the spin distribution to such a large extent.

Kabachnik also reported radicals from other oxides. Thus, $(t - \text{C}_4\text{H}_9)\text{PO}$ gave a single line with about 12 poorly-resolved components, spacing 0.37G . This was interpreted as an electron in a phosphorus d-orbital interacting very weakly with the phosphorus nucleus and the six α -protons. The spectra of the radicals from Ph_2MePO and PhMe_2PO were poorly resolved, and no unequivocal analysis could be made. Cowley and Hnoosh,⁵⁴ however, obtained a 29-line spectrum corresponding to $\text{PhMe}_2\text{PO}^\cdot$, with $a_P = 5.7\text{G}$, $a_H(\text{ring}) = 3.50\text{G}$ (4 lines) and $a_H(\text{methyl}) = 0.875\text{G}$ (7 lines). This assignment was also supported by Hückel calculations.

Another interesting spectrum observed by Cowley and Hnoosh was that of the DMADPO anion, $(\text{Me}_2\text{N})\text{Ph}_2\text{PO}^-$, prepared by reduction with Na/K alloy in THF. This spectrum showed a 8.75G phosphorus splitting and a 4.9G nitrogen splitting, together with proton and metal splittings. This is in contrast to the work of Fraenkel *et al.*,⁹⁵ who found that concentrated solutions of alkali metals in HMPA, $(\text{Me}_2\text{N})_3\text{PO}$, gave an ESR singlet due to the solvated electron. More dilute solutions of alkali metal showed⁹⁶ a 35-line spectrum, interpreted as an electron with a double solvent shell, the inner shell having four tetrahedral molecules and the outer shell having six octahedral molecules, the hfs arising from the phosphorus nuclei only. Cowley and Hnoosh also obtained the spectrum from the radical $(\text{Me}_2\text{N})_2\text{PhPO}^\cdot$, but this was too complex for analysis.

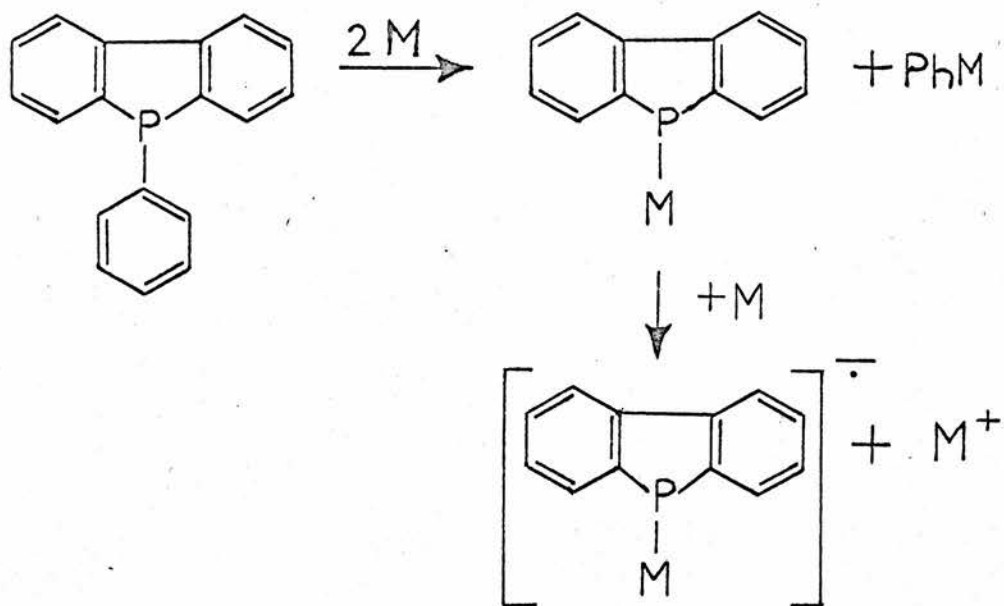
The preparation of the TPP anion was first attempted by Hanna,⁹⁷ by reaction of TPP with K in DME; a spectrum was obtained which was analysed as a phosphorus doublet of 8.36G, a proton splitting of 2.30G and, on dilution, a small splitting of 0.23G (10-12 lines). This was rationalised by assuming the electron to be localised in one benzene ring only, the electron residing in the antisymmetric benzene antibonding orbital, giving rise to equal splittings from the ortho and meta protons and zero from the para. The phosphorus splitting was assumed to arise from spin polarization of the 3s orbital by the s.d. in the d orbital. No explanation was given of the further splitting on dilution.

On reinvestigation of this radical, Britt and Kaiser⁹⁸ showed this assignment to be incorrect. They showed that the secondary splitting consisted of 7 lines, and that the small splitting consisted of 3 groups of 4 lines each, with splittings 0.8G and 0.2G respectively. By a series of careful experiments, the radical was shown to be $(C_6H_5)_2PK^{\cdot-}$, the formation of the radical following the scheme

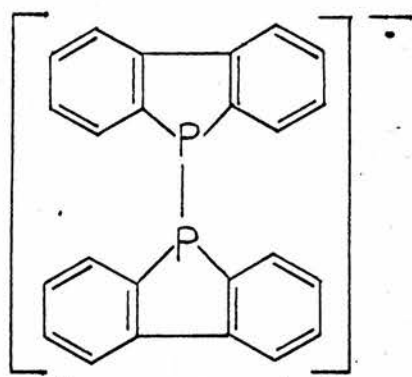


The septet splitting was assumed to arise from the ortho and para protons of the two rings, the small triplet from the meta protons (the outer two lines not being visible), and the small quartet from the potassium ion. The radicals obtained by reaction with Na and Li were only stable below $-50^{\circ}C$, and showed pronounced linewidth effects. This was ascribed to the gegenion being in a different location to that in the potassium case, and jumping from ring to ring.

A similar phenyl cleavage reaction was observed by the same authors⁹⁹ in the reaction of PBP (phenylbiphenylenephosphine) with alkali metals in THF. A stepwise reaction was again found (Figure 1(a)). The ESR spectrum consisted of a phosphorus doublet, 8.5G, and a triplet, 2.4G. The triplet could not be assigned, and no other splittings could be analysed, partly due to linewidth effects. Another complication was the formation of the dimer radical anion (Fig. 1(b)), $a_P = 8.8G$. Another reaction of this type was recently



(a)



(b)

Figure 1

observed by Hnoosh,¹⁰⁰ in the alkali metal reduction of 4,4'-bis(di-phenylphosphine)biphenyl. The spectrum, not fully resolved, consisted of a phosphorus triplet, 3.05G, together with proton splittings; no alkali metal splitting was found.

An electrolytic reduction of TPP¹⁰¹ produced only large amounts of the biphenyl anion. A weak, unresolvable signal was seen that could be attributed to the anion, but no further evidence was found.

Large amounts of biphenyl were also produced¹⁰² in the alkali metal reduction of the phosphazene $(\text{Ph}_2\text{PN})_3$, together with a complex, transient signal that could not be analysed. A more comprehensive study by Allcock and Birdsall¹⁰³ on a number of phosphazenes showed that no biphenyl was produced on electrolytic reduction. The simple phosphazenes $(\text{Ph}_2\text{PN})_3$ and $(\text{Ph}_2\text{PN})_4$ gave only a broad, structureless signal, but more complex compounds gave signals with much fine structure. No analysis of these signals was made owing to instability, but the authors concluded that conjugation was limited to the phosphorus atom and attached groups; no evidence was found for any conjugation over the phosphazene ring.

The radical anions of several other phosphines, all with some alkyl substituents, have also been observed. The radical $\text{PhMe}_2\text{P}^\cdot$ was observed by Kabachnik,⁹³ and a definite analysis made by Eliseeva et al.,¹⁰⁴ who found $a_p = 8.4\text{G}$, together with ring proton splittings. Under higher resolution, a further partially resolved splitting was seen, probably corresponding to methyl splittings. A spectrum obtained

by Kabachnik from the reaction of Ph_2MeP with K consisted of two quintuplets, 5.65G and 2.1G. It is difficult to assign these splittings to either the anion or the phenyl-cleaved anion, and it seems likely that this is a poorly-resolved biphenyl anion spectrum. The reaction of K with 4,4'-bis(dimethylphosphine)biphenyl⁵⁴ gave the anion radical, exhibiting a 57-line spectrum, with $a_p = 5.7\text{G}$. Ring proton and metal splittings were also observed, but no methyl splittings.

Little progress has been made in the preparation of phosphine radical cations. The only such species characterised¹⁰⁵ are a series of $p-(\text{CH}_3)_2\text{N}-$ and $p-\text{CH}_3\text{O}-$ substituted triphenylphosphine cations. These were produced by oxidation with silver perchlorate in benzene, in nitroaromatic or nitroalkane solvents, and Bentrude¹⁰⁶ has estimated the splittings in the $(p-\text{Me}_2\text{NC}_6\text{H}_4)_3\text{P}^+$ cation to be $a_p = 12\text{G}$, $a_N = 6.2\text{G}$. Bersohn¹⁰⁷ has reported the unsubstituted TPP cation to have a phosphorus splitting of 2.32G, but no details of the preparation or analysis were given.

The relatively new technique of photolysis of di-t-butyl peroxide in the presence of a substrate has been applied¹⁰⁸ to tertiary alkyl phosphines, but no simple phosphorus radicals have yet been produced, the predominant reaction being displacement of an alkyl group from the phosphine. However, it seems likely that some slight variation of this method will eventually produce some interesting phosphorus-containing radicals.

The synthesis of the phosphorins by Märkl⁵⁶ provided a ring

system which Dimroth et al. found to be very easily oxidised to the cation^{57,59} and anion.⁵⁸ Oxidation by 2,4,6-triarylphenoxy, lead tetraacetate and mercuric acetate was easily accomplished, and introduction of p-MeO- groups even allowed oxidation by PbO_2 . The radicals were perfectly stable over several days at 0°C and in the absence of air. The phosphorus splittings varied between 21G and 27G, the larger splittings occurring in the pentaphenyl compounds and the t-butyl compounds. (The former is presumably due to reduced delocalisation due to steric effects pushing the phenyl groups out of the plane of the phosphorin ring, and the latter due to the absence of delocalisation into aryl rings.)

The reduction of 2,4,6-triphenylphosphorin with Na/K alloy gave an unresolved doublet, $a_{\text{P}} = 32.4\text{G}$. (The corresponding cation had $a_{\text{P}} = 23.2\text{G}$.) Further contact with the metal resulted in a second reduction, to the diamagnetic dianion. This could again be further reduced to the trianion radical, which exhibited a single line split into about 10 components. No obvious phosphorus hfs was observed in the latter. All three species were stable for several days out of contact with air and metal. (It is interesting to note that, for this species, a_{P}^- is greater than a_{P}^+ , in contrast with the situation with proton splittings (Section 5).

More recently, Dimroth has prepared some 1,1-dialkyloxy-, 1,1-diaryloxy-,^{109,110} and 1,1-dialkylamino-phosphorins, and has prepared radical ions from these. Oxidation of 1,1-dimethoxy-2,4,6

-triphenyl phosphorin gave a spectrum with $a_P = 20.1G$. No methyl splittings were seen, showing the electron to be confined mainly to the ring. Reduction of the same compound gave a radical with a 31.6G doublet which, on further reduction, gave a broad singlet with some fine structure. These oxidations and reductions are similar to those of 2,4,6-triphenylphosphorin, and presumably give analogous species.

As with the phosphorus radicals in the solid state, there is some doubt as to the structure of many radicals in solution, particularly the anions from phosphines and phosphine oxides. The ease of formation of radical cations from the phosphorins is in contrast with the apparent difficulties with the other phosphorus systems. The studies on radicals with the phosphorus outside the π -system suggest that phosphorus splittings depend on both electronic and steric effects. Apart from the Hückel calculations on phosphine and phosphine oxide radical anions, no attempt has been made to relate experimental spin distributions to calculated spin distributions where the phosphorus is in the π system.

CHAPTER II

EXPERIMENTAL

	Page
1. General	35
(a) Vacuum System	35
(b) Purification Techniques	36
(c) Spectrometer	38
(d) Hyperfine Splitting and g-Value Measurement	39
(e) Computer Simulations	40
2. Radical Anions from Phospholes: A. Reactions at Room Temperature with Alkali Metals	42
(a) Reaction of Pentaphenylphosphole and 1,2,5-Triphenylphosphole with K	42
(b) 1-Methyl-2,5-diphenylphosphole with K	47
(c) 1-Vinyl-2,3,4,5-tetraphenylphosphole with K	47
(d) Phospholes with Na	47
(e) Phospholes with Li	48
Radical Anions from Phospholes: B. Reactions at Low Temperature with Alkali Metals	49
(a) MeDPPL with K and Na in DME	49
(b) MeDPPL with K and Na in THF	51
(c) TPPL with K and Na in DME, and with Na in THF	54
(d) TPPL with K in THF	55
(e) PPPL with K and Na in DME and THF	56
(f) ViTPPL with K and Na in DME and THF	57
(g) Other Phospholes with K and Na in DME and THF	58
(h) Phospholes with Li in DME and THF	58
3. Radical Anions from Phosphole Oxides	58
(a) Reaction of 1,2,5-Triphenylphosphole Oxide with K in DME and THF	59
(b) TPPL O with Na in DME and THF	60
(c) TPPL O with Li in DME and THF	61
(d) Reaction of Pentaphenylphosphole Oxide with K in DME and THF	62
(e) PPPLO with Na in DME and THF	64
(f) PPPLO with Li in DME and THF	64
4. Attempted Preparations of Cations from Phospholes and Phosphole Oxides	64
(a) Dissolution in Strong Acids	64
(b) The System $\text{Pb}(\text{OAc})_4/\text{DME}$	65
(c) The System $\text{Pb}(\text{OAc})_4/\text{BF}_3\text{-Et}_2\text{O}/\text{CH}_2\text{Cl}_2$	65
(d) The System $\text{SbCl}_5/\text{CH}_2\text{Cl}_2$	65
(e) The System $\text{AgClO}_4/\text{C}_6\text{H}_6/\text{CH}_3\text{NO}_2$	65
(f) The System $\text{CF}_3\text{CO}_2\text{H}/\text{CH}_3\text{NO}_2$	66

	Page
5. <u>Radical Ions from Phosphorins: A. Anions</u>	66
(a) Reaction of 2,4,6-Triphenylphosphorin with K in DME and THF	67
(b) 2,6-Ditertiarybutyl-4-phenylphosphorin with K in DME and THF	68
(c) 2,4,6-Tritertiarybutylphosphorin with K in DME and THF	69
<u>Radical Ions from Phosphorins: B. Cations</u>	70
(a) TPPN with $\text{Pb}(\text{OAc})_4$ in DME and THF	70
(b) DTBPPN with $\text{Pb}(\text{OAc})_4$ in DME and THF	72
(c) TTBPN with $\text{Pb}(\text{OAc})_4$ in DME and THF	74

1. General

(a) Vacuum System

All the radical ions discussed in this chapter were prepared in vacuo, apart from the attempted preparation of phosphole cations by dissolution in strong acids (Section 4(a)).

The pumping system was standard, consisting of a mercury diffusion pump with two cold traps, backed by a rotary oil pump. Pressures of 10^{-5} torr. were commonly obtained.

The apparatus used for alkali metal reduction is shown in Figure 2. The substrate was placed in the main tube A, and a small piece of metal placed in the side-arm B, which was sealed off with a piece of rubber tubing and a screw clip. A pressure of 10^{-2} torr. could be obtained in this way. Heating with a small flame forced the metal through the constriction C, which was then sealed off. After further pumping, the metal was carefully heated and distilled through the second

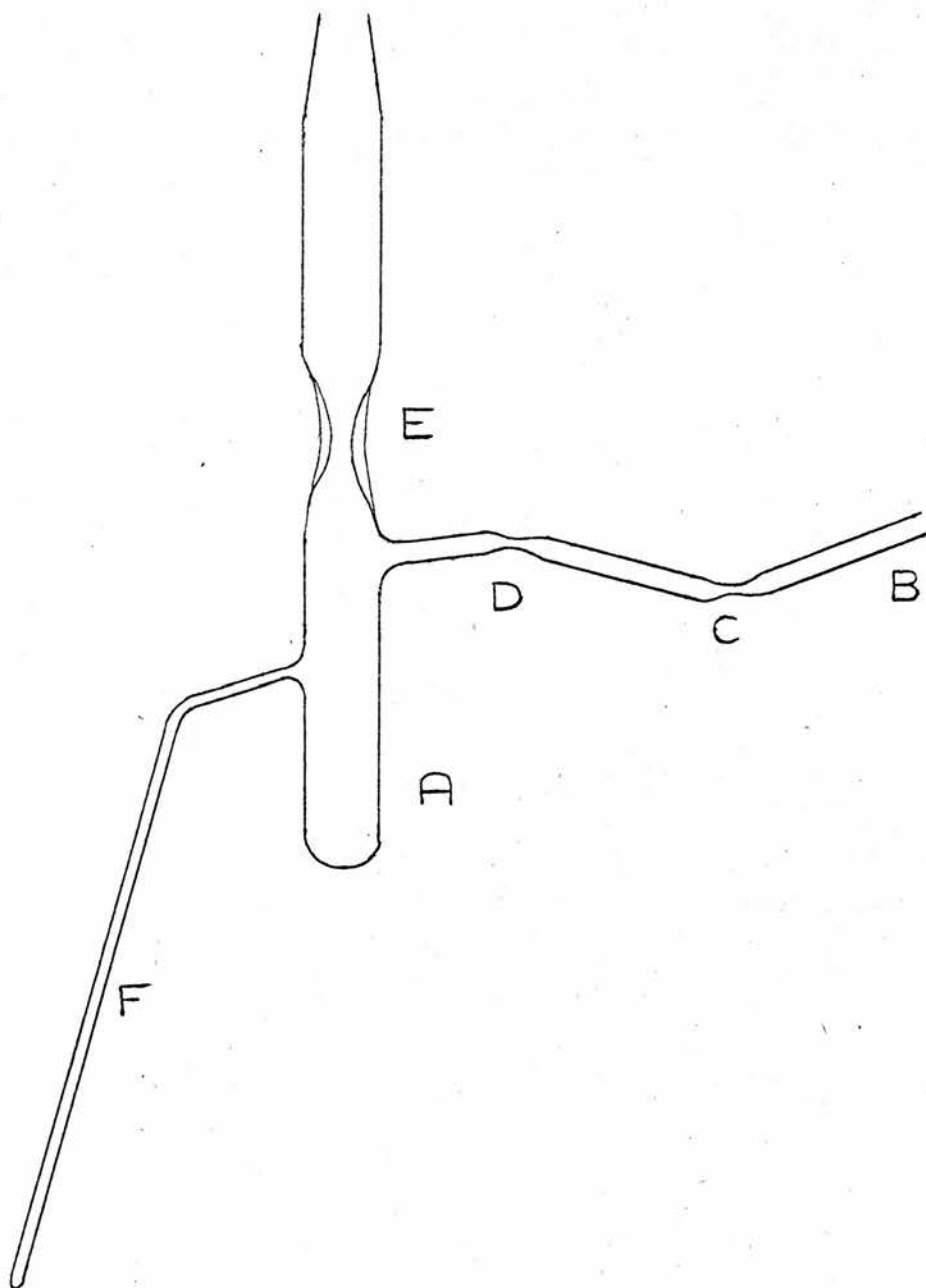


Figure 2

constriction D, leaving any oxide impurity behind. This constriction was sealed off, and the metal again distilled to give a mirror as required. The solvent was then distilled in, and the whole tube sealed at constriction E. After warming, the solution was brought into contact with the metal, tipped into side-arm F and examined in the spectrometer.

For reactive samples, and for samples which gave successive reactions, it was found necessary to restrict carefully the extent of the mirror, and also to ensure no contact with the solution until desired by keeping the mirror at the top of the tube A.

The substrate concentrations used were in the range $10^{-2}M$ - $10^{-3}M$, the actual concentration being adjusted to give optimum reaction rates and line-widths. Any further dilution to improve resolution was achieved by distillation of solvent into F.

The apparatus used for cation preparation was identical but for the absence of side-arm B. For the lead tetraacetate oxidation of phosphorins, the oxidant and substrate were placed in A, solvent distilled in, the tube sealed off and the system allowed to warm up and react. The techniques for the attempted preparations of phosphole cations are discussed in Section 4.

(b) Purification Techniques

(i) Solvents

Both DME and THF were dried and purified in the same way. They

were refluxed for 30 min. over sodium, distilled and stored over sodium. A suitable portion (25 ml.) was stored overnight over lithium aluminium hydride. This was then thoroughly degassed by several cycles of the freeze, pump, thaw method and dried further by using as the solvent for the preparation of the anthracene anion, by the technique described previously. Development of the blue colour of the ion was considered sufficient proof of dryness.

Nitromethane was dried by refluxing and storing over calcium hydride. Methylene chloride was dried by twice distilling from, and storing over, phosphorus pentoxide.

(ii) Reagents

Sodium and potassium, having been thoroughly washed in petroleum ether, were considered sufficiently pure after the distillation through the two constrictions. On account of the exothermic reaction of lithium with the glass on heating, small chips of lithium were introduced directly into A along with the substrate. This allowed time for an oxide coating to develop, and consequently reactions with this metal were painfully slow.

Trifluoroacetic acid was distilled twice in vacuo and used directly. Antimony pentachloride was thoroughly degassed, over 15 cycles being necessary to remove all traces of chlorine. Boron trifluoride etherate was degassed and used directly. Silver perchlorate and lead tetraacetate were used without further treatment. It was

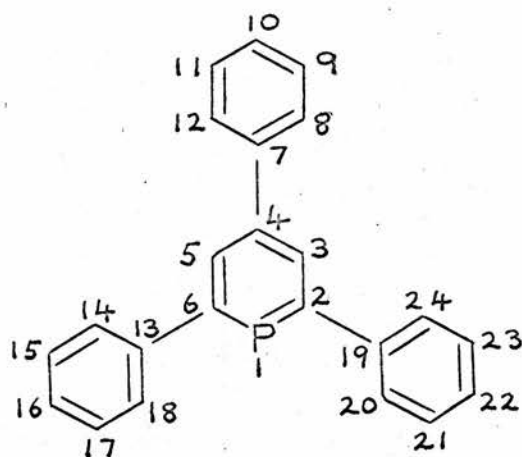
found that small traces of lead dioxide decomposition product in the latter did not affect any results.

(iii) Substrates

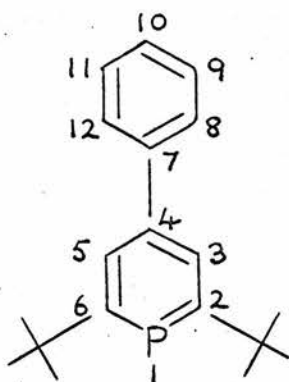
The phosphorins used (Fig. 3) were fresh samples prepared and donated by Professor K. Dimroth. The melting points were all within 2° of those reported, and further purification was considered unnecessary. The phospholes used (Fig. 4) were prepared and donated by Dr. E.H. Braye and were several years old. Although the melting points were all within 4° or less of those quoted, the possibility existed of contamination by the oxide. The ESR results, however, did not show any spurious signals from the oxides, and no attempt at purification was made.

(c) Spectrometer

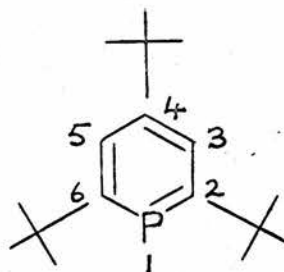
Spectra were recorded on a Decca Radar X3 spectrometer, employing 100 Kc./sec. magnetic field modulation and phase sensitive detection. The microwave klystron operated at a specified frequency of 9270.0 Mc./sec. A wide range of microwave power levels and modulation amplitudes was available. Superheterodyne detection was available, but since this is really only of use with very narrow lines (less than 50 mG.) and with samples which saturate easily, no attempt was made to use it in this work. The magnetic field was provided by a Newport Instruments type F 11-inch electromagnet employing water cooling. The field homogeneity was 20 mG, and a wide range of field sweep speeds



(1)



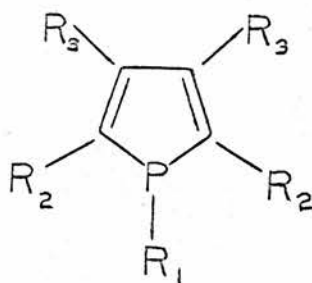
(2)



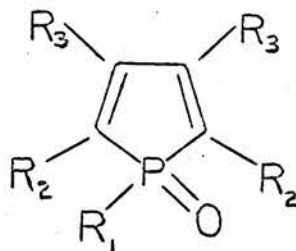
(3)

- (1) 2,4,6-triphenylphosphorin (TPPN)
 (2) 2,6-ditertiarybutyl-4-phenylphosphorin (DTBPPN)
 (3) 2,4,6-tritertiarybutylphosphorin (TTBPN)

Figure 3



- (1) $R_1 = \text{CH}_3$, $R_2 = \text{Ph}$, $R_3 = \text{H}$ (MeDPPL)
- (2) $R_1 = R_2 = \text{Ph}$, $R_3 = \text{H}$ (TPPL)
- (3) $R_1 = R_2 = R_3 = \text{Ph}$ (PPPL)
- (4) $R_1 = -\text{CH} = \text{CH}_2$, $R_2 = R_3 = \text{Ph}$ (ViTPPL)



- (5) $R_1 = R_2 = \text{Ph}$, $R_3 = \text{H}$ (TPPLO)
- (6) $R_1 = R_2 = R_3 = \text{Ph}$ (PPPLO)

Figure 4

was available. The field could be accurately set at 10G intervals by means of a proton resonance meter situated in the field behind the microwave cavity. The cavity operated in the TE 102 mode. Spectra were recorded on a Smith's I-t chart recorder.

For low-temperature studies a Decca variable temperature accessory MW235 was employed. The temperature was varied by passing nitrogen gas at a constant rate through the metal coil (immersed in liquid air) of a heat exchanger, and then through a Dewar vessel inserted into the cavity. Sample tubes were placed in this Dewar stem. The temperature at the sample was measured by a platinum resistance thermometer and fine control of the temperature was achieved electronically. With this system temperatures accurate to $\pm 2^{\circ}\text{C}$ were obtained.

(d) Hyperfine Splitting and g-Value Measurement

Room temperature measurements were made by comparison with a saturated aqueous sodium carbonate solution containing a minute quantity of Frémy's salt (potassium nitrodisulphonate), for which $a_{\text{N}} = 13.091 \pm 0.004\text{G}^{111}$ and $g = 2.00550 \pm 0.00005^{112}$. A sealed capillary containing this solution was taped to the outside of the sample tube. The concentration of the Frémy's salt was optimised by trial and error so as to facilitate accurate determination of the separation of the lines in both standard and sample. In cases where this was not possible, a more approximate calibration was made by running the standard immediately before and after the sample to eliminate the possibility of chart motor speed variation. No discrepancies were found in practice.

In samples with a large number of hyperfine lines, as many pairs as possible were chosen for measurement, spread over the entire spectrum. Together with improving the accuracy of the measurement, this also eliminated possible errors arising from chart motor speed variation and non-linearity of the magnetic field sweep. The hyperfine splittings were calculated using a separation of 26.18G between the high and low field lines of Frémy's salt.

For g-value measurement, the value of the field at the centre of the Frémy's salt spectrum was calculated by

$$H_F = \frac{h\nu}{g\beta} = \frac{6.6252 \times 10^{-27} \times 9270 \times 10^6}{2.0055 \times 0.92732 \times 10^{-20}} \\ = 3302.37G$$

The g-value of the sample was then calculated from the relationship

$$g = \frac{h\nu}{\beta H_S} = \frac{h\nu}{\beta(H_F + \Delta H)} = \frac{g_F H_F}{H_F + \Delta H}$$

where H_S is the centre of the sample spectrum and ΔH is the separation between the two centres, taken as positive if $H_S > H_F$.

Where the centre of the sample spectrum was obscured by the Frémy's salt lines, the position was found using the nearest unhidden hyperfine lines.

(e) Computer Simulations

Computer simulation is an extremely useful technique for analysing

experimental spectra in which it is not possible to deduce an unequivocal assignment by measuring the spectra and performing line simulations by hand. It is especially useful in cases where the spectra are only partially resolved. Estimated splitting constants and numbers of equivalent nuclei may be fed into a suitable programme, which will calculate the shape of the spectrum assuming a given line shape. This may then be plotted to give a "theoretical" spectrum. The input data is then adjusted until the calculated spectrum matches the experimental spectrum.

The spectral simulation programme used in this work was written by J.B. Holz (University of North Carolina) and modified for use with the IBM 1627 plotter. The programme could calculate and plot up to 5000 points and up to 200 groups of 10 equivalent lines, but had no facility for simulating varying line-widths.

The following experimental section is divided into the preparation and characterisation of radicals from phospholes, phosphole oxides and phosphorins. The reactions of phospholes are divided into room temperature and low temperature reactions; distinct types of radicals are obtained in each case. The signal strengths are roughly classified as intense, medium, weak, very weak.

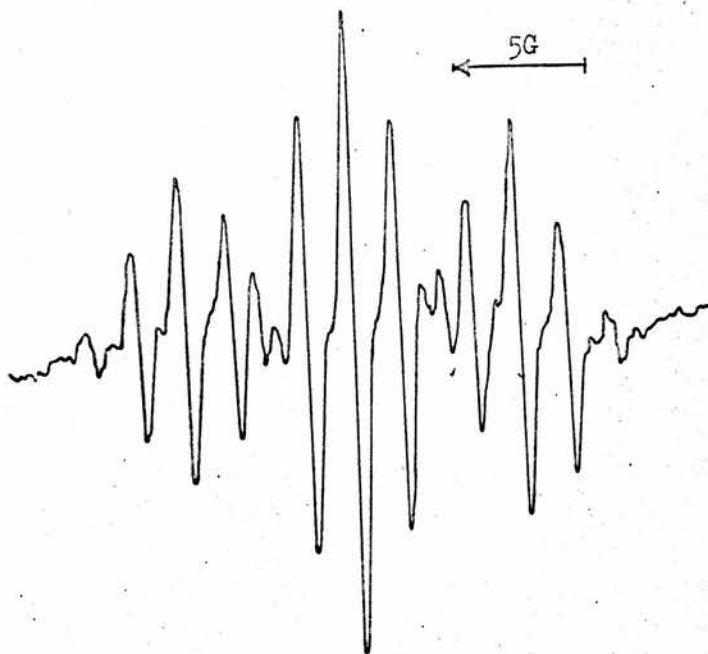


Figure 5

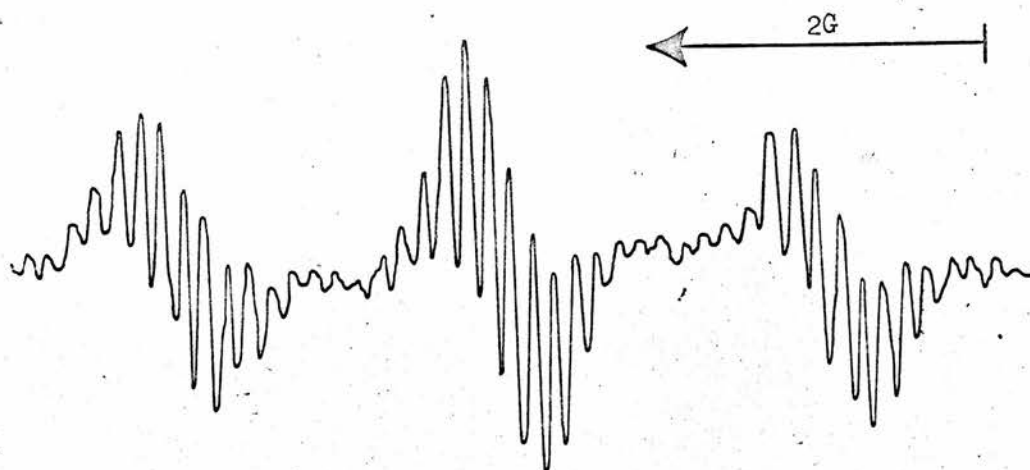


Figure 6

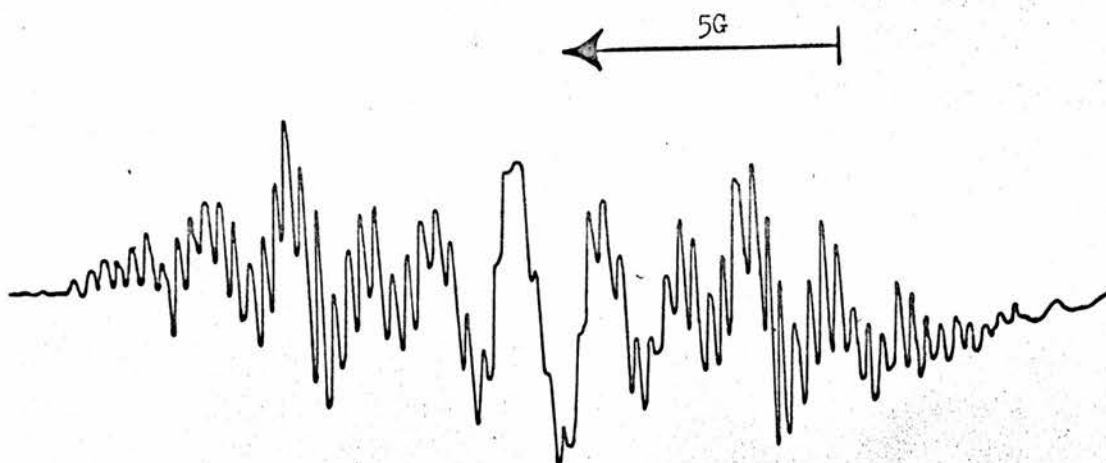


Figure 7

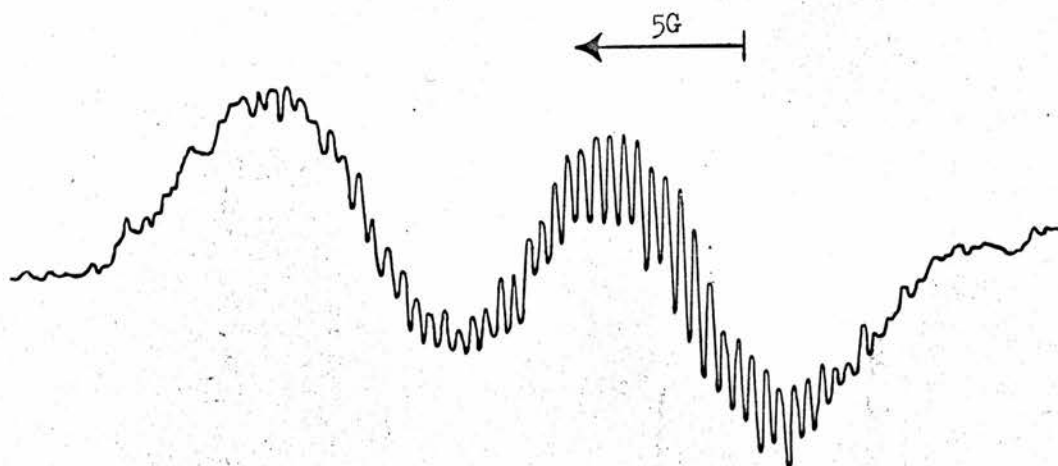


Figure 8

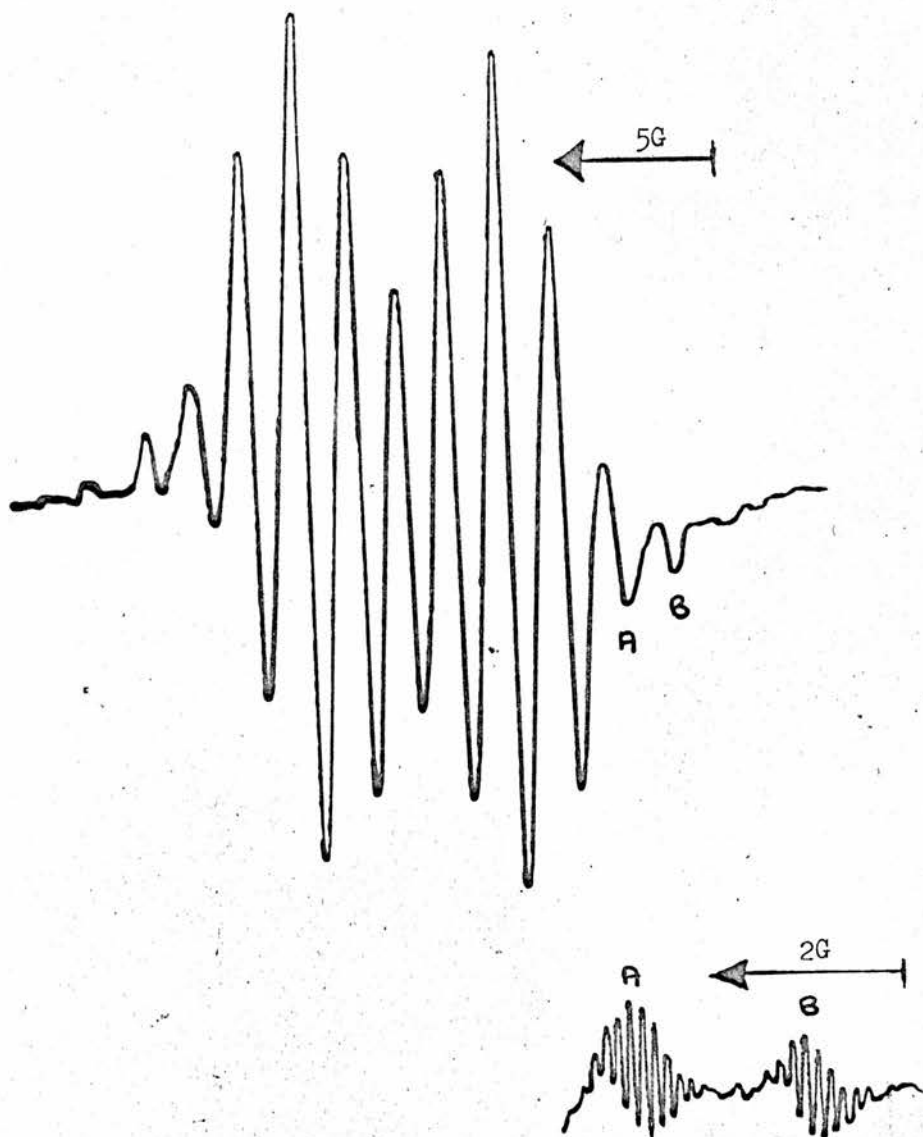


Figure 9

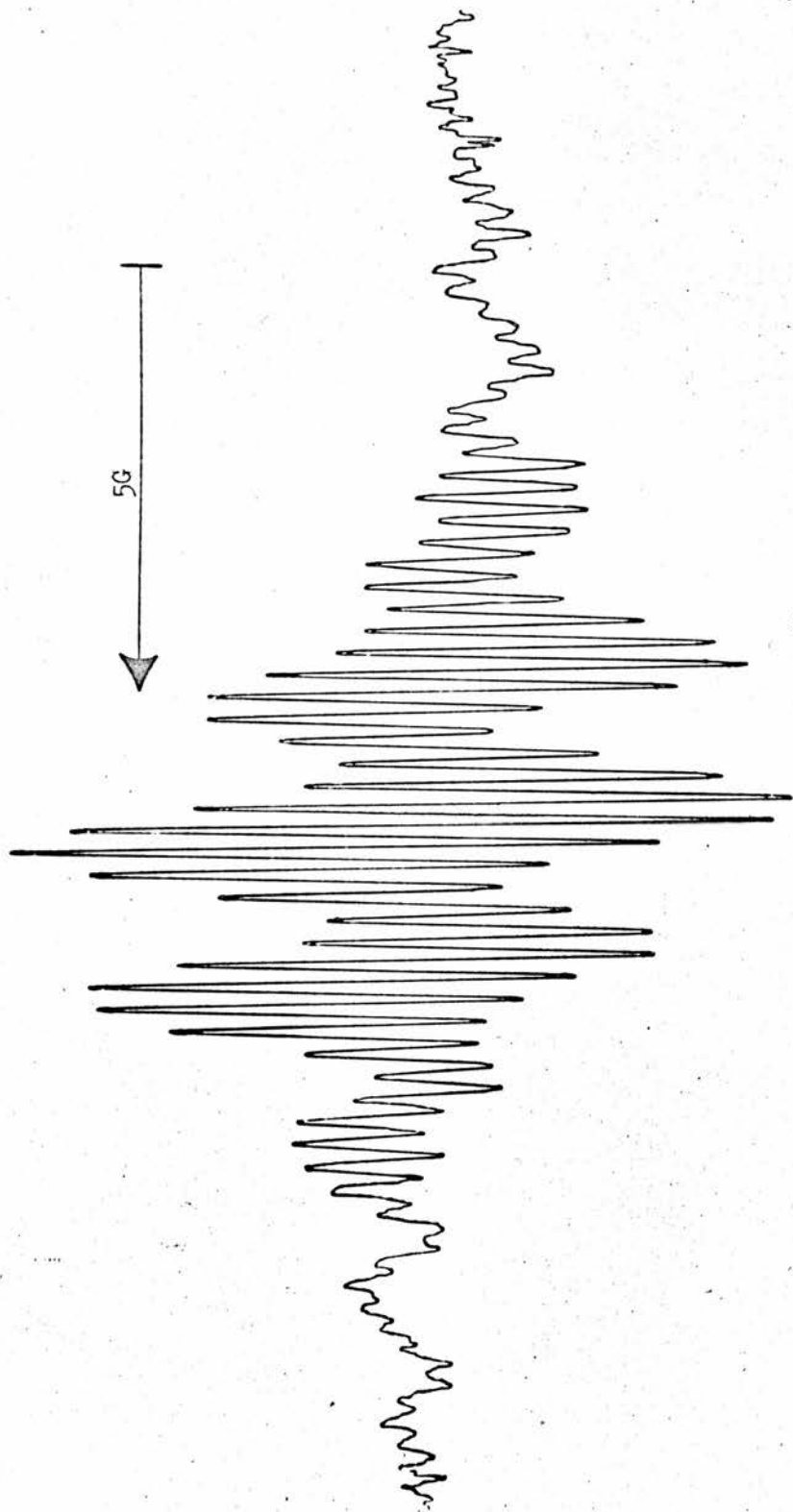


Figure 10

2. Radical Anions from Phospholes:

A. Reactions at Room Temperature with Alkali Metals

(a) Reaction of Pentaphenylphosphole and 1,2,5-Triphenylphosphole with K

Each reaction was carried out in both DME and THF. Reaction initiation times varied from minutes to hours, and depended more on the extent and cleanliness of the potassium mirror than on the phosphole concentration. In each run a red colour gradually developed, but no signals were observed until the colour had intensified considerably. Four distinct signals were seen from each phosphole in each solvent.

Signal A (Fig. 5) consisted of a 1:2:1 triplet split into a 1:4:6:4:1 quintet. The splitting constants at 25°C were:

$$\text{(in DME)} - a_1 = 6.28 \pm 0.08\text{G (3 lines)}$$

$$a_2 = 1.75 \pm 0.05\text{G (5 lines)}$$

$$\text{(in THF)} - a_1 = 6.08 \pm 0.08\text{G (3)}$$

$$a_2 = 1.66 \pm 0.05\text{G (5)}$$

The spectra could be computer simulated unambiguously. On lowering the temperature the major splitting increased considerably. From TPPL in DME, a_1 increased steadily from 6.17G at +40° to 6.96G at -50°. The secondary splitting did not change. At high dilution and low microwave power (700 μ W), the signal from PPPL in THF showed further fine structure (Fig. 6), each of the lines being split into about 12 components, separation 0.13G. Another high resolution spectrum from

PPPL in DME showed a marked increase in the width of the central group of lines at temperatures below 0° (Fig. 7).

Signal B (Fig. 9) consisted of a 1:1 doublet with a further splitting into about 9 lines. From PPPL in DME,

$$a_1 = 6.37 \pm 0.05G \text{ (2)}$$

$$a_2 = 1.66 \pm 0.07G \text{ (about 9)}$$

Although 9 lines were clearly visible, the intensity ratios did not correspond to this number. The intensities of the central lines corresponded closely to a 1:4:6:4:1 quintet. As with signal A, high dilution and low microwave power permitted further resolution (inset, Fig. 9), consisting of about 10 lines, separation 0.14G. Resolution of this degree was not obtained on every line owing to varying line-widths, which could explain the anomalous intensities.

Signal C (Fig. 10) consisted of 9 lines, the intensities agreeing with 8 equivalent nuclei; from a PPPL sample in DME, $a = 1.77 \pm 0.07G$. At high dilution and low microwave power, each line split further into about 7-9 lines, separation 0.3G (the spectrum shown in Figure 10 shows these fine splittings).

Signal D (Fig. 8) was broad with the general shape of a poorly resolved doublet, splitting about 10G. No fine structure was apparent at normal concentrations, but at high dilution further lines appeared on the low-field half of the spectrum, separation 0.4G.

Signals A, B, C all had the same g -value of 2.0027, and signal D had $g = 2.0033$. In most runs, D was present with one or more of A, B,

C superimposed. The splitting constants for A, B, C quoted above refer to the few cases where D was not present.

In the course of about 40 reactions it was found that each of the signals A, B, C was interconvertible with the other two. The order of appearance of the signals was not predictable. Below are listed some general observations:

- (1) Samples prepared on the vacuum line in the same batch gave the same sequence of signals. This suggests that the pressure in the system at the time of preparation may have a critical influence.
- (2) Fast reactions, produced by a high phosphole concentration or, more usually, by a more extensive potassium mirror, favoured the formation of D.
- (3) The first samples prepared using a new batch of solvent were more likely to give A, B, C than the later samples. This suggests the probability of a volatile impurity being distilled over with the solvent.
- (4) Temperature had a critical influence. Low temperatures stabilised A, B, C against formation of D. Samples run by first forming the phosphole monoanion at low temperature (Section B) and then by allowing further reaction gave A. A, B or C could be prepared from samples in which D had been formed initially by cooling the solution and reacting with potassium below 0°C . The appearance of signals in this case coincided with the appearance of a dark blue colour in the red solution.

PBP. The splitting of 10G from D is similar to the phosphorus splittings of the radicals formed by further 1-electron addition to these species. Thus D could result from a 1-electron addition to I. However, the poor resolution of the signal suggests the possibility of an **asymmetric** species; this could be the result of the fission of a phosphorus-carbon ring bond in I, followed by a 1-electron addition.

Signal A has identical splitting constants to the radical observed recently¹¹⁴⁻¹¹⁸ in the reaction of benzene with Na/K alloy in DME/THF mixed solvent. That A is the same radical as this would seem to be confirmed by the appearance of the very small splittings at low power levels and by the same temperature dependence of the main splitting, as first observed by Bolton.¹¹⁶

Although the analysis of B is less straightforward, owing to the peculiar intensities, the splittings are the same as in A, except for the loss of one proton contributing to the main splitting. Together with the identical *g*-values, this indicates very closely related structures for the two radicals. Similarly, C has the same *g*-value and 1.75G splitting, but has lost the protons giving the 6.3G and 0.13G splittings. Thus, all three radicals appear to have closely related structures. The significantly different *g*-value of D indicates a very different structure from A, B, C.

The origin and structure of these radicals are discussed more fully in Chapter IV.

(b) 1-Methyl-2,5-diphenylphosphole with K

Reactions were slower than with TPPL and PPPL, but a similar red colour was produced. Some very weak signals observed were ascribed to small amounts of impurities. An intense signal was obtained in both DME and THF after the red colour had intensified, and was identical to signal D, with the same splittings and g-value. No type A, B, C signals were seen either separately or superimposed on D. Since the monoanion of this phosphole has a distinct spectrum (Section B), this radical would appear to result from cleavage of a P-C ring bond, followed by 1-electron addition. The similarity of this signal to signal D indicates that D is formed by an analogous reaction; this is in contrast to the work on TPP and PBP.

(c) 1-Vinyl-2,3,4,5-tetraphenylphosphole with K

Reaction was slow but gave the usual red colour. A very weak type D signal was seen, but the radical decomposed after about 5 mins. No type A, B, C signals were seen.

(d) Phospholes with Na

Reactions with TPPL, PPPL, MeDPPL and ViTPPL at room temperature did not give any intense signals. All reacted to give an initial pale blue, fluorescent solution. TPPL and PPPL both gave very weak doublet signals, almost certainly the monoanions, which were produced in much higher yields at low temperature (Section B). Further reaction gave

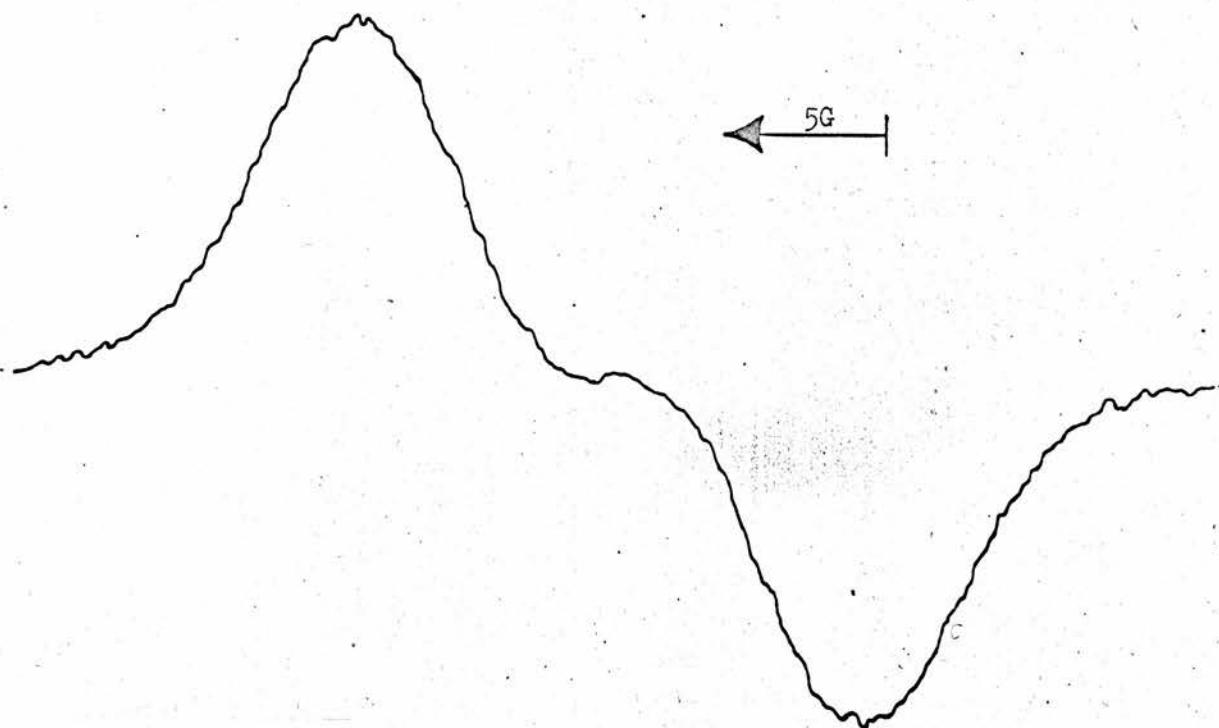


Figure 11a

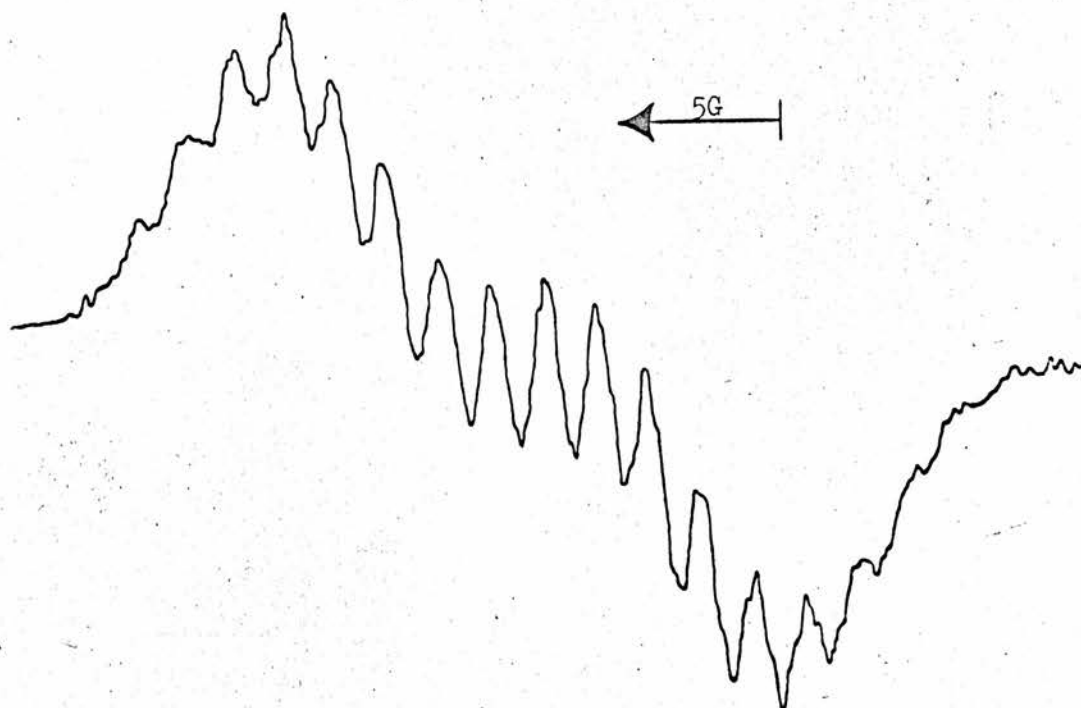


Figure 11b

pale maroon solutions which, with two exceptions, gave no further signals. Samples of TPPL in DME gave a moderately strong signal, shown in Figure 11. The overmodulated signal (Fig. 11a) closely resembled the envelope of signal D. At modulation amplitude 0.7G, this resolved into about 18 lines, separation $1.48 \pm 0.04\text{G}$ (Fig. 11b), each of which split again at modulation 0.2G into three lines each, separation 0.45G, the resolution being better on the low-field side. The similarity of this signal to signal D suggests that some sort of cleavage reaction has occurred. The different fine structures may be due to either the P-C ring cleavage having occurred without prior P-phenyl cleavage or the gegenion contributing to the splittings by ion-pairing. The absence of A, B, C type signals supports the former. However, ion-pairing does occur with the phosphole oxides (Section 3).

A sample of TPPL in THF reacted at low temperature to give first the monoanion and then the red colour showed a fairly weak biphenyl signal which, after several hours at room temperature, gave an intense signal D. This shows that both P-C ring and P-phenyl cleavages are possible with sodium under suitable conditions.

(e) Phospholes with Li

Reactions of all four with this metal took at least two weeks to initiate. As the red colour intensified, a weak signal D was seen from TPPL, PPPL, MeDPPL. No other signals were observed.

B. Reactions at Low Temperature with Alkali Metals

Reactions were performed in the following manner. After sealing off the sample tube the solution was allowed to warm to room temperature to allow dissolution of the phosphole, taking great care to avoid contact with the potassium mirror. The entire tube was then immersed in a solid CO_2 /acetone bath at -80°C , and the solution allowed to react with the potassium in this bath. Some solution was tipped into the side-arm, which was inserted into the ESR cavity, initially at -60°C .

(a) MeDPPL with K and Na in DME

Reaction with the potassium mirror produced an immediate brilliant blue colour, showing an intense ESR signal; reaction with sodium took several minutes to initiate but produced the same colour. The spectra obtained were the same in both cases, although the signal strength was higher by a factor of about 3 in the sodium reactions.

The spectrum consisted basically of a well-separated doublet, one component of which is shown in Figure 12, recorded at modulation amplitude 0.07G. The other component was identical. Each component was split into at least 35 lines, arranged in 6 main groups. Spectra run under high gain conditions did not show any clear outside lines. Under high resolution, each of the lines was seen to consist of a number of overlapping lines.

Measurements on the spectra, together with computer simulations,

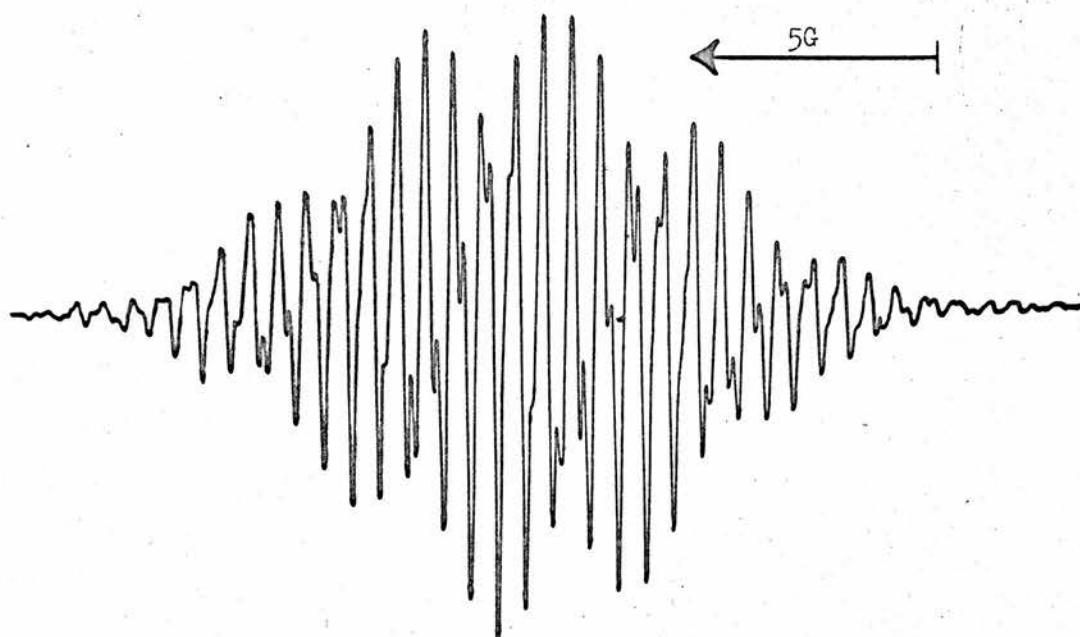


Figure 12

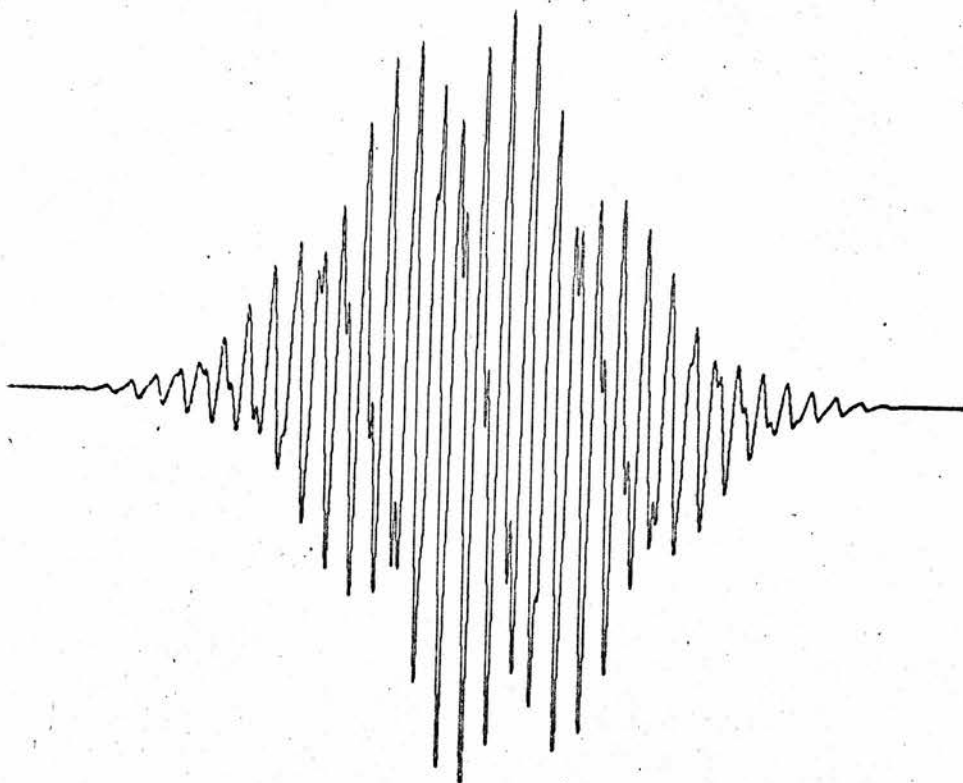


Figure 13

gave the following splitting constants:-

$$a_1 = 23.5 \pm 0.3G \text{ (2 lines)}$$

$$a_2 = 2.48 \pm 0.05G \text{ (6)}$$

$$a_3 = 1.31 \pm 0.05G \text{ (7)}$$

$$a_4 = 0.62 \pm 0.04G \text{ (5)}$$

The computed half-spectrum is shown in Figure 13, using the following input data:-

$$\text{line-width} = 0.19G$$

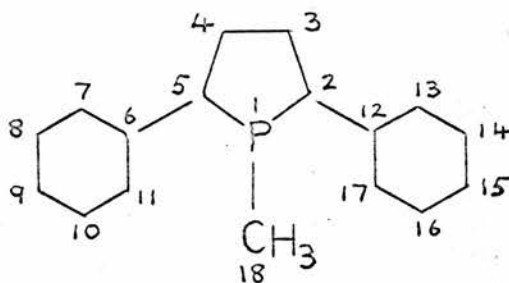
$$a_2 = 2.47G \text{ (6)}$$

$$a_3 = 1.34G \text{ (7)}$$

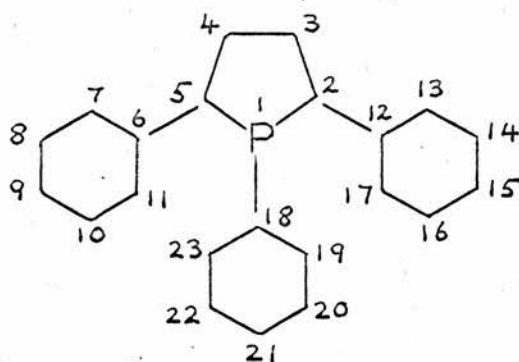
$$a_4 = 0.66G \text{ (5)}$$

The large 23.5G doublet may be confidently assigned to the phosphorus nucleus; this splitting is of similar magnitude to those observed by Dimroth in the spectra of phosphorin cations and anions. The 2.47G splitting by 5 equivalent nuclei must arise from identical splittings from the 3 methyl protons and the 2 phosphole ring protons at positions 3, 4 (Fig. 14). The 1.34G splitting from 6 equivalent nuclei arises from the ortho- and para- protons on the two phenyl rings, and the 0.66G splitting by 4 equivalent nuclei from the meta-protons on these rings. These assignments were supported by McLachlan spin density calculations (Chapter III).

As may be seen from the simulated spectrum, the curve envelope and the positions of all the main lines are reproduced exactly.



Numbering system for MeDPPL



Numbering system for TPPL

Figure 14

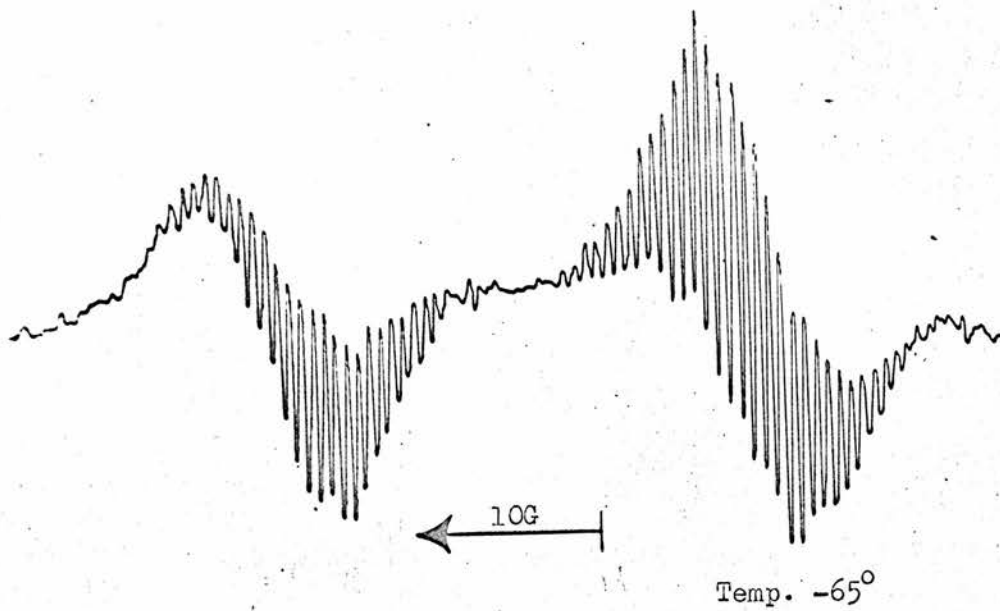


Figure 15

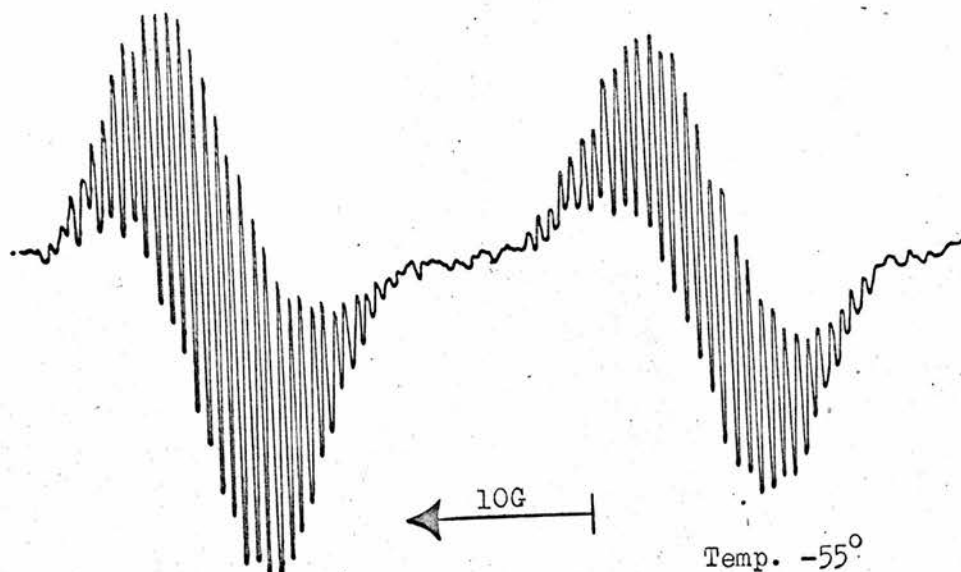


Figure 16

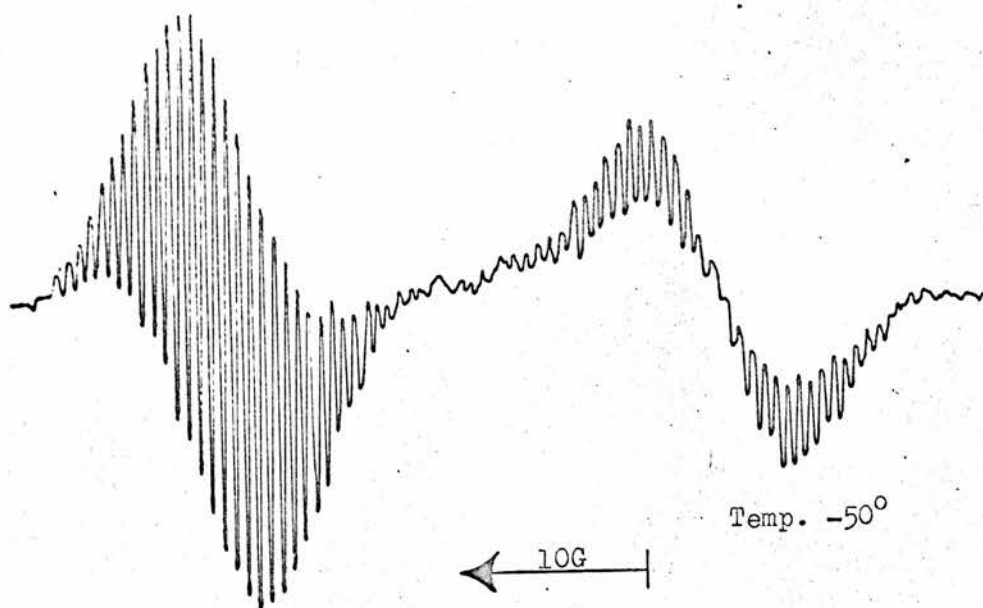


Figure 17

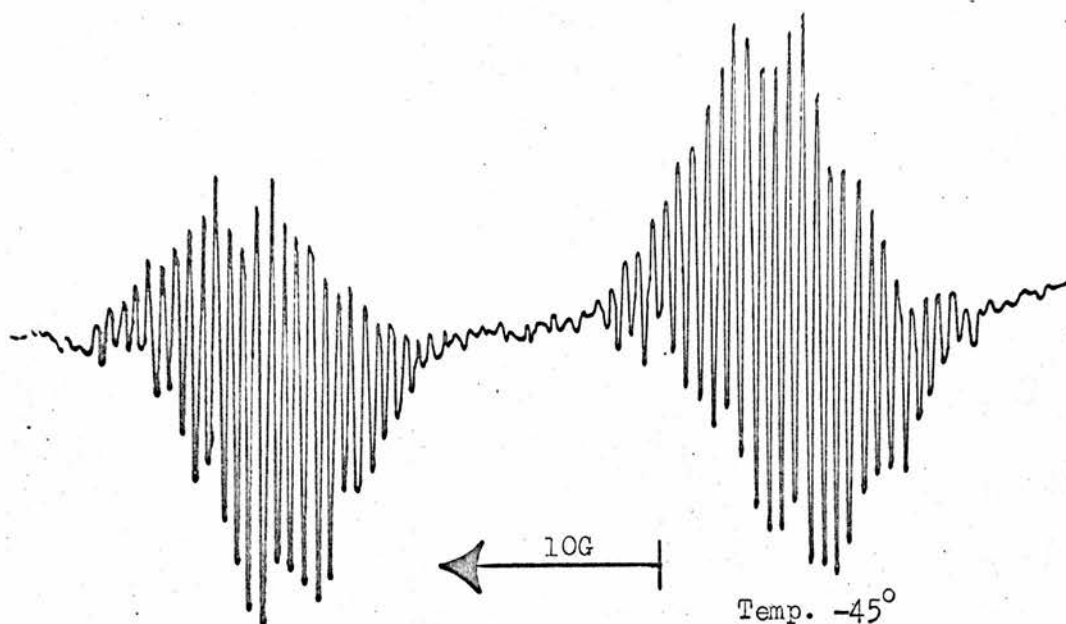


Figure 18

However, the positions and intensities of the finest lines are not reproduced very well. This could arise from slight inequivalence of some of the protons; for example, the 3 methyl proton splittings may differ slightly from the 2 ring proton splittings. It was found to be impractical to attempt simulation of these inequivalences owing to the large number of feasible possibilities. The simulations were further complicated by the fact that changing the input splittings by only 0.01G sometimes changed the appearance of the spectrum considerably.

No change in the splitting constants or in the general appearance of the spectrum was noted in the temperature range -40° to -65° . At -30° the line-width increased sufficiently to prevent resolution of the finest lines. Above this temperature the radical decayed rapidly, giving a greenish solution. The radical was stable for several hours below -30° . No evidence was found for metal ion splittings. The greater radical yield on reaction with sodium is probably due to the absence of the competitive reactions which can occur with potassium, as described in Section A.

(b) MeDPPL with K and Na in THF

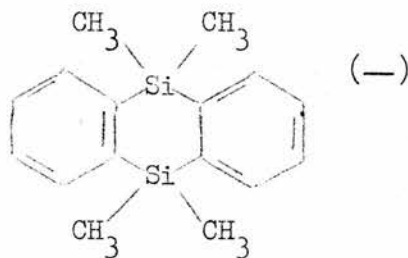
Reaction with sodium gave the same signal as on reaction in DME, with a similar signal strength. On reaction with potassium, however, a very different signal was observed (Figs. 15-18). The signal, of only medium strength, again consisted of a well-separated doublet, but the fine structure differed considerably from that in DME. No obvious

groupings of the lines could be seen, and a peculiar line-width effect was found. At -65° (Fig. 15) the highfield component was much less well resolved than the lowfield component, and was distinctly asymmetrical. At -55° (Fig. 16) both components had the same structure and symmetry, with the lowfield group of slightly lower intensity. At -50° (Fig. 17) the spectrum was the reverse of that at -65° , with almost all the resolution on the lowfield peak having been lost. At -40° the spectrum was again similar to that at -65° . The radical decomposed rapidly above -30° . In certain spectra run at -45° (Fig. 18) and at -60° , in which the two components were of similar appearance, there were clear indications of groupings similar to those in the DME spectrum. This group separation of about 2.5G, together with the separation of the individual components of about 0.6G, suggests that this is a different form of the same species observed in DME.

Measurement of the large phosphorus splitting was complicated by the asymmetry of the components. It was estimated that the splitting of about 24G at -65° increased steadily to about 28G at -30° . (This variation was not found with Na/THF or Na, K/DME.) However, the splitting of 24G at about -60° does support the previous conclusion that this is the same species as observed in DME.

No evidence for potassium splittings was found at any temperature, although it would appear that the difference in the spectra is a result of gegenion pairing in this solvent, since these unusual spectra were not seen with the systems Na/THF or Na, K/DME.

It is now well-established in the spectra of aromatic anions that ion-pairing to give metal splittings can sometimes occur in THF but not with the same anion in DME. For example, the spectrum of the biphenyl anion¹¹⁹ in THF shows a potassium splitting of 0.04G, which is not present in DME. (The line-widths in the present work would prevent observation of splittings of this magnitude.) Even if ion-pairing is occurring here, it is difficult to propose a reasonable mechanism to explain this complex line-width effect. In a study of the 5,5,10,10-tetramethyl-5,10-dihydrosilanthrene anion¹²⁰



in which alternating line-widths are observed, the authors suggested that the K^+ gegenion oscillates between the two silicon nuclei, and is associated with the silicon d-orbitals. A similar mechanism may be feasible here, in which the gegenion takes up positions on either side of the phosphole ring, and is closely associated with the phosphorus d-orbitals. This mechanism would be particularly important if the configuration about the phosphorus was non-planar, making the two sites non-equivalent. Restricted rotation of the methyl group would make the situation even more complex. Close association with the phosphorus

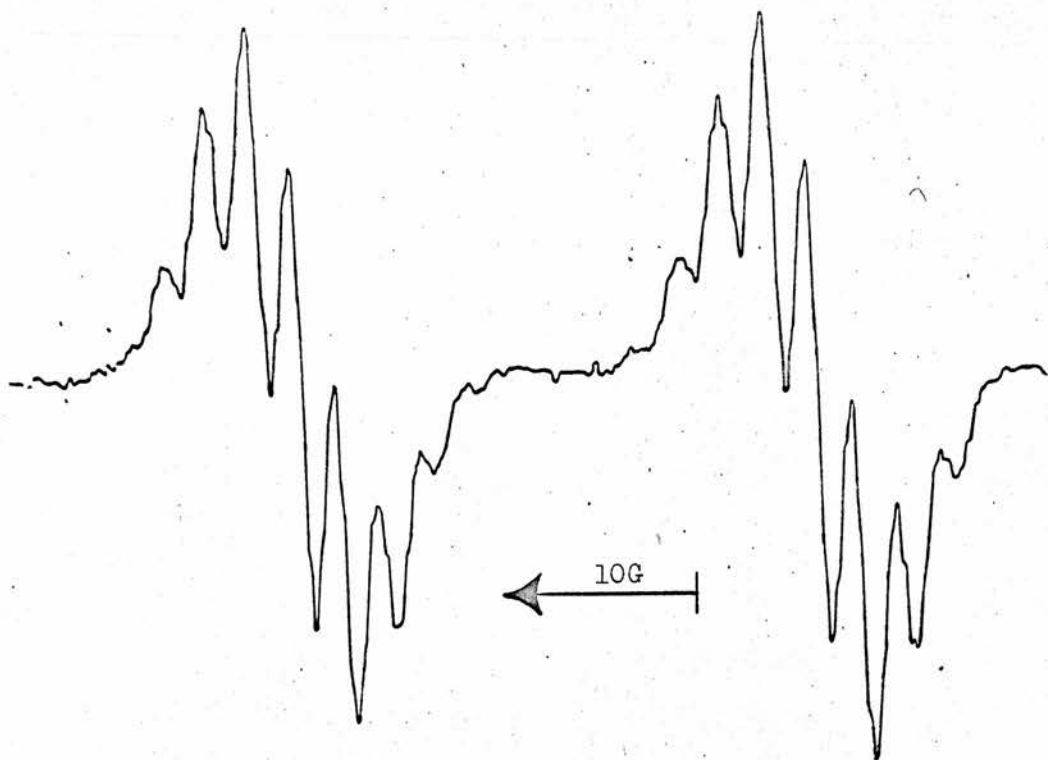


Figure 19

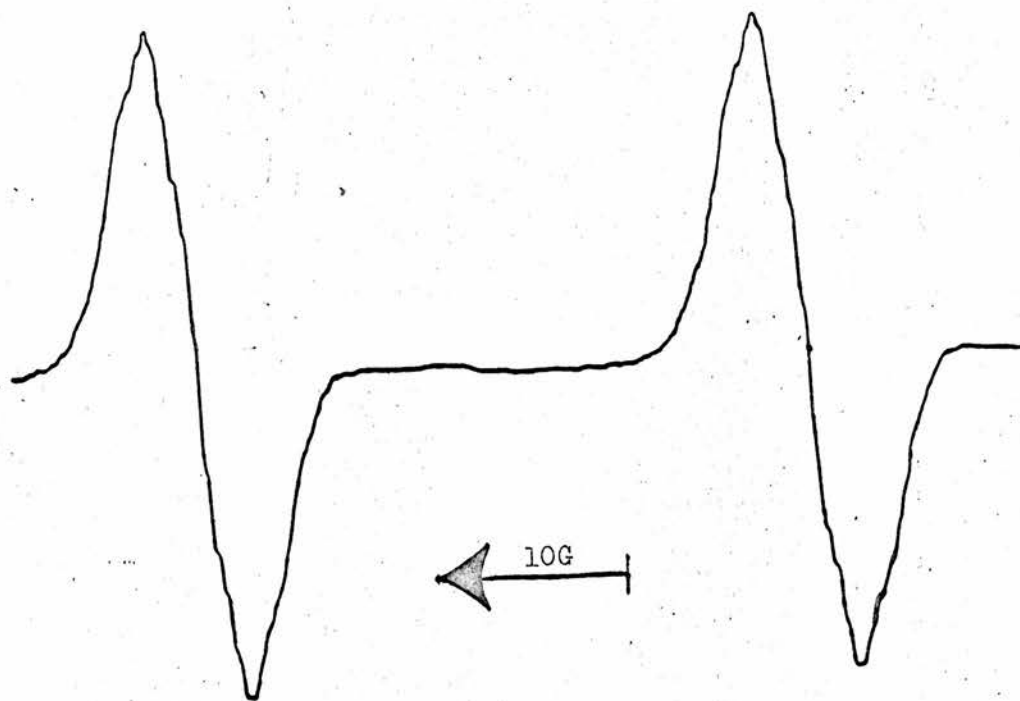


Figure 20

is also indicated by the significant change of the phosphorus splitting with temperature. The spectra are, however, much too complex and poorly resolved to permit detailed analysis of the possible mechanisms.

(c) TPPL with K and Na in DME, and with Na in THF

A brilliant blue colour was produced immediately on reaction with potassium, and after a few minutes on reaction with sodium. As in (b) the sodium samples gave much more intense signals than the potassium samples. The spectrum (Fig. 19) again showed a well-separated doublet, each component being split into 9 lines (the outer two being observed under high gain conditions), the intensity ratios corresponding to 8 equivalent protons. At slow sweep speeds, each of these lines split into 5 or 7 incompletely resolved lines. The high line-width of 0.4G prevented observation of any smaller splittings. The measured splitting constants (at -40°C) were

$$a_1 = 26.5 \pm 0.4\text{G} \text{ (2 lines)}$$

$$a_2 = 2.26 \pm 0.06\text{G} \text{ (9)}$$

$$a_3 = 0.43 \pm 0.04\text{G} \text{ (5 or 7)}$$

Computer simulations gave no help in assigning the 0.43G splitting to 5 or 7 lines owing to the poor resolution of the experimental spectrum. The simulations did, however, confirm the other assignment.

No changes in splitting constants were found in the temperature range -20° to -60° , the radical decomposing rapidly above -20° . The radical was stable for several hours below this temperature.

The 26.5G splitting may be assigned with confidence to the phosphorus nucleus. The 2.26G splitting may be assigned to the phosphole ring protons and to the ortho- and para-protons on the phenyl rings attached to positions 1 and 5, i.e. protons at positions 3, 4, 7, 9, 11, 13, 15, 17 (Fig. 14). This assignment is also supported by McLachlan calculations (Chapter III). If the 0.43G splitting does arise from 4 equivalent protons, these would be the meta-protons at 8, 10, 14, 16. Since assignment to 6 equivalent protons would be difficult to explain from the structure of this molecule, this assignment would seem likely.

It is interesting to note that no measurable splittings arise from the phenyl group attached to the phosphorus, indicating that this ring is pushed well out of the plane of the phosphole ring. The large splittings from the other two phenyl rings indicate that these are probably planar with the phosphole ring. This result would be expected from purely steric considerations, since the considerable crowding would push the phenyl ring on the phosphorus out of the plane, rather than pushing the other two rings out of the plane, so as to bring the loss of delocalisation energy to a minimum.

(d) TPPL with K in THF

The signal from the usual blue solution was superficially similar to that in (c), the linewidth having increased, this preventing observation of the smallest splitting. The values of the other two splitting

constants had changed to

$$a_1 = 28.1 \pm 0.4G \text{ (2)}$$

$$a_2 = 2.06 \pm 0.06G \text{ (9)}$$

No changes of splittings or line-width were observed in the temperature range -20° to -60° , the appearance of the signal being the same throughout. The splitting constants are significantly different from those in (c), and lend support to the idea that the K^+ gegenion in THF is closely associated with the radical. However, this system does not give any further information as to the structure.

(e) PPPL with K and Na in DME and in THF

Each metal in each solvent gave the usual blue colour with an intense ESR signal (Fig. 20). This consisted of a featureless doublet with no fine structure, even at low modulation amplitude, slow sweep and high dilution. The separation was $31.3 \pm 0.4G$, with line-width $4.5G$. No variation of splitting was seen in the temperature range -30° to -60° , and the radical decomposed rapidly above -30° . The potassium samples were stable for about 3 hours at cardice/acetone temperature, and the sodium samples stable for several days.

The doublet may again be assigned to the phosphorus. The absence of proton splittings from the phenyl rings is not surprising, since steric effects will push most or all of the 5 rings out of the plane of the phosphole ring, reducing the spin density in these rings. This is seen in the larger a_p value of $31.3G$, compared with $26.5G$ in

TPPL, indicating an increased spin density in the phosphole ring despite the presence of two more phenyl rings.

The greater stability of the sodium samples may be attributed to lack of competitive reactions; the potassium samples at cardice/acetone temperatures eventually gave the radicals described in Section A.

No anomalous effects were noted in the K/THF system. In particular, the value of a_p did not change, indicating that association with K^+ does not occur here. This may be due to the severe steric crowding round the phosphole ring not allowing close proximity of K^+ with its solvent shell.

(f) ViTPPL with K and Na in DME and THF

Each metal in each solvent again gave an intense blue colour, but the ESR signal was weak, and consisted of a featureless doublet similar in shape to that from PPPL (Fig. 20), with separation $27.6 \pm 0.6G$. The radical was very unstable even at -60° , decomposing completely within 10 min. to give a reddish solution.

Less steric interaction than in PPPL and possible delocalisation over the vinyl group would explain the lower phosphorus splitting. However, the reasons for the low signal strength and the radical instability are not clear. The initial intense colour would indicate that the radical is being formed in reasonably high yield, but is disappearing quickly to give a low steady-state concentration. The

disappearance could occur via some reaction of the vinyl group, such as dimerisation of two radicals.

(g) Other Phospholes with Na and K in DME and THF

Reactions were attempted with 2,3,4,5-tetraphenylphospholes with the groups $-\text{CH}_2\text{CO}_2\text{H}$, $-\text{CH}_2\text{Cl}$ and $-(\text{CH}_2)_3\text{Br}$ on the phosphorus, but no colourations or signals were seen in any of the systems.

(h) Phospholes with Li in DME and THF

No reactions were evident with any of the phospholes after 7 days at cardice/acetone temperature. On bringing to room temperature, a red colouration was produced after a further 7 days, but no signals were obtained.

3. Radical Anions from Phosphole Oxides

In order to obtain a comparison with the reactions of phosphine oxides with alkali metals, the phosphole oxides TPPL₂O and PPPL₂O (Fig. 4) were reduced with potassium, sodium and lithium in DME and THF. (An unsuccessful attempt to oxidise MeDPPL to MeDPPL₂O was made, and shortage of MeDPPL precluded any further attempts.)

Reactions were found to proceed satisfactorily at room temperature, and the radicals producing the blue colour were assumed to be monoanions, no evidence being found for the phenyl-cleaved product.

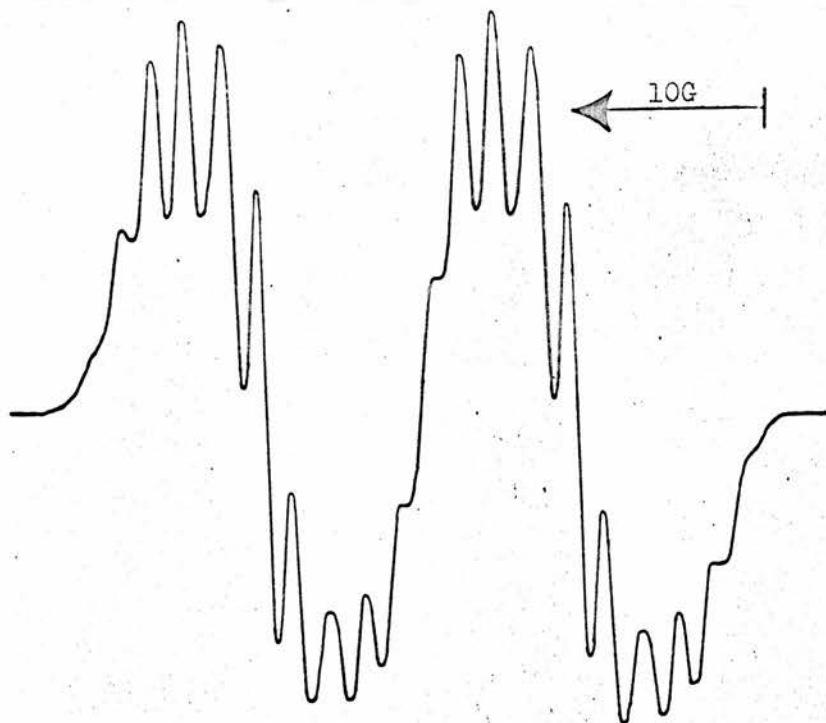


Figure 21

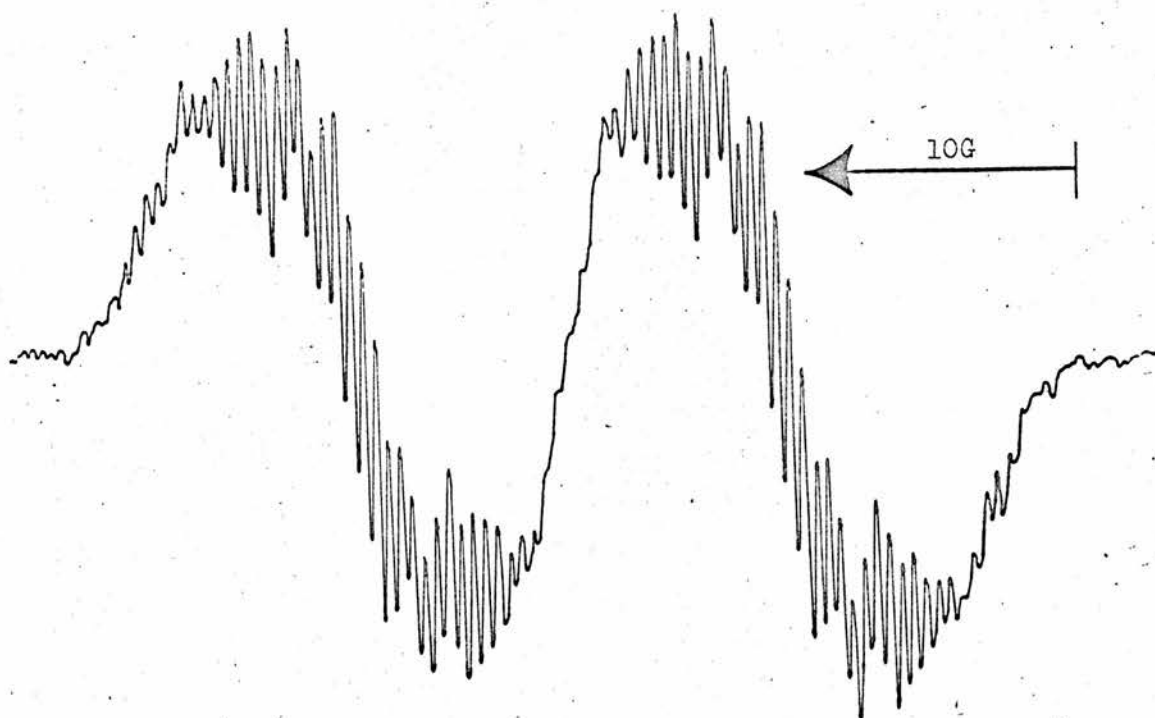


Figure 22

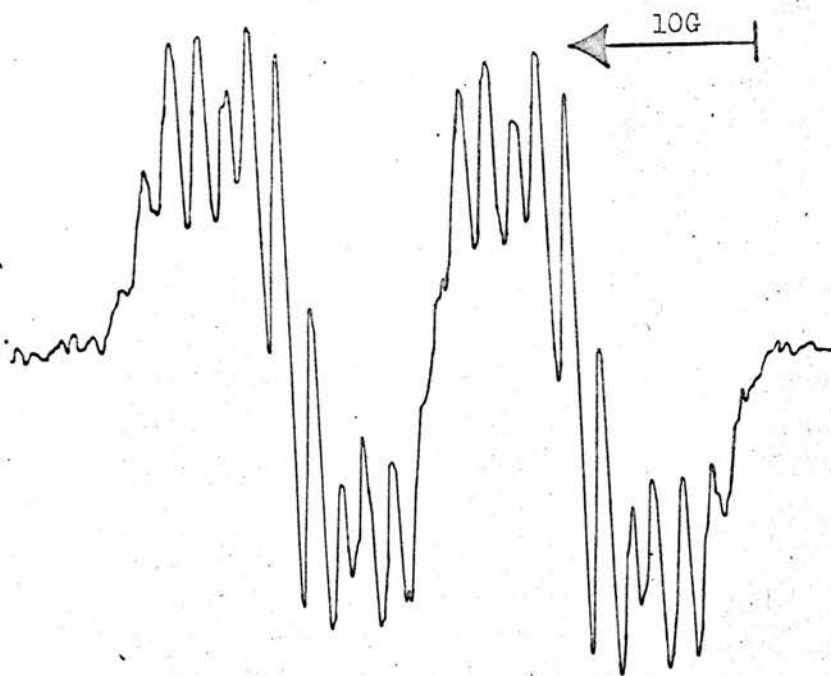


Figure 23

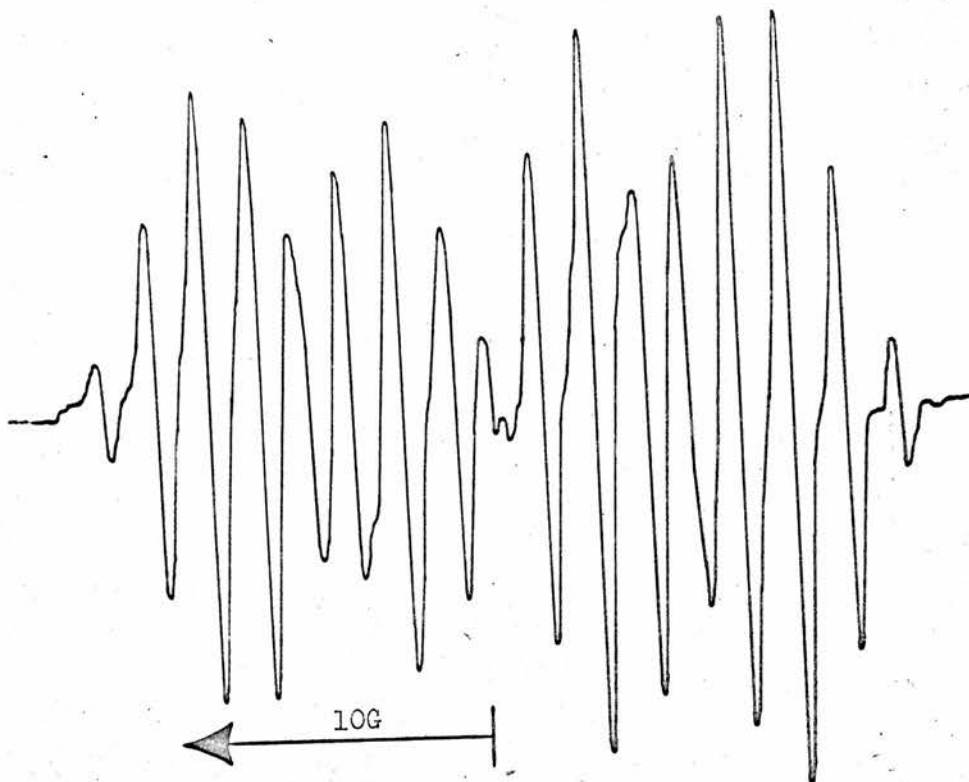


Figure 24

(a) Reaction of 1,2,5-Triphenylphosphole Oxidewith K in TFE and THT

Reaction in each solvent gave identical results: a rapid change of the yellow solution to give an intense blue colour with a medium strength ESR signal (Fig. 21). The spectrum consisted of an overlapping doublet, each component consisting of 11 partially resolved lines or groups of lines. Measurement against Frémy's salt gave

$$a_1 = 16.22 \pm 0.09\text{G} \quad (2)$$

$$g = 2.0024 \pm 0.0001$$

The separations of the secondary structure varied from 1.56G to 2.05G; these are not, therefore, lines due to a secondary splitting of the main line, but are probably groupings of unresolved lines, the line-width of each grouping being about 0.9G.

The 16.22G splitting must arise from the phosphorus nucleus. The low value of this, compared with the 26.5G splitting from TPPL, and the lower signal strength may be explained by the electron being delocalised on to the oxygen.

Further reaction over a period of 1-2 hours gave a murky red-brown solution, which exhibited a medium strength asymmetrical signal. However, although each sample gave a superficially similar signal, closer examination showed each to differ significantly. The asymmetry of the signals prevented measurement of any splittings; almost certainly these were mixtures of signals from a number of radicals. These could have been formed by phenyl-phosphorus cleavage followed by

subsequent reaction with K. No further analysis was attempted.

(b) TPPIO with Na in DME and THF

As in (a), reaction in both solvents gave an immediate intense blue colour with a medium strength ESR signal (Fig. 22). This again consisted of an overlapping doublet, but the fine structure consisted of narrow individual lines instead of the groupings. However, the poor resolution did not make analysis of this fine structure possible.

Measurement against Frémy's salt gave

$$a_1 = 15.75 \pm 0.05G \quad (2)$$

$$a_2 = 0.45 \pm 0.04G$$

$$g = 2.0024 \pm 0.0001$$

This is not a better-resolved example of the spectrum obtained with potassium, since runs at increasing modulation amplitudes did not show any groupings. However, the phosphorus splitting and g-value are sufficiently close to those in (a) to be able to assume that these radicals are the same.

The distinct differences in the fine structure and the smaller phosphorus splitting must be attributed to the effect of the gegenion. It is not clear whether the differences are due to the close proximity of gegenion perturbing the spin distribution, or whether they are due to unresolved gegenion splittings; in view of the significantly lower phosphorus splitting, the former would seem most likely, although the

possibility of gegenion splittings also being present cannot be ruled out.

It may be noticed that the 0.45G splitting is very close to the 0.43G splitting in the anion of TPPL; this could, then, be assigned to the meta-protons at positions 8, 10, 14, 16 (Fig. 14).

(c) TPPLO with Li in DME and THF

Reaction with Li chips took about 3 weeks to initiate; an intense blue colour was again produced in each solvent, with a medium strength ESR signal (Fig. 23). The spectrum was superficially similar to that on reaction with potassium, but closer examination showed that each component of the doublet consisted of about 13 incompletely resolved lines (cf. 11 with K), and the intensities were distinctly different. At low modulation amplitude and high dilution, a small splitting was observed, but it was not possible to estimate the number of lines. Measurement against Frémy's salt gave

$$a_1 = 14.95 \pm 0.1G \text{ (2)}$$

$$a_2 = 1.50 \pm 0.05G \text{ (} \geq 13 \text{)}$$

$$a_3 \approx 0.25G$$

$$g = 2.0024 \pm 0.0001$$

The differences between this and the previous signals must again be attributed to the gegenion. The small 0.25G splitting, which is the smallest observed in any of the phospholes and phosphole oxides, could arise from the Li nucleus, although there is no clear evidence

for this.

Despite the poor resolution, the secondary structure could be interpreted as arising from a 1:2:1 triplet, 5.54G, split into a 1:3:3:1 quartet, 1.50G. Although the triplet could be assigned to the 2 phosphole ring protons, it would be difficult to assign the quartet, unless this arose from the ortho- and para-protons in the phenyl ring attached to the phosphorus; since in the phospholes (in particular TPPL) no splitting is observed from this ring at all, this would seem unlikely. This analysis could therefore be an oversimplification. Again, the gegenion appears to have a distinct influence on the spin distribution.

(d) Reaction of Pentaphenylphosphole Oxide
with K in DME and THF

Reaction in each solvent gave an intense blue colour exhibiting an intense, broad, featureless doublet signal very similar to that from the PPPL anion (Fig. 20). At very high dilution some fine structure of separation 0.2G could just be seen. Measurement against Frémy's salt gave

$$a_P = 16.40 \pm 0.1G \text{ (2)}$$

$$\text{line-width} = 4G$$

$$g = 2.0020 \pm 0.0001$$

The lack of resolution is not surprising, considering the poor resolution of the PPPL anion. Again, the smaller phosphorus splitting

may be attributed to delocalisation over the oxygen.

On further reaction, the solution became red-brown. In the DME samples a new, medium strength signal appeared (Fig. 24). The 17-line spectrum was easily analysed as the following overlapping sets:-

$$a_1 = 12.65 \pm 0.08\text{G} \text{ (2 lines)}$$

$$a_2 = 6.36 \pm 0.07\text{G} \text{ (2)}$$

$$a_3 = 1.75 \pm 0.03 \text{ (5)}$$

$$g = 2.0027 \pm 0.0001$$

The spectrum could be computer simulated with the above splittings. The similarity of the splittings a_2 and a_3 to those in radicals A, B, C (Section 2A) together with the identical g -values, suggests that this radical (E) has a closely related structure. This is supported by the appearance in the THF samples of signal B at this stage of the reaction. Although it would be tempting to assign the large 12.65G splitting to a phosphorus nucleus, the other evidence does not support this. It would also be difficult to assign the above splitting constants to some radical derived from this phosphole oxide.

The appearance of this signal suggests that the asymmetric signals described in (a) could be a mixture of some or all of A, B, C, E, or even other signals. (One of the asymmetric signals did appear to have a doublet of doublets similar in separation to E.)

(e) PPPLO with Na in DME and THF

A similar blue colour and intense, featureless doublet was obtained. However, the splitting had decreased to $16.11 \pm 0.08\text{G}$, with $g = 2.0022 \pm 0.0001$. This again indicates that the gegenion has a distinct effect on the spin distribution.

(f) PPPLO with Li in DME and THF

The reaction took three weeks to initiate, but the usual blue colour and doublet was produced. Again, the phosphorus splitting had decreased, to $15.25 \pm 0.08\text{G}$, with $g = 2.0023 \pm 0.0001$. The change of splitting constant again indicates gegenion interaction.

4. Attempted Preparations of Cations from
Phospholes and Phosphole Oxides

Although the only cations of phosphine type compounds prepared and characterised at the start of this work had electron donating groups present, it was decided to attempt oxidation of the phospholes using a number of oxidising systems, in the hope that the oxidation potentials of some of these compounds would be sufficiently low.

(a) Dissolution in Strong Acids

All six phospholes and oxides dissolved in both conc. H_2SO_4 and oleum to give bright yellow solutions, but no ESR signals were seen in any of the systems. Presumably protonation of the phosphorus is the

predominant reaction.

(b) The System $\text{Pb}(\text{OAc})_4 / \text{DME}$

This system had been used previously in the oxidation of the phosphorins.^{57,59} The phosphole and lead tetraacetate were placed in tube A (Fig. 2), the system pumped down to 10^{-5} torr. and solvent distilled in. No colour changes or signals were seen from any of the phospholes. On standing for 12 hours, a yellow powdery solid was deposited in most of the samples.

(c) The System $\text{Pb}(\text{OAc})_4 / \text{BF}_3\text{-Et}_2\text{O} / \text{CH}_2\text{Cl}_2$

This system had previously been successful in the preparation of triarylamminium cations,¹²¹ the BF_3 etherate acting as a catalyst. The BF_3 etherate was distilled in after the solvent, but although a bright orange-red colour was produced, no signals were seen.

(d) The System $\text{SbCl}_5 / \text{CH}_2\text{Cl}_2$

Solvent was distilled on to the phosphole to give solutions from 10^{-2} to 10^{-4} molar. On distilling in a small amount of SbCl_5 , an immediate orange colour was produced in all the samples, but no signals were observed. After about 15 min. the solutions were pale yellow. PPPL gave a blue colour after 4 days, but with no signals.

(e) The system $\text{AgClO}_4 / \text{C}_6\text{H}_6 / \text{CH}_3\text{NO}_2$

This system had been used previously to prepare the cations of the

anions and methoxy substituted triphenylphosphines.¹⁰⁵ AgClO_4 was placed in A, with the phosphole in a side-arm. Benzene was distilled into A and the AgClO_4 dissolved to give the complex. CH_3NO_2 was then distilled in, the solution warmed and the phosphole dissolved. No colour changes or signals were observed. After 12 hrs. a yellowish solid was deposited.

(f) The System $\text{CF}_3\text{CO}_2\text{H} / \text{CH}_3\text{NO}_2$

Sufficient CH_3NO_2 was distilled into A to make a 10^{-3} molar solution. Varying amounts of $\text{CF}_3\text{CO}_2\text{H}$ were distilled in, but no colour changes or signals were seen.

5. Radical Ions from Phosphorins

Since the preparation of radical ions from some phosphorins had previously been investigated by Dimroth et al.,⁵⁷⁻⁵⁹ it was decided to prepare and investigate closely the anions and cations of three representative phosphorins (Fig. 3) by the simplest methods available: potassium reduction to the anions, and lead tetraacetate oxidation to the cations. Little time was spent on investigating the effect of factors such as alkali metal, solvent or temperature. All preparations were performed at room temperature.

A. Anions: /

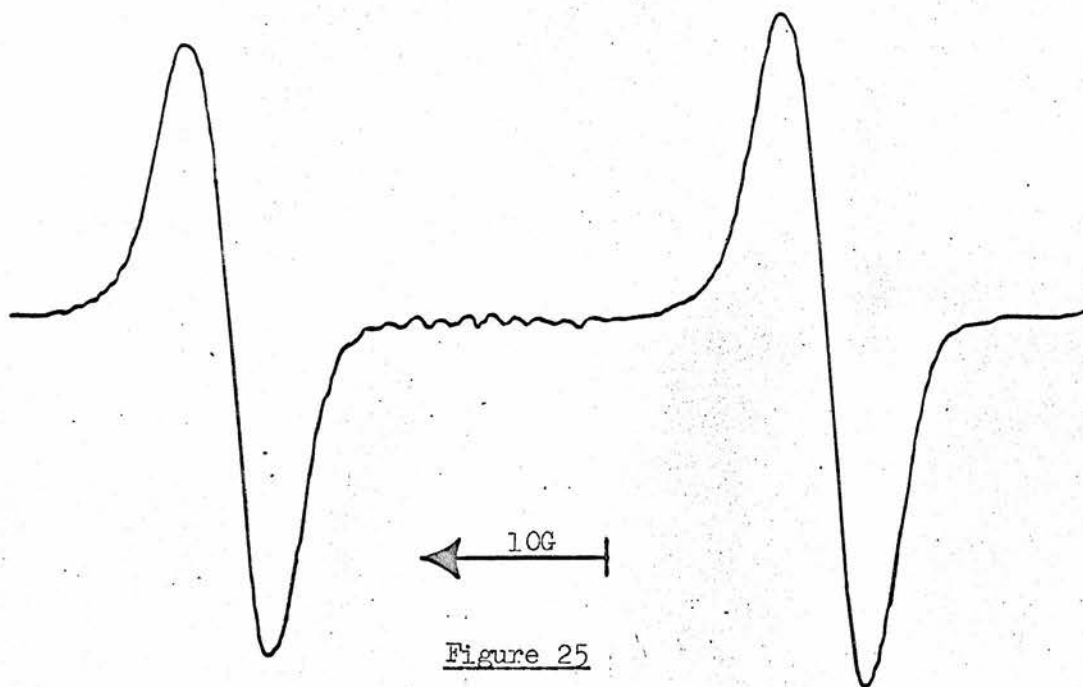


Figure 25

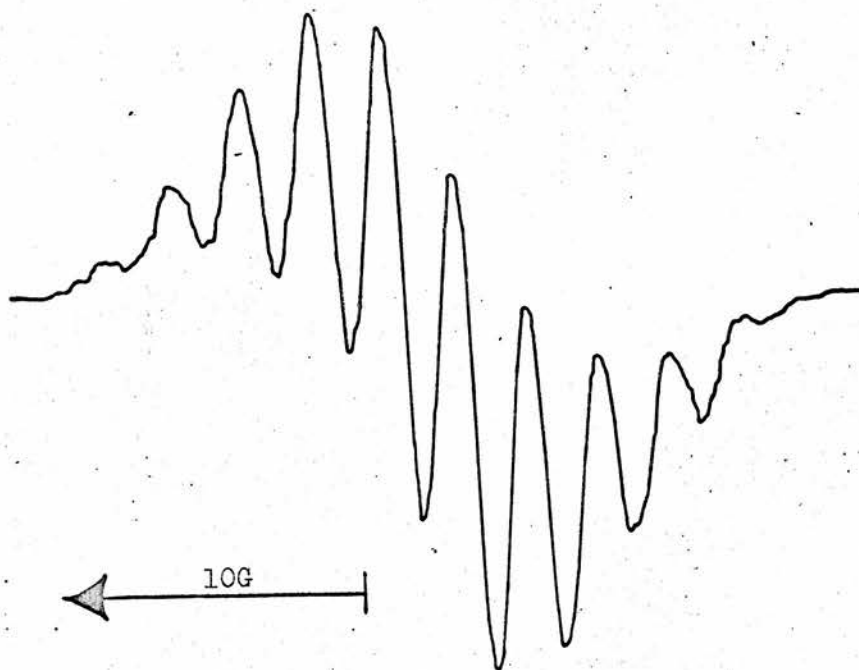


Figure 26

A. Anions:

(a) Reaction of 2,4,6-Triphenylphosphorin
with K in DME and THF

The reaction sequence was as observed by Dimroth.⁵⁸ Rapid reaction gave a dark green solution exhibiting an intense, featureless doublet ESR signal (Fig. 25). No fine structure could be seen under any conditions. Measurement against Frémy's salt gave

$$a_p = 32.90 \pm 0.15G$$

$$\text{line-width} = 4G$$

$$g = 2.0044 \pm 0.0001$$

Lowering the temperature to -60° increased the line-width to 4.8G but no other changes were apparent. At all temperatures, the line-width of the lowfield peak was slightly less than that of the highfield peak.

On further reaction with potassium, the signal disappeared and the green solution changed to a red, diamagnetic solution, which Dimroth attributed to the dianion stage. Further reaction gave a dark blue-green solution, with a new, intense signal (Fig. 26), which Dimroth attributed to the trianion stage. This signal consisted of 11 equally spaced lines, but the intensities did not correspond to 10 equivalent protons. There was no obvious phosphorus doublet splitting. Measurement against Frémy's salt gave

$$a = 2.36 \pm 0.06G \text{ (11)}$$

$$\text{line-width} = 1.2G$$

$$g = 2.0027 \pm 0.0001$$

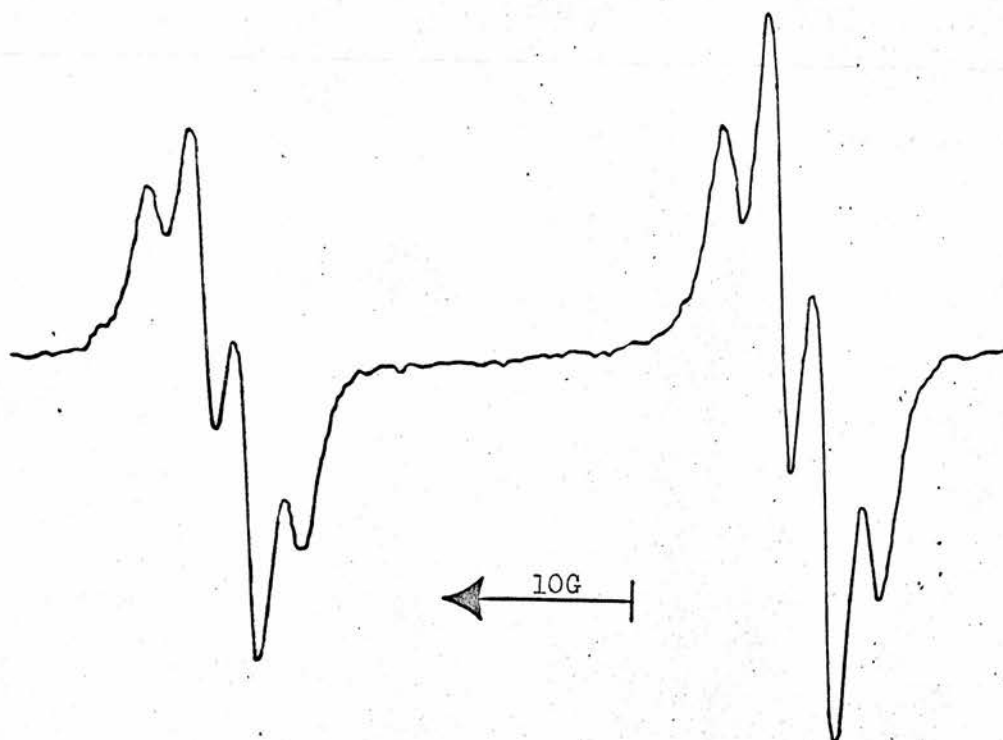


Figure 27

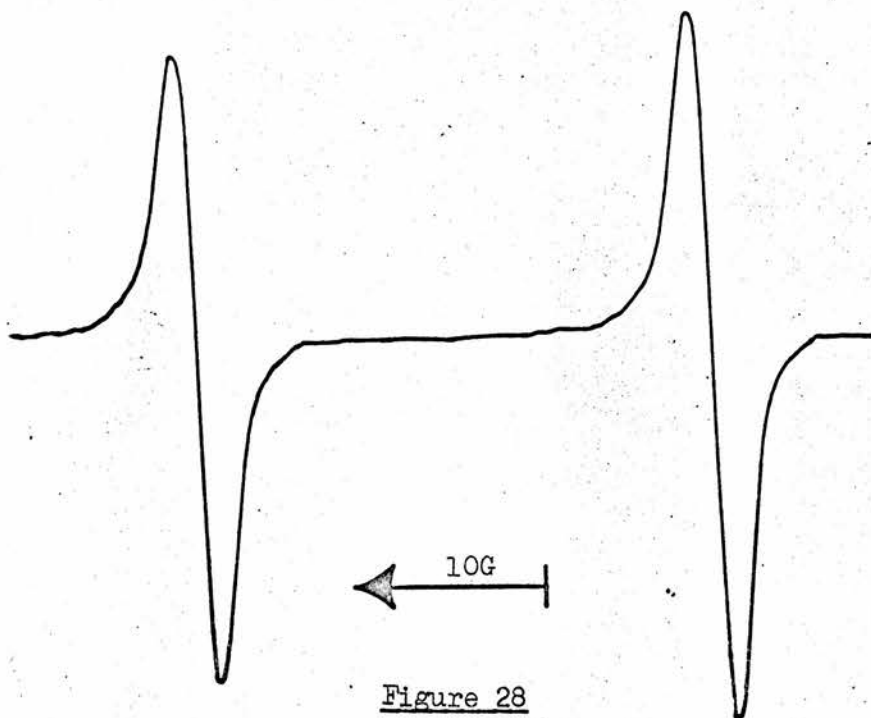


Figure 28

No further resolution could be seen under any conditions.

The poor resolution of both these signals gives little information on the spin distributions in these radicals. The only significant feature is the large phosphorus splitting in the monoanion compared with the trianion; the 2.36G splitting in the latter may be a proton or a phosphorus splitting.

(b) 2,6-Ditertiarybutyl-4-phenylphosphorin
with K in DME and THF

Reaction was rapid and gave a dark green solution with an intense ESR signal (Fig. 27), consisting of a doublet, each component being split into 4 lines. As with the TPPN anion, the line-width of the lowfield peak was distinctly lower than that of the highfield peak. At slow sweep speeds and high dilution, a further splitting was evident on some of the peaks, but the number of lines could not be ascertained. Measurement against Frémy's salt gave

$$a_1 = 30.40 \pm 0.1\text{G} \quad (2)$$

$$a_2 = 2.36 \pm 0.07 \quad (4)$$

$$a_3 \doteq 0.6\text{G}$$

$$\text{line-width} \doteq 0.5\text{G}$$

$$g = 2.0045 \pm 0.0001$$

On further reaction, the signal disappeared after about 15 min. and the solution became red; no further signals appeared on prolonged

contact. By analogy with TPPN, this must be the diamagnetic dianion stage.

The large splitting can be assigned to the phosphorus nucleus. The quartet splitting from 3 equivalent protons may be assigned to either positions 3, 5, 10 or positions 8, 10, 12 (Fig. 3). The small splitting would then arise from positions 8, 12 or 9, 11 in the former case, or positions 3, 5 or 9, 11 in the latter case. McLachlan calculations (Chapter III) suggest that the quartet could arise from 3, 5, 10 and the small splitting from 8, 12. However, as described in this chapter, some doubt can arise from this assignment.

(c) 2,4,6-Tritertiarybutylphosphorin with K
in DME and THF

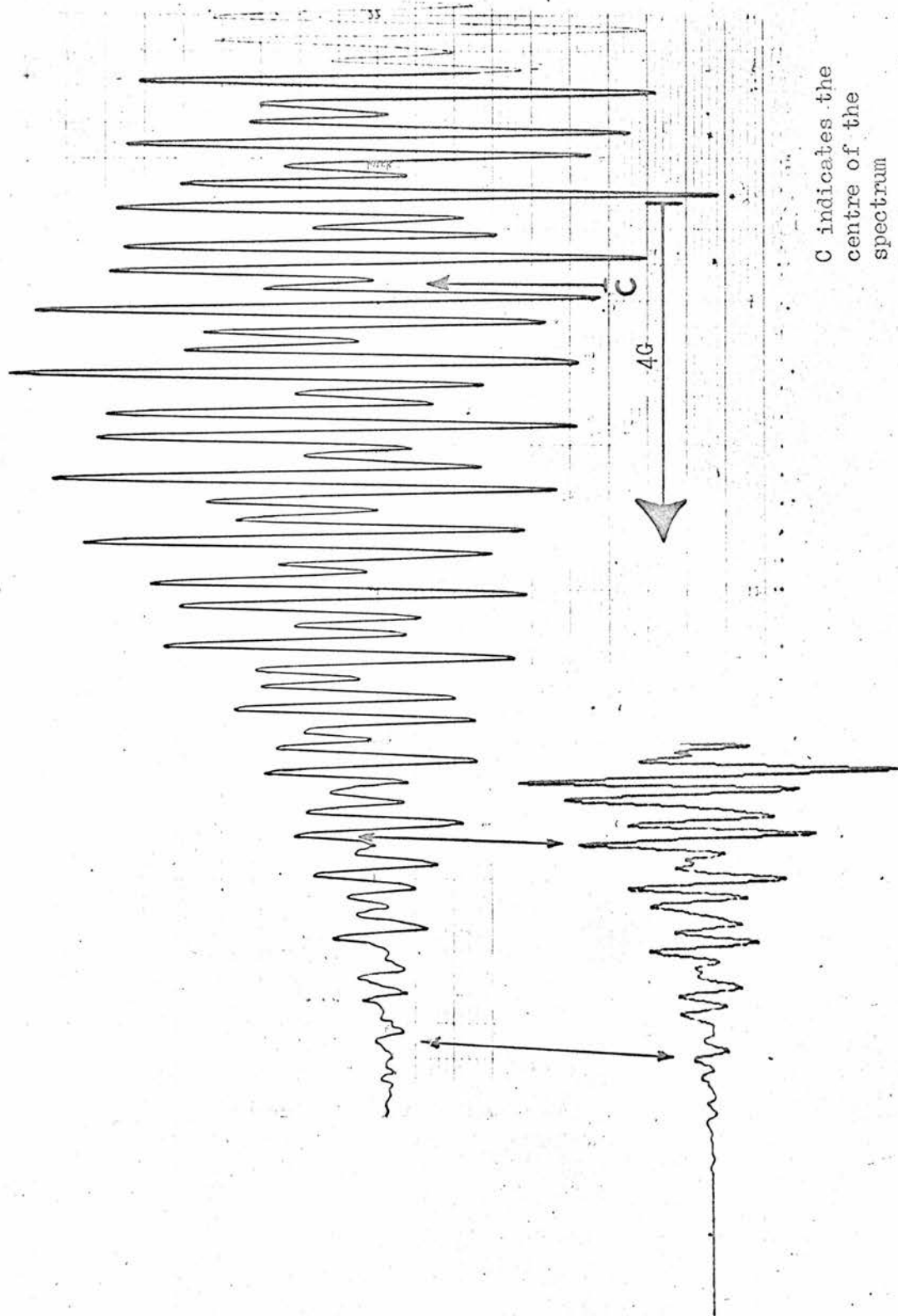
Reaction was fast, giving a green solution with a medium ESR signal (Fig. 28) which disappeared after about 1 hr. to give a pale green solution. No further signals were seen on prolonged contact with potassium. The signal consisted of a featureless doublet, and no further resolution could be seen under any conditions. Measurement against Frémy's salt gave

$$a_P = 26.91 \pm 0.15G$$

$$\text{line-width (lowfield peak)} = 2.1G$$

$$\text{line-width (highfield peak)} = 2.3G$$

The splitting constants from positions 3, 5 must be less than 2.1G, the width of the narrowest peak. The low value is supported



C indicates the
centre of the
spectrum

Figure 29

by McLachlan calculations (Chapter III). It is interesting to note that TPPN can undergo 3-electron addition, DTBPPN can undergo 2-electron addition and TTBPN can undergo only 1-electron addition; this order parallels the extent of the delocalised π system.

B. Cations

(a) TPPN with $\text{Pb}(\text{OAc})_4$ in DME and THF

Reaction at room temperature gave a pale yellow-green solution exhibiting an intense doublet ESR signal, which reached maximum strength after about 30 min. (The radical was stable for several days at room temperature.) Each component consisted of at least 40 lines, separation 0.3G, with an even intensity distribution. On lowering the temperature to -50° , and diluting the sample until colourless, many of the lines split further to give a better resolved, complex spectrum of at least 72 lines. One half of one component of this spectrum is shown in Figure 29. This spectrum was much better resolved than that published by Dimroth,⁵⁷ who apparently prepared the radical under nitrogen. High gain conditions did not show any clear outside lines. Measurement against Frémy's salt gave

$$a_p = 24.21 \pm 0.06\text{G} \quad (2)$$

$$\text{line-width} \doteq 0.09\text{G}$$

$$\text{spread} \doteq 18.8\text{G} \quad (\text{each component})$$

$$g = 2.0022 \pm 0.0001$$

The complexity and incomplete resolution of this spectrum did not permit any easy analysis. However, by preparing the cation of the corresponding phosphorin deuterated in the phenyl rings at 2, 6, Dimroth found $a_3 = a_5 = a_8 = a_{10} = a_{12} = 2.4\text{G}$. These equalities are analogous to those found in the spectrum of the 2,4,6-triphenylphenoxy radical,¹²² with $a = 1.75\text{G}$, and it was therefore considered likely that the spin distributions of these two radicals would be similar. Measurements of the outermost visible lines suggested possible splittings of about 0.7G and 0.5G , and by analogy with the phenoxy radical the former was assigned to positions 9, 11, 14, 16, 18, 20, 22, 24, and the latter to positions 13, 15, 21, 23. These sets of assignments were also supported by the McLachlan calculations.

A large number of computer simulations were performed, keeping the 2.40G splitting constant and varying the other two splittings, but no exact fit could be found. However, a simulation of the outer 13 lines was achieved using

$$a_1 = 2.40\text{G} \quad (6)$$

$$a_2 = 0.70\text{G} \quad (9)$$

$$a_3 = 0.50\text{G} \quad (5)$$

$$\text{line-width} = 0.10\text{G} \quad (\text{see inset, Fig. 29})$$

The inner lines did not give a good fit; this suggests that a_2 and a_3 are close to the true values but that the value of a_1 is in error. This may be expected, since the line-width of the deuterated cation would not permit accurate measurement of this splitting, and would

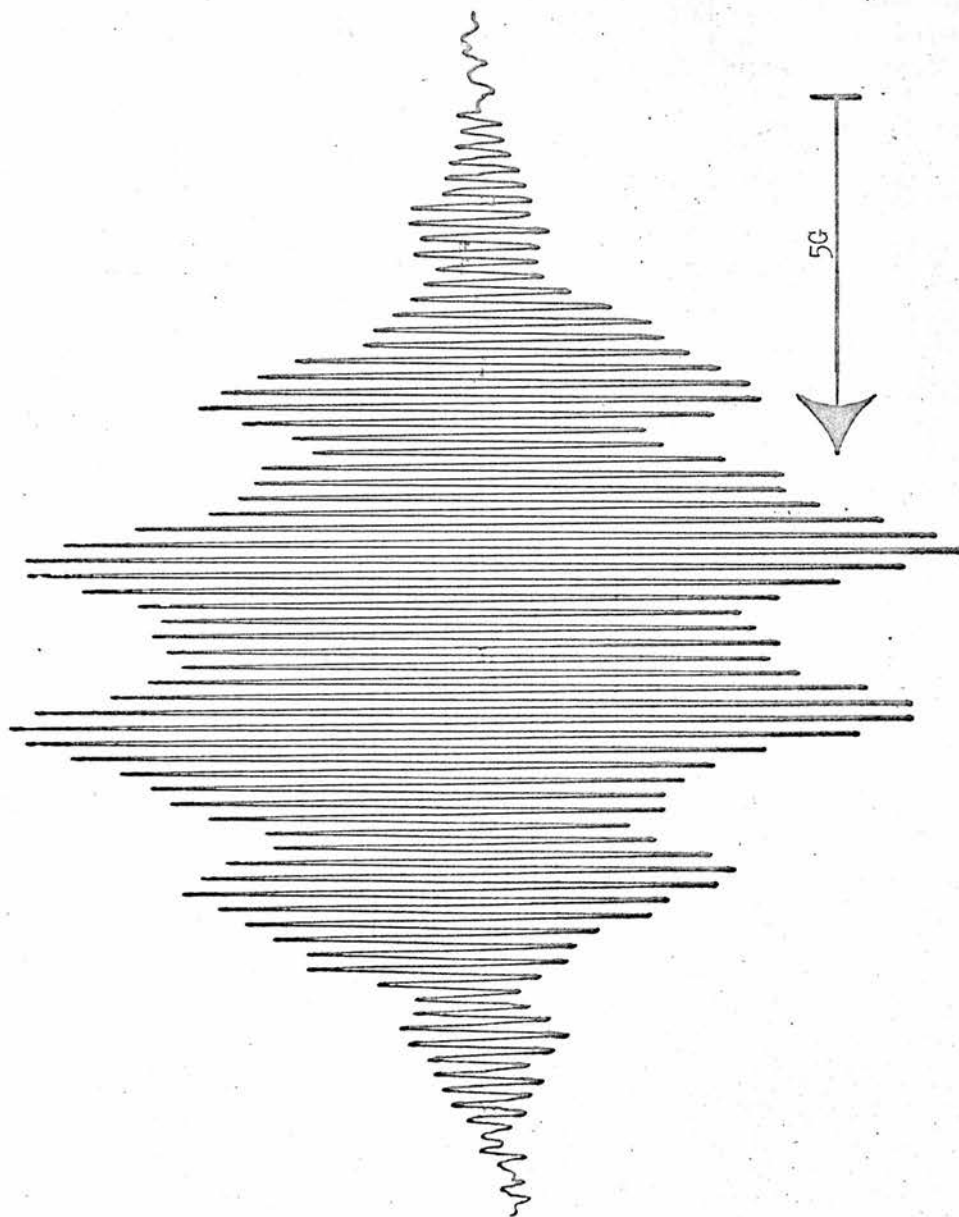


Figure 30

also hide any small differences in the splittings at the various positions. (It should also be noted that Dimroth's paper does not state which solvent was used.) The simulated spread of 19.2G, compared with the observed spread (measured between the same outer lines) of 18.8G, confirms that these assignments are reasonably close to the true ones. In the time available, however, no fit could be found by varying the 2.40G splitting.

The small values of the splittings in the 2,6-phenyl groups suggest that, like the phenoxyl, these groups are pushed more out of the plane of the ring than is the 4-phenyl group.

(b) DTBPPN with $\text{Pb}(\text{OAc})_4$ in DME and THF

Reaction at room temperature gave a pale yellow solution, with a doublet ESR signal, one component of which is shown in Figure 30. This built up into an intense signal after about 1 hr., and was present for several days at room temperature. Each component was split into at least 76 lines, arranged in 6 groups with relative intensities 1:5:10:10:5:1, in agreement with 5 equivalent protons. Within each group the intensities varied smoothly; this made measurement of the group splitting difficult. High gain conditions did not show any clear outside lines. Measurement against Frémy's salt gave

$$a_P = 24.14 \pm 0.09\text{G} \quad (2)$$

$$a_1 = 2.33 \pm 0.06\text{G} \quad (6)$$

$$a_2 = 0.21 \pm 0.04\text{G}$$

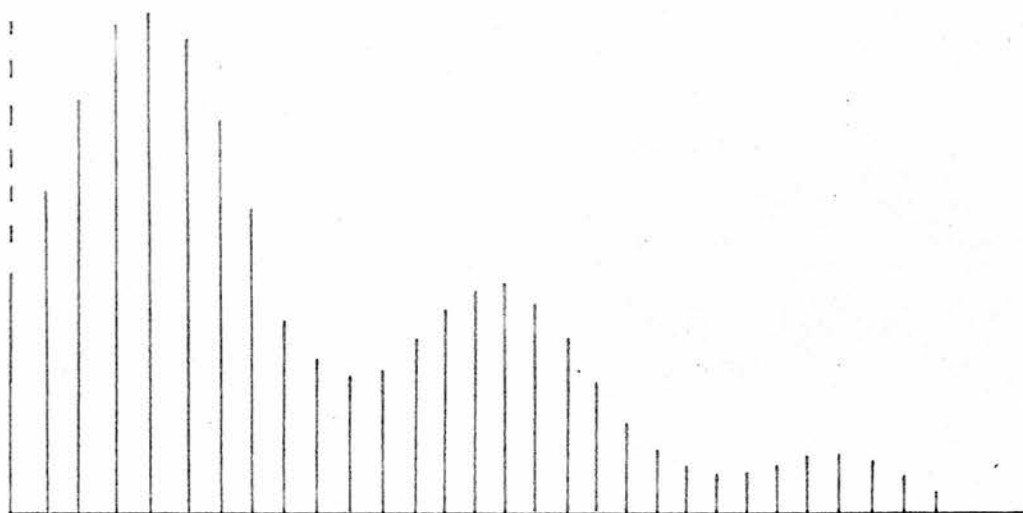


Figure 31

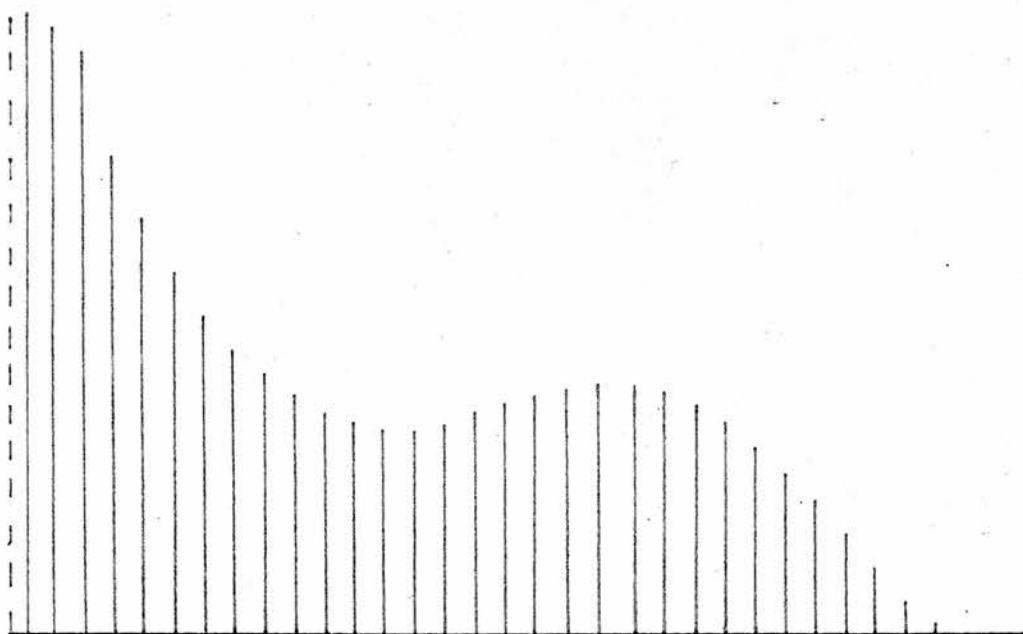


Figure 32

$$\text{line-width} \doteq 0.09\text{G}$$

$$\text{spread} \doteq 16\text{G (each component)}$$

$$g = 2.0020 \pm 0.0001$$

At slow sweep speeds, low modulation amplitude (0.03G) and high dilution, further lines with a separation of about 0.06G were just visible. Resolution did not improve in the temperature range -60° to $+40^{\circ}$.

The 2.33G splitting may be assigned to equivalent protons at positions 3, 5, 8, 10, 12; this splitting was reported by Dimroth⁵⁹ to be 2.5G. The large number of fine lines must arise from the 18 t-butyl protons and the 2 protons at 9, 11; sweeps at higher modulation amplitudes did not show any triplet splitting attributable to the latter protons. Assuming the 0.21G splitting to be from the t-butyl protons, line simulations showed that the splitting from 9, 11 must be approximately a small, integer multiple of this value. Multiples of 1, 2 and 3 (i.e. 0.21G, 0.42G, 0.63G) gave the correct curve envelope, and the value 0.63G gave the closest intensity ratios (Fig. 31). Multiples of 4 and above gave incorrect envelopes.

This combination of splittings predicted a spread of 16.6G, compared with the observed spread of 15.8G. Owing to the low relative intensity of the outside line compared with that of the central line - a ratio of 1:48,620 - some of the outside lines will not be visible: hence the lower value for the observed spread. The fine separation of 0.06G must arise from incomplete overlap of some of the lines.

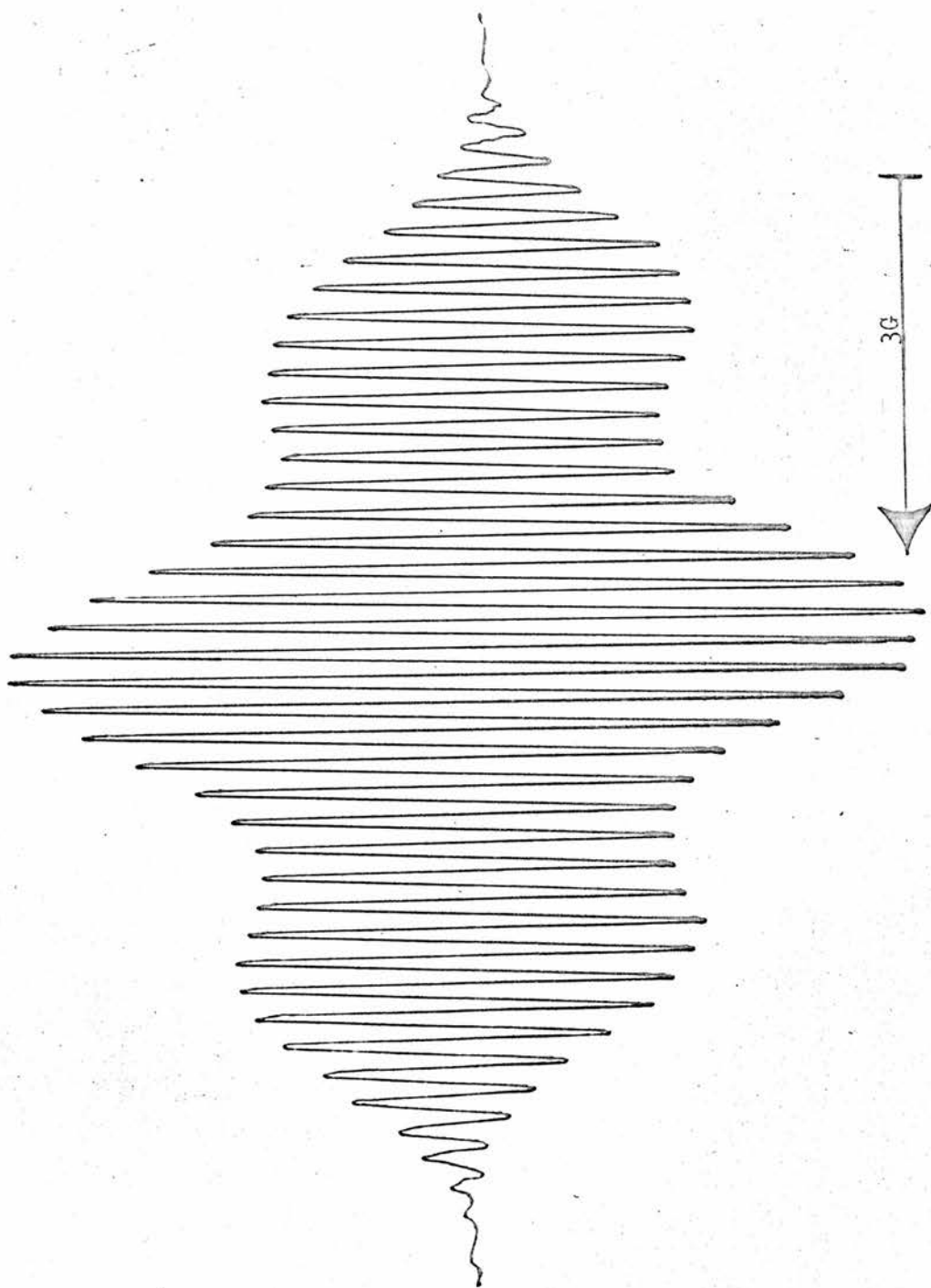


Figure 33

(c) TTBPN with $\text{Pb}(\text{OAc})_4$ in DME and THF

Reaction was slower than with the other phosphorins, taking about $1\frac{1}{2}$ hrs. to initiate; the medium signal obtained was at maximum intensity after about 3 hrs., and was stable for several days at room temperature. The spectrum (one component of which is shown in Figure 33) consisted of a doublet, each component being split into at least 42 lines arranged in three groups; the relative intensities of 1:2:1 indicated 2 equivalent protons. The central lines were all of similar intensity, making measurement of the group splitting difficult. High gain conditions did not show any clear outside lines. Measurement against Frémy's salt gave

$$a_P = 26.70 \pm 0.08G \quad (2)$$

$$a_1 = 2.62 \pm 0.06G \quad (3)$$

$$a_2 = 0.23 \pm 0.03G$$

$$\text{line-width} \doteq 0.1G$$

$$\text{spread} \doteq 11G$$

$$g = 2.0021 \pm 0.0001$$

Under high resolution conditions, lines with a separation of about 0.05G were just visible, about the resolution limit for 100 Kc. detection. The 2.62G triplet can be assigned to the meta-protons at 3, 5. As with the cation of DTBPPN, the smallest splitting of 0.21G can be assigned to the 18 ortho-*t*-butyl protons. The form of the spectrum indicates that the splitting from the 9 para-*t*-butyl protons must be approximately a small integer multiple of 0.23, and line

simulations were performed with the values 0.23, 0.5 and 0.7. The value of 0.5 gave the best envelope and intensities (Fig. 32). The fine separation of 0.05G would then arise from incomplete overlap.

These splitting constants predict a spread of 13.9G; if the lower limits (within experimental error) are used, a spread of 12.6G; this is still considerably larger than the observed 11.0G. This can be understood by considering the intensities of the outer lines in a system in which 10 lines are split by 19 lines; the outermost line is a factor of the order of 10^6 smaller than the innermost lines. Therefore, a considerable number of the outer lines will not be visible.

It is interesting to compare the t-butyl splittings with those in the 2,4,6-tritertiarybutylphenoxy radical.¹²³ The corresponding splittings are 0.07G for the ortho groups and 0.37 for the para groups. The authors attributed the low ortho splitting to interaction with the oxygen, and considered the Q-value of the para-t-butyl group of 0.84G to be the "true" Q-value. (This Q was estimated from spin densities calculated for 2,4,6-trimethylphenoxy.) No such interaction can occur directly in this phosphorin radical, and the ortho splitting is consequently much higher. Comparison with McLachlan spin densities (Chapter III) gives Q-values of 0.75G for the ortho and 2.0G for the para. These values are in reasonable agreement considering that small changes in the McLachlan input parameters cause large changes in spin densities at the 2, 4, 6 positions.

CHAPTER III

SPIN DENSITY CALCULATIONS

	Page
1. <u>π-Electron Calculations</u>	77
(a) The Simple Hückel Method	77
(b) The McLachlan Method	80
(c) Computer Programme	84
(d) Choice of Parameter Values	85
(e) Results	90
(i) TTBPn anion and cation	90
(ii) DTBPn anion and cation	92
(iii) TPPn anion and cation	94
(iv) MeDPPL anion	96
(v) TPPL anion	98
(vi) Others	99
2. <u>All-Valence Electron Calculations</u>	100
(a) The CNDO Theory	101
(b) Computer Programme	104
(c) Results	108
(i) PH, PN, PO, PH ₃ , PF ₃	115
(ii) PH ₂ , NH ₂	116
(iii) PF ₂ , NF ₂	116
(iv) PCl ₂	117
(v) PF ₄ ⁺ , PF ₄ ⁻	117
(vi) PF ₄	117
(vii) PCl ₄	118
(viii) PO ₂	118
(ix) PO ₃	118
(x) PO ₃ ²⁻	119
(xi) PO ₄ ²⁻	119
(xii) HPO ₂ ⁻ , FPO ₂ ⁻	119
(xiii) Phosphorins	120
(xiv) Phospholes	121

In this chapter, the calculation of spin densities in various radical species is outlined. These were performed with the intention of obtaining information on the electronic and geometric structures of the

radicals, and also with a view to estimating Q-values for phosphorus.

The Hückel and McLachlan π -electron calculations are reviewed first, followed by the results of the calculations on phosphorin and phosphole radical ions. In the second section, Pople's CNDO all-valence electron method is reviewed. As explained in this section, it proved desirable to test the programme on small phosphorus radicals and model systems; the results of these calculations are also presented.

More comprehensive treatments of Hückel theory are to be found in books by Streitwieser¹²⁴ and Pilar.¹²⁵ The McLachlan method has not been reviewed as extensively; the best source is McLachlan's original paper,¹²⁶ and a review has appeared in a book by Memory.¹²⁷ For CNDO and related theories, the best sources are the original papers¹²⁸ and a recent book by Pople and Beveridge.¹²⁹

1. π -Electron Calculations

(a) The Simple Hückel Method

As outlined in Chapter I the Hückel method is a simple π -electron method assuming σ - π separability. It is possible to write Roothaan's equations¹³⁰ in terms of a set of π molecular orbitals, each of which is constructed from linear combinations of suitable atomic orbitals. Solution of these equations would then provide a set of SCF π -MO's. In the Hückel method, no attempt is made at exact solution, and the

elements of the π Hartree-Fock matrix F_{π} are simply "guessed". The AO's used are carbon 2pz orbitals, and the problem lies in solving the determinant

$$\det (F_{\pi} - \epsilon \Delta) = 0 \quad . . . (31)$$

where each element has the form $F_{rs} - \epsilon \Delta_{rs}$; F_{rs} is the matrix element of the Hartree-Fock operator in the π basis, Δ_{rs} is the overlap integral and the ϵ are the Hartree-Fock eigenvalues.

F_{π} is defined by

$$F_{\pi} = h^{\text{core}} + \sum_j (2J_j - K_j) \quad . . . (32)$$

where h^{core} is a core hamiltonian including the kinetic energy of the π electrons, the nuclear- π attractions, and coulombic and exchange interactions between pairs of electrons, one σ and one π . J_j and K_j are coulomb and exchange operators respectively, and represent the coulomb and exchange interactions between the π electrons.

This may also be written

$$F_{\pi} = h^{\text{core}} + G_{\pi} \quad . . . (33)$$

Explicit evaluation of these matrix elements would involve calculation of a large number of integrals. In order to avoid this complexity, no attempt is made in the Hückel method to evaluate the F_{π} ; for conjugated hydrocarbons, values are given as follows:-

$$\begin{aligned} F_{rr} &= \alpha_r \\ F_{rs} &= \begin{cases} \beta_{rs} & \text{for nearest neighbours} \\ 0 & \text{otherwise} \end{cases} \quad r \neq s \quad . . . (34) \end{aligned}$$

α_r and β_{rs} are known as the coulombic and resonance integrals, and are regarded as empirical parameters, α_r being characteristic of the r th atom and β_{rs} being characteristic of the rs bond. The overlap integrals are usually neglected unless $r=s$

$$A_{rs} = \delta_{rs} \quad . . . (35)$$

(A_{rs} for nearest neighbours is sometimes given the calculated value of 0.25). This approximation has been shown to be reasonable provided all the resonance integrals are considered equal. The total energy can then be written

$$\begin{aligned} E &= \sum_i n_i \epsilon_i - \sum_i \langle \pi_i | G_{\pi} | \pi_i \rangle \\ &= \sum_i n_i \epsilon_i + G \quad . . . (36) \end{aligned}$$

where n_i is the occupation number of the i th orbital and ϵ_i is the energy of an electron in the i th orbital. G is regarded as a constant term or, more usually, as zero. Setting G equal to zero is, in effect, neglecting all electron repulsions.

The charge density — bond order matrix is then

$$P_{rs} = \sum_j n_j c_{rj} c_{sj} \quad . . . (37)$$

and the spin densities are

$$p_r = c_{ro}^2 \quad . . . (38)$$

where c_{ro} refers to the orbital of the unpaired electron.

Although the theory is not strictly valid for heteroatoms, these are usually treated by changing the values of the appropriate α_r and

β_{rs} by

$$\begin{aligned}\alpha_r &= \alpha + h_r \beta \\ \beta_{rs} &= k_{rs} \beta\end{aligned}\quad \dots (39)$$

where h_r , k_{rs} are empirical parameters, and α , β are reference integrals. The choice of these parameters for phosphorus is discussed in Section (d).

The neglect of interelectronic interactions means that Hückel theory predicts all spin densities to be positive, as can be seen from equation 38. However, negative spin densities are known to occur in many radicals, as was first shown by NMR studies on the pyrene anion.¹³¹ A comparatively simple modification of the method, the McLachlan method,¹²⁶ does introduce the necessary electron correlation in an approximate way, and is discussed in the next section.

(b) The McLachlan Method

This method is based on the SCF formalism, in which each electron moves in the potential field of the nuclei and the self-consistent field formed by the averaged fields of the other electrons.

Two types of wave function are commonly used; in the RHF (Restricted Hartree-Fock) method, the wave function takes the form

$$\Psi = |\psi_1^2 \psi_2^2 \dots \psi_n^2 \psi_0| \quad \dots (40)$$

in which the $2n$ electrons, spins α and β , occupy the orbitals $\psi_1 \dots \psi_n$ in pairs, and the unpaired electron (spin α) occupies ψ_0 . Ψ is then an eigenfunction of S^2 , the total spin angular momentum operator. As

in Hückel theory, solution of Roothaan's equations gives π spin densities which are the squares of the coefficient of the unpaired orbital; therefore negative spin densities again cannot be calculated.

The McLachlan method, however, uses the UHF (Unrestricted Hartree-Fock) formalism, in which the wave function takes the form

$$\Psi = |\psi_1^\alpha \psi_1^{1\beta} \dots \psi_n \psi_n^{1\beta} \psi_0^\alpha| \quad \dots (41)$$

in which the electrons of spin α and β occupy different, orthonormal sets of orbitals $\psi_1 \dots \psi_n, \psi_1^1 \dots \psi_n^1$, with the unpaired electron of spin α in ψ_0 . (Unfortunately, this wave function is no longer an eigenfunction of S^2 , being contaminated by states of multiplicity higher than 2. The most important contaminating states may be removed by application of a projection operator,¹³² giving somewhat better spin densities.)

In this formalism, the spin density is

$$\rho = |\psi_0|^2 + \sum_i (|\psi_i|^2 - |\psi_i^1|^2) \quad \dots (42)$$

so that ρ can become negative at a node of ψ_0 . The orbitals ψ_i, ψ_i^1 are expressed in terms of π atomic orbitals

$$\psi_i = \sum_s c_{is} \phi_s, \quad \psi_i^1 = \sum_s c_{is}^1 \phi_s \quad \dots (43)$$

The coefficients are determined by the elements of the Fock matrices F and F^1 , where

$$\begin{aligned}
 F &= V + K - J, \quad F^1 = V + K - J^1 \\
 \text{with } V_{rs} &= \beta_{rs} - \delta_{rs} \sum_{t \neq r} \delta_{rt} \\
 & \quad (= \text{field of core of nuclei and } \sigma \text{ electrons}) \\
 K_{rs} &= \delta_{rs} \sum_t (P_{tt} + P_{tt}^1 + P_{tt}^0) \delta_{rt} \\
 & \quad (= \text{coulomb field of all } \pi \text{ electrons}) \\
 J_{rs} &= (P_{rs} + P_{rs}^0) \delta_{rs}, \quad J_{rs}^1 = P_{rs}^1 \delta_{rs} \\
 & \quad (= \text{exchange fields for } \pi \text{ electrons of } \alpha, \beta \text{ spin})
 \end{aligned} \tag{44}$$

(The integral notation is that of Pariser and Parr.¹³³) The bond order matrices are defined by

$$P_{rs} = \sum_i c_{ir} c_{is}, \quad P_{rs}^1 = \sum_i c_{ir}^1 c_{is}^1, \quad P_{rs}^0 = c_{or} c_{os} \dots \tag{45}$$

The difference between F and F^1 is therefore due to the exchange field $J - J^1$ of the odd electron.

In a perturbation treatment, McLachlan starts with the SCF orbitals of the neutral molecule as a zero-order approximation. For alternant molecules, $P_{rr} = P_{rr}^1 = \frac{1}{2}$, and for atoms in the same set, $P_{rs} = P_{rs}^1$. For an ion, F then starts with the values

$$\begin{aligned}
 F(o)_{rr} &= \beta_{rr} + \frac{1}{2} \delta_{rr} \\
 F(o)_{rs} &= \beta_{rs} + P(o)_{rs} \delta_{rs}
 \end{aligned} \dots \tag{46}$$

To first order, this gives

$$J(1)_{rs} - J(o)_{rs} = P^0(o)_{rs} \delta_{rs} = G_{rs} \dots \tag{47}$$

where G_{rs} , the exchange potential of the odd electron, causes electrons

of α and β spin to move in different orbitals, and alters the spin density by changing the values of the coulomb integral α_r and the resonance integrals β_{rs} for electrons of α spin. A similar result holds for neutral radicals. The perturbed spin density is then given by

$$\rho_{rs} = \rho(o) - \frac{1}{2} \sum_{tu} \pi_{rs,tu} G_{tu} \quad . . . (48)$$

where the $\pi_{rs,tu}$ are polarizability coefficients.¹³⁴ All the atom-bond polarizabilities are neglected, and the χ_{rr} are assumed equal, giving

$$\rho_r = c_{or}^2 - \frac{1}{2} \chi_{rr} \sum_s \pi_{rs} c_{os}^2 \quad . . . (49)$$

McLachlan shows Hückel orbitals to be satisfactory, providing the resonance integral is suitably chosen; in fact, the term $\frac{1}{2}\chi$ is replaced by $\lambda = \frac{1}{2}\chi/\beta$, where β is the average of the quantities

$$\beta_{rs}(\text{eff}) = \beta_{rs} - \frac{1}{2} P_{rs} \chi_{rs} \quad . . . (50)$$

for all bonds in the molecule. Using Pariser and Parr's values for the integrals,¹³³ λ has the value 1.2. In practice, values from 1.0 to 1.2 have been commonly used.

In order to avoid calculation of the π_{rs} , equation 42 is used in practice, $\psi_0, \psi_1^1 \dots \psi_n^1$ being the Hückel orbitals and $\psi_1 \dots \psi_n$ being calculated with β_{rs} unchanged but with $\alpha_r = 2\lambda c_{or}^2 \beta$.

As in simple Hückel theory, heteroatoms are treated by modifying the values of the coulomb and resonance integrals by the h, k parameters.

As may be seen from the above, there are several approximations involved which hold strictly for only alternant hydrocarbons, involving values of the bond order matrices, polarizabilities and integrals. The most serious potential defect, however, is that for radicals with high negative spin densities the perturbation may no longer be regarded as small. Despite this, however, this theory has been used successfully with many systems, including systems with heteroatoms. When dealing with second-row heteroatoms, as in the following calculations involving phosphorus, 3p and not 2p orbitals are being used on the heteroatom. In this work, this effect is assumed to be included in the parameterisation.

In the following sections, only the McLachlan spin densities are presented. The Hückel spin densities were, in general, much poorer; for instance, predicting near-zero spin densities at the 3,5 positions of the phosphorin cations. Agreement was also poorer in the calculations on phospholes.

(c) Computer Programme

The McLachlan calculations were performed on an IBM 360/44 computer, using a programme written by D.H. Levy in Fortran II for an IBM 7090,¹³⁵ and suitably modified for the 360 by Dr. C. Thomson. Input data included the constant λ and the non-zero elements of the initial secular determinant. Output included the Hückel eigenvalues, eigenvectors and spin densities, followed by the McLachlan spin densities

for both the cation and the anion.

(d) Choice of Parameter Values

Although much work has been performed on parameter values for other heteroatoms,¹²⁴ little work has been published on values for phosphorus. Below is reviewed the past work, followed by the estimation of ranges of initial guesses for this work.

In a Hückel-type treatment, Brown¹³⁶ estimated the h and k parameters for phosphorus in the phosphole system. The π system consisted of $2p_z$ orbitals on the carbons, and a $3p_z$ orbital on phosphorus. The h parameter was estimated assuming a proportionality to the difference between the electronegativities of phosphorus and carbon,

$$h_P = M(\chi_P - \chi_C) \quad . . . (51)$$

The electronegativities were calculated from ionisation potentials and electron affinities, which in turn were calculated from cycles of transition energies between appropriate states. The parameter k was calculated assuming a proportionality between the resonance integral and the overlap integral; these considerations gave

$$h_P = 1.36$$

$$k_{CP} = 1.13$$

Little comparison was made between the theoretical results and experimental evidence owing to lack of experimental results at the time of

publication. Similar calculations were also performed with dxz , dyz orbitals on the phosphorus, the small parameter values obtained suggested that these orbitals were relatively unimportant.

In their paper on the anion radicals of phosphines,⁵⁴ Cowley and Hnoosh performed Hückel calculations on the anions prepared (Fig. 34). No details of the calculations were given, but the h and k parameters used⁵⁵ were

$$\begin{aligned} h_O &= 2.0, \quad h_P = 0.5, \quad h_N = 0.5 \\ k_{PO} &= 0.7, \quad k_{PN} = 0.5, \quad k_{PC} = 1.25 \end{aligned}$$

The Hückel spin densities are shown in Table II, the experimental spin densities being calculated from the McConnell relationship using the Q_{CH}^H values in the last column. In general, the agreement is very good. However, the anion A^- , which Hanna⁹⁷ had identified from the reaction of TPP with potassium, was later shown by Britt and Kaiser⁹⁸ to be the ion Ph_2PK^- . The good agreement here, then, is purely fortuitous, and would seem to cast doubt on the significance of the agreement for the other radicals.

The only other parameter values published have been those of Vilceanu et al.,¹³⁷ in Hückel calculations, including 3d orbitals, on 1,1-disubstituted phosphorins (phosphabenzene)s. The models tried, together with parameter values, are shown in Table III. The Fukui model¹³⁸ is a simple Hückel model, using one π electron and a d^3s hybrid. The Anti-Hückel model corresponds to Craig's phosphonitrilic structure,¹³⁹ with a dxy orbital involved, making the resonance

TABLE II

Phosphine	Position	a_i (G)	r_i (obs)	r_i (exp)	Q(G)
A ⁻	1(P)	7.8	-	.22	28.5
	3	2.4	.084	.085	
	4	.1	.003	.0003	
	5	2.4	.084	.086	
B ⁻	2(P)	5.25	-	.21	23.0
	4	1.75	.076	.083	
	5	-	-	.0001	
	6	1.75	.076	.084	
C ⁻	2(P)	7.9	-	.285	29.5
	4	2.6	.108	.112	
	5	-	-	.0001	
	6	2.6	.108	.113	
D ⁻	2(P)	8.75	-	.421	29.5
	4	3.50	.118	.106	
	5	-	-	.0001	
	6	3.50	.118	.113	
E ⁻	2(P)	7.2	-	.233	27.0
	4	2.44	.090	.091	
	5	-	-	.0001	
	6	2.44	.090	.091	
	15(N)	4.9	-	.188	
F ⁻	1(P)	5.7	-	.194	28.0
	3	2.2	.078	.077	
	4	.44	.015	.022	

TABLE III

Model	h_p	k_{CP}
I Fukui, strong interaction	-0.6	0.9
II Anti-Hückel	-0.6	0.9, -0.9
III Open chain	-0.6, -0.6	0.9, 0.9
IV Fukui, weak interaction	-3	0.3
V Anti-Hückel, weak interaction	-3	0.3, -0.3

integrals for the two P-C bonds of opposite sign.¹⁴⁰ The open-chain model corresponds to Dewar's allylic model for phosphonitrilics,¹⁴¹ using dxz and dxy hybrids, and halting conjugation at the phosphorus. This model has equivalent phosphorus atoms at each end of the carbon chain. Calculated quantities for models I and III were the only ones that provided the aromatic character observed experimentally (model I was also tested successfully on other phosphorus heterocycles).¹⁴² No parameter optimisations were attempted. Although no calculations were attempted, the authors considered d-orbitals unimportant in trivalent trico-ordinated phosphorus compounds, and suggested the parameters

$$h_P = -0.4$$

$$k_{CP} = 0.9$$

In treating a heteroatom X, distinction must be made between a heteroatom contributing 1 electron to the aromatic system, \dot{X} (e.g. nitrogen in pyridine), and one contributing 2 electrons, \ddot{X} (e.g. nitrogen in pyrrole). These situations correspond to effective nuclear charges of +1, +2 respectively, which means an increased α -value in the latter case. Thus, for phosphorus, h_P for phospholes should be greater than h_P for phosphorins. Streitweiser suggests

$$h_{\ddot{P}} - h_{\dot{P}} \doteq 1 - 1.5$$

Using Brown's value of $h_{\ddot{P}} = 1.36$, this gives $h_{\dot{P}} \doteq -0.2$.

h_X can also be estimated from electronegativities; since both h_X and electronegativities increase with increasing core potential, h_X

may be assumed to be proportional to the electronegativity difference of the two bonded atoms. This is usually expressed as

$$h_x = \chi_x - \chi_c \quad . . . (52)$$

where the χ are Pauling electronegativities. For phosphorus, this gives $h_P = -0.4$, which is comparable to the $h_P^* = -0.2$ above. (This is presumably the same argument as that used by Vilceanu to get $h_P = -0.4$.) In the present work, the initial ranges tried were $h_P = 1.0$ to -1.5 , $h_P^* = 0.5$ to 2.0 .

The resonance parameter is usually taken to be proportional to the overlap integral; since the latter is also a function of bond distance, k will decrease as the bond distance increases. Assuming an approximate phosphonitric bond distance of 1.6\AA for the phosphorin P-C bond, this would suggest $k_{CP}^* < 0.8$. In the present work, the ranges tried were $k_{CP}^* = 1.0$ to 0.3 , $k_{CP} = 0.7$ to 1.5 .

The t-butyl group could be treated either as having a small, negative inductive effect on the adjacent ring carbon, or as a conjugated system.¹⁴³ In the latter, a C-Y-Z model is used with Y the α -carbon and Z a carbon group pseudo-orbital (C_3). This model, however, involves 5 more parameters, each of which would strictly need optimising. The $h_C = -0.45$ parameter was used as a first guess for the inductive model.

Ring twist was treated initially by varying k as $\cos\theta$, θ being the angle of twist. As will be seen, however, it was found that

certain cases needed k greater than 1.

For MeDPPL, both inductive and heteroatom models were considered to describe the P-CH_3 grouping. Owing to the difficulty of additional parameterisation in the latter, only the inductive model was tested thoroughly.

The McLachlan parameter λ was varied between 1.0 and 1.2; the results quoted are for $\lambda = 1.2$.

The numbering schemes are shown in Figures 3 and 14. The experimental spin densities presented in the tables were calculated from the McConnell relationship, using $|q_{\text{CH}}^{\text{H}}| = 25\text{G}$.

(e) Results

(i) TTBPN anion and cation

Initial calculations with $h_{\text{C}} = -0.45$ suggested k_{CP} to be in the range 0.4 to 0.55, h_{P} in the range -0.95 to -0.8. Varying h_{C} gave good agreement between -0.4 and -0.55. Final values were

$$h_{\text{P}} = -0.85, \quad k_{\text{CP}} = 0.45, \quad h_{\text{C}} = -0.45$$

The spin densities are shown in Table IV. The spin densities at position 3 are in excellent agreement for the cation, and are correctly below the highest allowed value in the anion. The spin densities of 0.309, 0.249 at 2,4 are not in the same order as would be expected from the experimental *t*-butyl splittings of 0.23G, 0.5G, giving

effective Q-values of 0.75G, 2.0G. These values would be expected to be the same, but the spin densities at these positions depend critically on the parameter values, and may well be slightly in error. However, the values are reasonably close to the "true" Q-value of 0.8G calculated elsewhere.¹²³ One unusual point is the spin density of greater than 1 on the phosphorus in the anion.

TABLE IV

Atom	Cation		Anion	
	$\rho_i(\text{exp})$	$\rho_i(\text{calc})$	$\rho_i(\text{exp})$	$\rho_i(\text{calc})$
1(P)	-	.329	-	1.067
2	-	.309	-	-.090
3	.105	-.100	<.08	-.012
4	-	.249	-	.136

Calculations were also performed using the conjugated model for the t-butyl groups; the same phosphorus parameters were used, with the t-butyl parameters

$$h_C = -0.45, \quad h_Y = -0.1, \quad h_Z = -0.5$$

$$k_{CY} = 1.0, \quad k_{CZ} = 2.0$$

The results are presented in Table V. The spin distributions are very

TABLE V

Atom	Cation		Anion	
	$\rho_i(\text{exp})$	$\rho_i(\text{calc})$	$\rho_i(\text{exp})$	$\rho_i(\text{calc})$
1(P)	-	.319	-	1.108
2	-	.257	-	-.102
3	.105	-.076	<.08	.008
4	-	.211	-	.087

similar to those in the inductive model; the slightly poorer agreement with experiment is almost certainly due to not optimising the parameters. No attempt was made to do this in the present work.

(ii) DTBPPN anion and cation

Parameters h_P , h_C and k_{CP} were kept as for TTBPB and $k(4,7)$ varied from 0 to 1. However, the spin densities calculated in the phenyl ring in the cation were much too low, and those in the anion much too high. Good agreement could only be found with $k(4,7) > 1$. The results in Table VI use

$$h_P = -0.85, \quad h_C = -0.45, \quad k_{CP} = 0.45, \quad k(4,7) = 1.3$$

TABLE VI

Atom	Cation		Anion	
	$\rho_i(\text{exp})$	$\rho_i(\text{calc})$	$\rho_i(\text{exp})$	$\rho_i(\text{calc})$
1(P)	-	.228	-	.779
2	-	.281	-	-.128
3	.093	-.091	.094	.118
4	-	.235	-	-.072
7	-	-.050	-	.131
8	.093	.100	(.024)	.034
9	.025	-.040	<.02	-.012
10	.093	.089	.094	.140

The agreement for positions 3, 8, 10 in the cation is excellent; the s.d. at 9 is slightly high, but in tolerable agreement. The anion results are not quite as good. Even allowing for inaccuracies in the experimental spin densities arising from errors in measurement due to the high line-widths, the agreement between 3 and 10 is poor. (The

high values here may indicate that a lower Q_{CH}^H should be used.) No other parameter sets improved the densities. However, there exists the possibility that the experimental spectrum, which was poorly resolved, could consist of a doublet split into a triplet, the splitting constants being in approximately the same ratio as the calculated spin densities, 140:118. This would lead to two possible sets: 2.36G (1H) and 1.99G (2H), or 2.80G (1H) and 2.36G (2H). It was not possible to decide which of these was the case, if either, owing to the poor spectral resolution, and also the fact that the overlap of about 0.4G would be of the same order as the splittings at the 9, 11 positions.

The results for the conjugated model, using the same parameters, are presented in Table VII. Again, the spin distribution is very similar, especially in the anion.

TABLE VII

Atom	Cation		Anion	
	$\rho_i(\text{exp})$	$\rho_i(\text{calc})$	$\rho_i(\text{exp})$	$\rho_i(\text{calc})$
1(P)	-	.216	-	.795
2	-	.236	-	-.116
3	.093	-.077	.094	.118
4	-	.214	-	-.068
7	-	-.040	-	.130
8	.093	.097	(.024)	.035
9	.025	-.036	<.02	-.013
10	.093	.090	.094	.142

It is difficult to present a physical interpretation of the value

of 1.30 for $k(4,7)$. This value would indicate a very strong conjugation between the two rings. Although this could be interpreted as arising from a short C-C bond, X-ray studies on crystalline 2,6-dimethyl-4-phenylphosphorin¹⁴⁴ show a bond length of 1.481 Å, exactly as expected for a $C(sp^2) - C(sp^2)$ bond.¹⁴⁵ (The bond twist was found to be 38.8° .) It would seem, then, that the only justification for using this value is simply that it gives better spin distributions.

(iii) TPPN anion and cation

Owing to the uncertainty in the experimental spin distribution in the cation, and the lack of observable proton splittings in the anion, it was more difficult to fit the calculated spin densities. Using the initial values $h_P = -0.85$, $k_{CP} = 0.45$, $k(2,19)$ and $k(6,13)$ were varied from 0.5 to 1.0 to simulate ring twist; a value of 0.7 was found suitable, corresponding to 45° twist. Once again, $k(4,7)$ needed to be greater than 1. As may be seen in Table VIII, two sets of parameters were necessary:-

$$\begin{aligned} \text{set 1: } h_P &= -0.6, k_{CP} = 0.45 \\ k(6,13) &= k(2,19) = 0.7, k(4,7) = 1.10 \\ \text{set 2: } h_P &= -0.85, k_{CP} = 0.4 \\ k(6,13) &= k(2,19) = 0.7, k(4,7) = 1.15 \end{aligned}$$

Set 2 gave reasonable agreement for the cation, but predicted a phosphorus s.d. of only -0.02 in the anion; this would mean a $Q(\text{effective})$

TABLE VIII

Atom	Cation			Anion		
	$\rho(\text{exp})$	$\rho^1(\text{calc})$	$\rho^2(\text{calc})$	$\rho(\text{exp})$	$\rho^1(\text{calc})$	$\rho^2(\text{calc})$
1(P)	-	.221	.127	-	1.063	-.020
2	-	.241	.274	-	-.150	.086
3	.096	-.064	-.076	-	.075	.219
4	-	.235	.253	-	-.050	-.045
7	-	-.036	-.040	-	.075	.003
8	.096	.072	.085	-	.031	-.011
9	.028	-.020	-.032	-	-.015	.000
10	.096	.064	.077	-	.092	-.010
13	-	-.018	-.021	-	.006	.071
14	.028	.028	.030	-	-.014	.044
15	.020	-.011	-.012	-	-.001	-.010
16	.028	.024	.026	-	-.010	.103

of about 1500G. The s.d. of 0.2 at 3, 5 would also give rise to an observable splitting in the experimental spectrum. Set 1, with relatively small parameter changes, gave a more reasonable spin distribution for the anion; the phosphorus s.d. of 1.063 is comparable to that in the anions of the other phosphorins. This set does, however, give slightly poorer spin densities in the cation.

The large cation spin densities in the cation at 3, 8, 10 are not as high as expected, but the smaller spin densities are in excellent agreement. The calculations indicate that the s.d. at 8 may be significantly higher than at 3 and 10; this fits in with the previous supposition (Chapter II, Section 5B(a)) that the poor computer simulations may be due to inequalities at these positions. The anion calculations predict relatively low spin densities on the carbons;

this agrees with the lack of observable splittings in the experimental spectrum.

The predicted ring twist at positions 2, 6 of 45° compares favourably with that of 46° predicted for the corresponding phenoxyl.¹²² It is again difficult to explain the $k(4,7)$ bond parameter of above 1.

Calculations were also performed on the trianion, using both parameter sets. Both, however, predicted large phosphorus spin densities which would give splittings greater than 15G. This is not seen in the experimental spectrum; owing to the difficulty of analysing this spectrum it was not considered worth while performing any parameter variations.

(iv) MeDPPL anion

Only the inductive model for the $P-CH_3$ group was tested thoroughly; the heteroatom model was extremely sensitive to the $P-CH_3$ parameters, and a fit was not obtained in the time available.

No agreement was found at all with any combination of parameters for the anion, i.e. the unpaired electron in the π orbital no. 10. However, there was extremely good agreement with the spin densities calculated for the cation, i.e. the unpaired electron in orbital no. 9. This might indicate errors in calculation of the eigenvalues, and an incorrect ordering of almost degenerate energy levels, but, in all cases, the gap between the two levels was at least 0.9 β . It is most unlikely that any error could be of this magnitude. If the levels

are, in fact, ordered correctly, it would then appear that the π system has 2 electrons less than expected. This would arise if the phosphorus was not donating electrons to the π system. This possibility is discussed further in Chapter IV.

The spin densities were very insensitive to variations of h_P in the range 0.8 to 1.6, and k_{CP} in the range 0.8 to 1.4. There was, however, an extreme sensitivity to the ring twist parameter at (2,12) and (5,6). An increase of this by 0.1 caused a 20% increase of the spin densities in the phenyl ring. The spin densities in Table IX were calculated with the parameters

$$\begin{aligned} h_P &= 1.4, \quad k_{CP} = 1.0 \\ k(2,12) &= k(5,6) = 0.85 \end{aligned}$$

TABLE IX

Atom	$\rho(\text{exp})$	$\rho(\text{calc})$
1	-	-.035
2	-	.287
3	.099	.113
6	-	-.015
7	.052	.059
8	.025	-.022
9	.052	.058

The proton splittings are in very good agreement with the experimental splittings; the value at position 3 is slightly high, but the other two are almost exact. One disturbing feature is the extremely low s.d. on the phosphorus. Exceptionally high Q-values would be needed

to give the observed splitting of 23.5G. It was not possible to increase the phosphorus s.d. above 0.09 by any combination of parameters. The ring twist parameter of 0.85 indicates a 30° ring twist. This is as expected, the methyl group pushing both rings out of the plane.

(v) TPPL anion

As with the previous calculations, no agreement was obtained with the calculated anion spin densities, but good agreement was obtained with the cation spin densities. (The gap between the two orbitals was about 0.97 β .) The densities were again insensitive to the phosphorus parameters, but were very sensitive to the ring twist parameters $k(5,6)$, $k(2,12)$. Varying the $k(1,18)$ parameter made virtually no difference to the densities. The densities in Table X were calculated with

$$h_P = 1.36, k_{GP} = 1.1$$

$$k(1,18) = 1.0, k(5,6) = k(2,12) = 1.20$$

TABLE X

Atom	$\rho(\text{exp})$	$\rho(\text{calc})$
1	-	-.034
2	-	.220
3	.090	.100
6	-	-.018
7	.090	.096
8	(.017)	-.034
9	.090	.098
12	-	.002
13	-	-.006
14	-	.000
15	-	-.005

The agreement with experiment is, in general, very good. The slightly higher calculated spin densities would indicate a lower Q_{CH}^H value of about 23. Although the s.d. at 8 is higher than the experimental value, the calculation supports the assignment of the 0.43G splitting to the 4 meta-protons and not to the third phenyl ring. The calculations, in fact, indicate zero spin densities in this ring. Although this may be expected from steric considerations - the middle ring being forced out of the plane by the other two rings - direct confirmation of this steric effect could not be obtained owing to the insensitivity of the spin densities to $k(1,18)$. Once again, the odd 1.2 ring twist parameter occurs, as in the phosphorins. However, that this is not less than 1 does provide indirect evidence that the rings are planar with the phosphole ring. As with MeDPPL, an unexpectedly low phosphorus s.d. is predicted.

(vi) Others

No detailed calculations were made on other phospholes owing to the difficulty of "blind parameterisation", i.e. estimating parameters without having experimental proton splittings as a comparison. Merely guessing what would seem to be reasonable values would almost certainly have given erroneous spin densities. For example, Cowley and Hnoosh's parameters were tried on the phospholes MeDPPL and TPPL, and also on TPPLO and PPPL; the spin distributions in the two known phospholes were so poor as to make the results for the oxides of no value at all.

To summarise, then, the calculations on all the phosphorin ions gave extremely good agreement with the experimental evidence, the only curious feature being the ring twist parameters of greater than unity. Although the phosphole calculations also gave very good agreement, this agreement was apparently with the wrong ion. The optimised phosphorus parameter values were close to those estimated initially.

3. All-Valence Electron Calculations

As may be seen from the previous section, although the McLachlan calculations provided some useful information on spin distributions, some aspects of the calculations were not entirely satisfactory. It was hoped that the more sophisticated CNDO theory would resolve some of the difficulties encountered here. Since the programme available (Section (b) infra) had not been used previously on radicals containing second-row elements, it was decided to perform calculations on some other systems in which it would be possible to check the calculated results with experimental evidence. Small radicals were chosen, since more information on geometries was available, and also since the calculations (which involve a substantial amount of approximation) would be more likely to give reliable results.

In this section a short review of the CNDO theory is given, together with details of the programme used. This is followed by the

results of the calculations on the small radicals and on the phosphorins and phospholes. The discussion of these results is left to Chapter IV.

(a) The CNDO Theory

A comprehensive account of the theory is to be found in the original papers,¹²⁸ and in the recent book by Pople and Beveridge.¹²⁹ Critical reviews have also appeared recently by Jug¹⁴⁶ and Jaffé.¹⁴⁷ An outline of the evaluation of the SCF equations and the appropriate approximations is given below. The closed shell treatment is given first, and then extended to open shells.

Valence electrons only are treated explicitly, the inner shells being treated as part of a non-polarizable core. These electrons are assigned to LCAO molecular orbitals,

$$\psi_i = \sum_{\nu} c_{\nu i} \phi_{\nu} \quad \dots (53)$$

and a variational treatment leads to Roothaan's equations,

$$\sum_{\nu} F_{\mu\nu} c_{\nu i} = \sum_{\nu} S_{\mu\nu} c_{\nu i} \epsilon_i \quad \dots (54)$$

where the Fock matrix

$$F_{\mu\nu} = H_{\mu\nu} + G_{\mu\nu}$$

and

$$H_{\mu\nu} = \left\langle \phi_{\mu} \left| -\frac{1}{2}\nabla^2 - \sum_A \frac{V_A}{r_{A\mu}} \right| \phi_{\nu} \right\rangle$$

$$\left. \begin{aligned} G_{\mu\nu} &= \sum_{\lambda\sigma} P_{\lambda\sigma} \left[\mu\nu | \lambda\sigma \right] - \frac{1}{2} (\mu\sigma | \nu\lambda) \\ (\mu\nu | \lambda\sigma) &= \langle \phi_\mu(1) \phi_\nu(1) | r_{12}^{-1} | \phi_\lambda(2) \phi_\sigma(2) \rangle \\ S_{\mu\nu} &= \langle \phi_\mu | \phi_\nu \rangle, \quad P_{\lambda\sigma} = 2 \sum_i C_{i\lambda} C_{i\sigma} \end{aligned} \right\} \dots (55)$$

The most important approximation involved is that of zero differential overlap (ZDO), in which overlap charge distributions of the type $\phi_\mu(1)\phi_\nu(1)$ are equated to zero. This has three main effects:-

- (1) The overlap integral $S_{\mu\nu} = \delta_{\mu\nu}$.
- (2) The electron interaction integrals $(\mu\nu | \lambda\sigma)$ are zero unless $\mu = \nu, \lambda = \sigma$. These are written $\delta_{\mu\lambda} = (\mu\mu | \lambda\lambda)$. The theory at this point is not invariant to rotation of axes or to hybridisation of orbitals on the same atom. A further approximation then made is that these integrals depend only on the nature of the atom and not on the orbitals involved, i.e. $\delta_{\mu\lambda} \approx \delta_{AB}$. In practice, these are calculated as 2-centre coulomb repulsion integrals using s functions.
- (3) Integral $(\mu | V_B | \nu)$ (with μ, ν on A) are zero if $\mu \neq \nu$. For the same reasons as in (2), this integral is taken to be the same for all orbitals on A, $(\mu | V_B | \mu) = V_{AB}$.

The core Hamiltonian elements are calculated as

$$\epsilon_\mu = H_{\mu\mu} = U_{\mu\mu} - \sum_{B \neq A} V_{AB} (\mu \text{ on A}) \dots (56)$$

In the CNDO/2 method, $U_{\mu\mu}$ is calculated from ionisation potentials and electron affinities as

$$\frac{1}{2}(I_{\mu} + A_{\mu}) = U_{\mu\mu} + (Z_A - \frac{1}{2})\delta_{AA} \quad \dots (57)$$

V_{AB} is approximated as

$$V_{AB} = Z_B \delta_{AB} \quad \dots (58)$$

The off-diagonal elements are calculated as

$$S_{\mu\nu} = H_{\mu\nu} = 0 \quad (\mu, \nu \text{ on same atom}) \quad \dots (59)$$

and as

$$S_{\mu\nu} = S_{AB}^0 S_{\mu\nu} \quad (\mu, \nu \text{ on different atoms}) \quad \dots (60)$$

where $S_{AB}^0 = \frac{1}{2}(S_A^0 + S_B^0)$ is an empirical parameter depending on the nature of the atoms A and B. The Fock matrix is then given by

$$F_{\mu\mu} = -\frac{1}{2}(I_{\mu} + A_{\mu}) + \left[(P_{AA} - Z_A) - \frac{1}{2}(P_{\mu\mu} - 1) \right] \delta_{AA} + \sum_{B \neq A} (P_{BB} - Z_B) \delta_{AB} \quad (61)$$

$$F_{\mu\nu} = S_{AB}^0 S_{\mu\nu} - \frac{1}{2} P_{\mu\nu} \delta_{AB}$$

For the open shell case, starting with two sets of MO's, $\psi_i^{\alpha}, \psi_i^{\beta}$, two analogous Fock matrices are produced, with corresponding charge density-bond order matrices

$$P_{\mu\nu}^{\alpha} = \sum_i^{\text{occ}} C_{i\mu}^{\alpha} C_{i\nu}^{\alpha}, \quad P_{\mu\nu}^{\beta} = \sum_i^{\text{occ}} C_{i\mu}^{\beta} C_{i\nu}^{\beta} \quad \dots (62)$$

The total charge density-bond order matrix is then

$$P_{\mu\nu} = P_{\mu\nu}^{\alpha} + P_{\mu\nu}^{\beta} \quad \dots (63)$$

and the spin density matrix is

$$Q_{\mu\nu} = P_{\mu\nu}^{\alpha} - P_{\mu\nu}^{\beta} \quad \dots (64)$$

The original CNDO/1 formalism was similar, but gave poor bond lengths and energies.

This method cannot, however, calculate s orbital spin densities in π -radicals, owing to the neglect of the one-centre exchange integrals which are responsible for these densities. A closely-related method, the INDO method,¹⁴⁸ does include these integrals and can calculate splitting constants in π -radicals. However, the computational difficulties in evaluating these integrals in calculations involving second-row elements have so far precluded any INDO calculations on these systems.

(b) Computer Programme

Calculations were performed on an IBM 360/44 computer using a programme written by P.A. Dobosh in Fortran IV for an IBM 360/67 computer.¹⁴⁹ The programme required several modifications as outlined below.

The parameters $\frac{1}{2}(I + A)$ and β^0 were as published previously,¹²⁸ and no effort was made to optimise these. (As discussed more fully in Chapter IV, the parameterisation for ions and radicals is almost certainly different from that for neutral molecules.) The basis sets used were

H, He	1s
1st row (Li - F)	2s, 2px, 2py, 2pz
2nd row (Na - Cl)	3s, 3px, 3py, 3pz, 3dxy, 3dxz, 3dyz, 3dz ² , 3d(x ² - y ²)

The orbital exponents were calculated in the programme using Slater's rules. In this version, the 3d orbitals were given the same exponent as the 3s and 3p, 4.36. It was not possible to vary this value without extensive rewriting of the programme; the problem of the value of the 3d exponents is discussed in Chapter IV.

The input data consisted of the options open shell or closed shell, the number of atoms, charge, multiplicity, atomic numbers and cartesian co-ordinates. The overlap and coulomb integrals were calculated first. An extended Hückel calculation was then performed, using the approximate Fock matrix $F_{\mu\mu} = \frac{1}{2}(I + A)$, $F_{\mu\nu} = \beta_{AB}^0 S_{\mu\nu}$. This was diagonalised and a set of orbitals and initial density matrix constructed. CNDO corrections were then added to the core Hamiltonian. The density matrix and the CNDO core Hamiltonian were then transferred to an SCF subroutine, and the Fock matrix constructed by adding the CNDO integrals. This was diagonalised, a new density matrix formed and a new Fock matrix constructed. This was repeated until the energy converged to 10^{-6} a.u. A maximum of 25 iterations was allowed. The open shell procedure was similar, separate subroutines being used for the α and β spins. Output included: integral values, α and β eigenvalues and eigenvectors, α and β charge density-bond order matrices, total density matrix, spin density matrix, total atomic charge densities, s-orbital spin densities, total energy and dipole moment.

The programme as received was much too large for the 360/44. Some space was saved by use of an overlay structure and by cutting down

the dimensions so that the programme could handle up to 75 basis functions or 35 atoms, but the bulk of the space was saved by changing all double precision constants and variables to single precision. This was found to cause some convergence problems, especially with the larger molecules. The electronic energy, instead of converging smoothly, oscillated over a small amplitude, this amplitude increasing as the size of the molecule increased. Consequently, a large number of calculations went the full 25 iterations without converging. By changing the maximum number of iterations, it was found that "convergence" to slightly different energies did not change the eigenvectors and spin densities significantly, although the total energies differed slightly. This was confirmed by running the original double precision programme on the IBM 360/50 at Edinburgh University; although the total energies were slightly different, the spin densities were exactly the same. The results also checked with calculations performed using a CNDO programme written in single precision by Segal for first-row molecules.

The convergence problem did, however, give rise to difficulties in geometry optimisation. An experimentally measured bond length was used as a first approximation, and the bond angle varied to give a maximum energy. Using this angle, the bond length was then optimised. Although divergence of the energy was not encountered very often, the amplitudes of the oscillations were apparently large enough for some systems to prevent a reasonable minimum from being obtained.

Consequently there is the possibility that the spin densities quoted for these systems do not correspond to the true equilibrium geometry.

Another problem that arose was that the results were not invariant to rotation of the co-ordinate axes. This became more noticeable as the size of the molecule increased. This is discussed further in Chapter IV.

In view of the problems mentioned above, and of the fact that no open-shell CNDO calculations or second-row elements had been reported previously, it was decided to first perform calculations on a series of phosphorus radicals on which there was ESR information, and on which there was some information on the probable geometry. Owing to the size of the phospholes and phosphorins investigated in this work, calculations could only be performed on simpler model systems.

For the majority of the calculations, only the spin densities are reported here; other properties are only included if sufficiently interesting or unusual. Calculations on some other molecules on which theoretical or experimental results have been reported previously are also given briefly. All bond lengths are expressed in Angstrom units, and all bond angles in degrees. Charge and spin densities are quoted to 3-figure accuracy. Initial geometries were estimated from spectroscopic data¹⁵⁰ or from solid state data.¹⁵¹

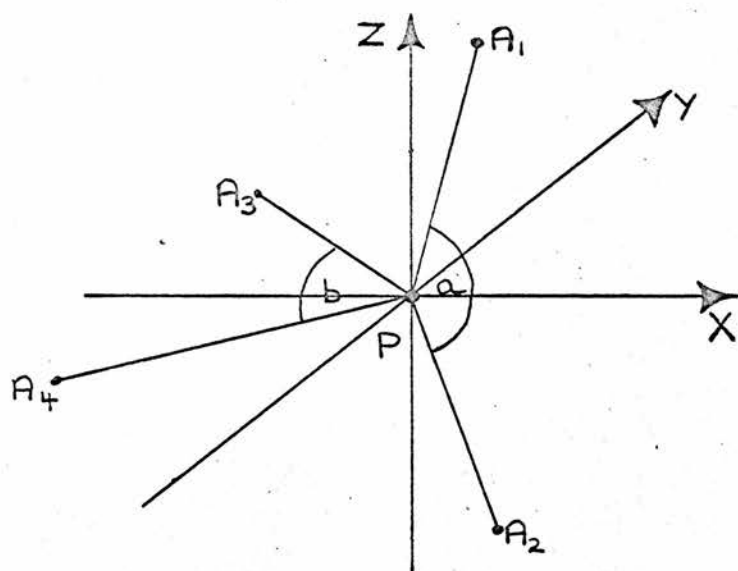
The axis systems used were as follows:-

- (1) PA : P at origin, A along Z axis.

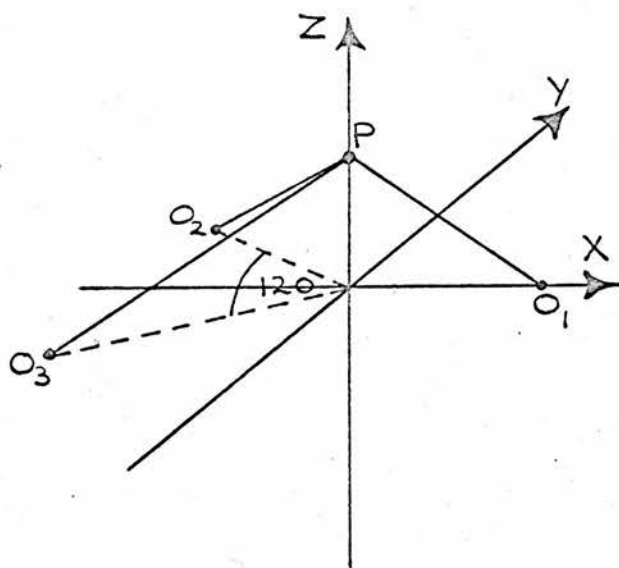
- (2) PA_2 : P at origin, PA_2 in the YZ plane with the Z-axis bisecting the APA angle.
- (3) AP_2O^- : P at origin, OPO in YZ plane with the X-axis bisecting the OPO angle, and PA in the XZ plane at an angle α to the XY plane (Fig. 35).
- (4) PO_3^- , PO_4^- : The O's in the XY plane, P along the Z axis (Fig. 35).
- (5) PA_4 : As in Fig. 35.
- (6) Phospholes and phosphorins. The co-ordinates of these molecules were calculated using a programme written in Fortran IV by M.J.S. Dewar.¹⁵² Input included the bond lengths, bond angles and dihedral angles. The programme was adapted to produce a punched output to be used as input to the CNDO programme. The output had atom 1 at the origin and the 1-2 bond along the positive X-direction. Thus the molecule resided mainly in the first quadrant in the XY plane.

(c) Results

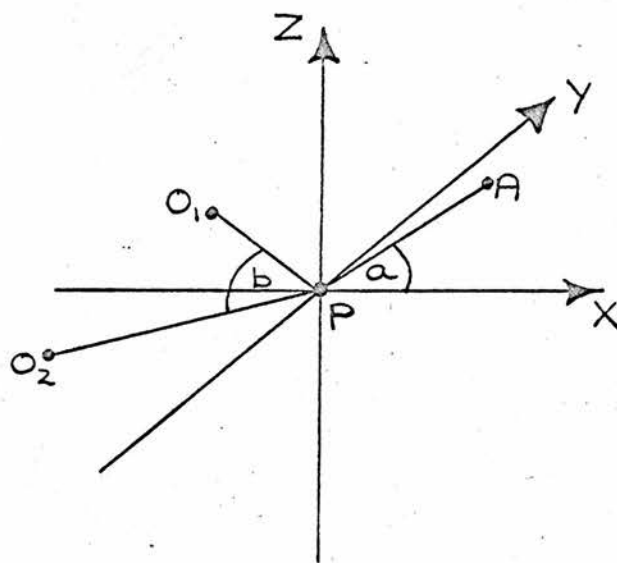
The results of the calculations are presented in tabular form in the following pages. Details of the various calculations are then given. Apart from the radicals on which there is ESR information, the results of some calculations on some neutral species and radicals for which there is other information are also presented.



PA_4 system

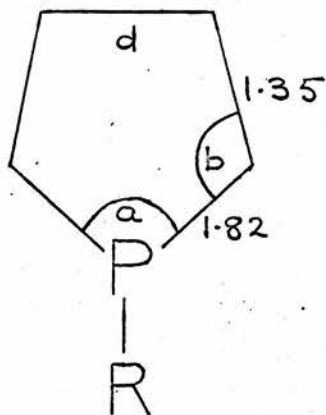
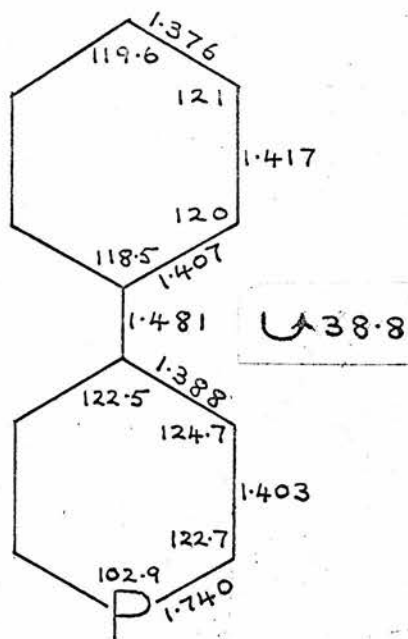


PO_3 system



$AP O_2^-$ system

Figure 35



- (i) $a = 90, b = 111, d = 1.48$
(ii) $a = 110, b = 92, d = 1.51$

CNDO geometries

Figure 36

TABLE XI

	Phosphorus				Hydrogen	D.M.
	s	p	d	total	s	
This work	1.750	2.623	.360	4.733	1.089	.83
Ref. 129 *	-	-	-	-	-	.84
Ref. 156 **	1.64	3.48	.26	5.38	.89	.34
Ref. 157 ‡	1.566	3.164	.188	4.918	1.024	-

* CNDO, PH = 1.4206, HPH = 92.8

** ab initio, no details given.

‡ ab initio, r = 1.4208, HPH = 93.8

TABLE XII

	Phosphorus				Fluorine			D.M.
	s	p	d	total	s	p	total	
This work	1.771	1.421	1.195	4.387	1.839	5.365	7.204	.38
Ref. 128	1.756	1.444	1.178	4.378	1.836	5.372	7.208	.62
Ref. 157	1.51	1.89	.71	4.11	1.90	5.42	7.32	1.44

TABLE XIII: Charge Densities (PH_2 , NH_2)

	P	H	N	H
s	1.861	1.094	1.653	.922
p	2.714	-	3.504	-
d	.237	-	-	-
Total	4.812	1.094	5.157	.922

TABLE XIV: $\text{PF}_2^+ \text{NF}_2^-$

	P	F	N	F
<u>Spin Densities</u>				
s	-	-	-	-
p	.937(.88)	.027(.06)	.817(.76)	.091(.12)
d	.009	-	-	-
<u>Charge Densities:</u>				
s	1.900	1.880	1.668	1.844
p	1.896	5.387	3.135	5.255
d	.669	-	-	-
Total	4.465	7.267	4.803	7.099

TABLE XV: PCl_2

	Spin Densities		Charge Densities	
	P	Cl	P	Cl
s	-	-	1.822	1.875
p	.718	.124	2.257	4.919
d	-.030	.032	.924	.205
Total	-	-	5.002	6.999

TABLE XVI: PF^+ , PF^-

	PF^+		PF^-	
	P	F	P	F
<u>Spin Densities</u>				
s	-	-	-	-
p	.957	.033	.974	.02
d	.01	-	.006	-
<u>Charge Densities</u>				
s	1.947	1.867	1.958	1.889
p	1.535	5.271	3.349	5.502
d	.381	-	.303	-
Total	3.863	7.137	5.610	7.390

TABLE XVII: Spin Densities (PF_4)

	Optimised angles ¹			Higuchi ²		
	P	F_1, F_2	F_3, F_4	P	F_1, F_2	F_3, F_4
s	.366	.010	.008	.335	.002	.003
p	-.096	.212	.148	.075	.161	.124
d	-.024	-	-	.010	-	-
E_T	-117.79141 a.u.			-117.77232 a.u.		

¹ a = 140, b = 106

² a = 186, b = 110

TABLE XVIII: Spin Densities (PCl_4)

	Optimised angles ¹			Higuchi ²		
	P	Cl_1, Cl_2	Cl_3, Cl_4	P	Cl_1, Cl_2	Cl_3, Cl_4
s	.268	.002	.002	.290	.000	.001
p	.186	.200	.046	.218	.166	.059
d	.044	.002	.000	.048	-.003	-.002
E_T	-72.65878 a.u.			-72.69893 a.u.		

¹ a = 180, b = 104

² a = 200, b = 106

TABLE XIX: Spin Densities (PO_3)

	P	O
s	.186	-.015
p	-.061	.371
d	.164	-

TABLE XX: Spin Densities (PO_2)

	P	O
s	.008	.001
p	-.177	.485
d	-.289	-

TABLE XXI: Spin Densities (PO_3^{2-})

	P	O
s	.205	-.004
p	-.239	.284
d	.195	-

TABLE XXII: HPO_2^-

	Charge Densities			Spin Densities		
	P	O	H	P	O	H
s	1.679	1.845	1.234	.146	-.011	.245
p	2.005	4.608	-	-.099	.318	-
d	1.176	-	-	.093	-	-
Total	4.860	6.453	1.234	-	-	-

TABLE XXIII: FPO_2^-

	Charge Densities			Spin Densities		
	P	O	F	P	O	F
s	1.728	1.854	1.897	.152	-.016	.008
p	1.717	4.599	5.498	-.156	.402	.071
d	1.254	-	-	.144	-	-
Total	4.698	6.453	7.395	-	-	-

TABLE XXIV: pz Spin Densities (phosphorin)

Atom	Cation	Anion	Trianion
1(P)	σ - radical	.602(.103)	-.003(.190)
2	-	.115	.201
3	-	-.050	.301
4	-	.165	-.191

(brackets indicate total d densities)

TABLE XXV: pz Spin Densities (2,4,6-Trimethylphosphorin)

Atom	Cation	Anion
1(P)	.496(.037)	.576(.099)
2	.104	.121
3	-.030	-.060
4	.227	.169

(brackets indicate total d densities)

TABLE XXVI: pz Spin Densities (4-Phenylphosphorin)

Atom	Planar		30° twist	
	Cation	Anion	Cation	Anion
1(P)	.357(.028)	.628(.075)	.373(.028)	.621(.081)
2	.082	.076	.084	.085
3	.005	-.023	.007	-.030
4	.243	.136	.247	.144
7	-.004	-.016	.004	-.013
8	.098	.037	.048	.018
9	-.047	-.019	-.027	-.011
10	.105	.035	.065	.020

(brackets indicate total d densities)

(i) PH, PN, PO, PH₃, PF₃

PH: Spectroscopic PH = 1.432. These calculations optimised at 1.52; accurate SCF calculations optimised at 1.41.¹⁵³ The total charge densities (4.905 on P, 1.096 on H) indicate significant charge build-up on H.

PN: Spectroscopic PN = 1.491. These calculations diverged for all bond lengths in the range 1.43 to 1.63.

PO: Spectroscopic PO = 1.448. A poor optimisation was found at 1.52. The total charge densities (4.606 on P, 6.394 on O) are much more exaggerated than those calculated by Boyd and Lipscomb (5.010 on P, 6.034 on O) in an ab initio calculation.¹⁵⁴ This used a 3d exponent of 1.40 and the experimental bond length. CNDO calculations using this bond length still predicted large charge shifts. The CNDO results showed the unpaired electron to reside mainly on the phosphorus (0.834 in the p orbitals, 0.059 in the d orbitals) with 0.107 in the oxygen p orbitals.

PH₃: Experimental geometry,¹⁵⁵ PH = 1.4206, HPH = 93.5. The PH length was taken as 1.4206, and the angle HPH optimised to 92. The charge densities and dipole moment are compared in Table XI with those calculated by Pople with the original CNDO programme¹²⁹ and with two ab initio calculations including d-orbitals.^{156,157} Some calculations were also performed on the species PH₃⁻ and PH₃⁺, and indicated that the former should have the same bond angle as PH₃, and that the latter should have a bond angle of 110.

PF₃: The experimental geometry, which is not known exactly, was taken to be PF = 1.54, FPF = 100. With PF kept at 1.54, FPF optimised at 107. The charge densities and dipole moment are presented in Table XII, together with the results from Segal and Santry's CNDO calculation¹²⁸ and from Hillier and Saunders' ab initio calculation.¹⁵⁷ Calculations on PF₃⁻ suggested that this molecule should be planar.

(ii) PH₂, NH₂

(The NH₂ calculation was performed as a comparison.)

PH₂: Experimental geometry (spectroscopic), PH = 1.429, HPH = 91.7.

Optimised geometry, PH = 1.52, HPH = 91.5.

NH₂: Experimental geometry (spectroscopic), NH = 1.024, HNH = 103.4.

Optimised geometry, NH = 1.06, HNH = 106.

In each case, unit s.d. was predicted in the phosphorus px orbital. The charge densities are presented in Table XIII.

(iii) PF₂, NF₂

PF₂: Experimental geometry unknown, but P-F bond length usually in the range 1.53-1.58.

Optimised geometry, PF = 1.73, FPF = 112.

NF₂: Experimental geometry (spectroscopic), NF = 1.37, FNF = 104.2.

Optimised geometry, PF = 1.23, FPF = 104.

The spin and charge densities for both species are presented in Table

XIV. The figures in brackets in these tables are the spin densities calculated by Wei ⁷⁵ by the extended Hückel method. The PF_2 geometries used were $\text{PF} = 1.58$, $\text{FPF} = 102$. The NF_2 geometries used were $\text{NF} = 1.40$, $\text{FNF} = 104$.

(iv) PCl_2

Experimental geometry unknown. With a bond length of 2.0, the bond angle optimisation was very erratic. The minimum energy was taken to be at 140° , but the energy improved dramatically as the angle was reduced below 90° . The bond length optimised well at 1.95. The spin and charge densities are presented in Table XV.

(v) PF^+ , PF^-

ESR experiments ⁶⁹ suggested the possible existence of one of these species. The bond lengths were varied in the range 1.6 to 1.8.

PF^+ Optimised at 1.69, with total energy $E_T = -34.16046$ a.u.

PF^- Optimised at 1.76, with total energy $E_T = -34.60173$ a.u.

The spin and charge densities are shown in Table XVI.

(vi) PF_4

The PF_2 bond length of 1.73 was assumed and axes were chosen as in Figure 35. The angle a was varied between 120 and 220, and angle b between 90 and 150. The optimisation was erratic, but a reasonable energy minimum was found at $a = 186$, $b = 110$. The calculation was also performed using the bond angles and axis system of Higuchi.¹⁵⁸ The spin densities and total energies are presented in Table XVII.

The results - for instance, spin and charge densities - were found to be dependent on the axis system used, although not to any serious extent.

(vii) PCl_4

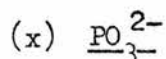
The PCl_2 bond length of 1.95 was used. Axes were as for PF_4 (Fig. 35). The energy minimisation was extremely erratic, and a poor minimum obtained at $a = 180$, $b = 104$ must be subject to error. A calculation was also performed with $a = 200$, $b = 106$ (i.e. pyramid-shaped, as the geometry predicted by Higuchi for PF_4), using the same axes as Higuchi. The spin densities and total energies are presented in Table XVIII. A marked sensitivity to the axis system was found.

(viii) PO_2

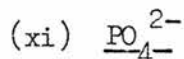
This was suggested as a possible alternative to the PO_3^{2-} radical.⁶ Taking $\text{PO} = 1.53$, OPO optimised to 150. All bond length optimisations between 1.53 and 1.66 diverged. The spin densities in Table XIX are for $\text{PO} = 1.52$, $\text{OPO} = 150$.

(ix) PO_3

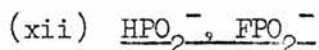
This was suggested as a possible alternative to PO_4^{2-} . Axes were as in Figure 35. With $\text{PO} = 1.53$, OPO optimised at 120 (planar). PO optimised at 1.62. Spin densities are presented in Table XX. The phosphorus 3s orbital s.d. was almost constant with respect to angular variation.



Axes were as for PO_3 . With $\text{PO} = 1.53$, OPO optimised at 120 (planar). PO optimised at 1.69. The spin densities at this geometry are presented in Table XVI. The phosphorus 3s s.d. was quite sensitive to the PO bond length; at 1.53, the s.d. was 0.339.



Axes were as for PO_3 with the fourth oxygen along the positive Z direction. Using the PO_3^{2-} bond length of 1.69, calculations were performed with tetrahedral angles. An extreme sensitivity to the accuracy of the co-ordinate input was found; the results were also sensitive to axis rotation. This may be due to the fact that, although oscillation did not occur, the electronic energy never quite converged. This was found to have serious effects on the results in other systems. The calculations did, however, indicate a phosphorus 3s s.d. of about -0.04, with most of the s.d. in the oxygen p orbitals.



The axis system for these radicals shown in Figure 35 was chosen to facilitate co-ordinate calculation.

HPO_2^- : Initial bond lengths, $\text{PH} = 1.42$, $\text{PO} = 1.54$. Angles a and b were varied in the ranges: a from 0 to 90, b from 90 to 150. A very good minimum was obtained at $a = 40$, $b = 135$. Assuming $\text{PO} = 1.69$, PH optimised at 1.54. The spin and charge densities are presented in Table XXII.

FPO₂⁻: Initial bond lengths PF = 1.54, PO = 1.54. A good minimum was obtained at a = 20, b = 130. Assuming PO = 1.69, PF was optimised at 1.78. Spin and charge densities are presented in Table XXIII.

(xiii) Phosphorins

Owing to programme size limitations, no calculations could be performed on the molecules on which ESR results were available. Instead, calculations were performed on the model systems

- (1) phosphorin
- (2) 2,4,6-trimethylphosphorin
- (3) 4-phenylphosphorin

The ring geometries were as found in the X-ray structure¹⁴⁴ of 2,6-dimethyl-4-phenylphosphorin. Average values of bond angles and lengths were used for equivalent positions (Fig. 36). All ring C-H lengths were taken as 1.08. Calculations were performed on the neutral molecule, the cation and the anion. In the following tables the pz spin densities are given, together with the phosphorus 3d s.d.

(1) Phosphorin (Table XXIV). The cation was predicted to be a σ -radical; examination of the orbitals showed that this probably arose from errors in the calculation of the B-eigenvalues, resulting in incorrect ordering of the orbitals. The anion was predicted to be a π -radical, as was the trianion.

(2) 2,4,6-Trimethylphosphorin (Table XXV). For the C-CH₃

grouping, C-C = 1.524, C-H = 1.09 was used. The relative orientation of the methyl groups was found to have negligible effect on the spin densities. Both cation and anion were predicted to be π - radicals.

(3) 4-Phenylphosphorin (Table XXVI). The angle between the two rings was varied from 0 to 80. Two distinct minima were found, at 0 and 30. The total energies (in a.u.) were

Neutral mol., -91.74828 and -91.73994 at 0,30 respectively;
cation, -91.38120 and -91.36665 at 0,30 respectively;
anion, -91.74632 and -91.73067 at 0,30 respectively.

Although the 30° angle is close to the 38.8° angle measured in the solid state by X-rays, the 0° energy minimum is lower in each case.

(xiv) Phospholes

No definite experimental geometries were available for any of the phospholes. NMR evidence on 1-methylphosphole⁶¹ suggested that the geometry was quite different from the analogues thiophen, furan and selenophen. In view of this uncertainty, two initial guesses were made at the geometry (Fig. 36). The P-C₁ bond was fixed at 1.82, and the C₁-C₂ bond fixed at 1.35. All C-H bonds were fixed at 1.08. The angle a at the phosphorus was taken at 90 and 110, and the angle b at C₁ calculated to give the bond d a length between 1.45 and 1.55. The two initial geometries were then

$$(1) \quad a = 90, b = 111, d = 1.48$$

$$(2) \quad a = 110, b = 92, d = 1.51$$

The configuration round phosphorus was initially taken to be planar.

The models used were

- (a) Phosphole, $P-H = 1.42$;
- (b) 1-Methylphosphole, $P-C = 1.85$, $C-H = 1.09$;
- (c) 1-Phenylphosphole. The phenyl geometry was assumed to be that of benzene (all angles 120 , $C-C = 1.40$, $C-H = 1.08$). Calculations were performed with the rings planar and at 35° ;
- (d) 1-Vinylphosphole. The vinyl geometry was $P-C = 1.85$, $C-C = 1.35$, $C-H = 1.08$, all angles 120 . The group was assumed planar;
- (e) Biphenylenephosphine. Benzene ring geometries were used, with $a = 110$, $b = 92$, $d = 1.46$.

All the calculations predicted the anions to be σ -radicals. Altering the configuration about phosphorus to pyramidal gave similar results.

CHAPTER IV

DISCUSSION

	Page
1. <u>Radicals from Phospholes and Phosphole Oxides</u>	123
(a) Anomalous Radicals	124
(b) Phosphole Anions	131
(i) Reaction mechanism	131
(ii) Structure of anions	132
(iii) Q-values	141
2. <u>Radicals from Phosphorins</u>	142
(a) Structure	142
(b) Q-Values	147
3. <u>CNDO Calculations</u>	148
(a) PH, PN, PO	148
(b) PH ₃ , PF ₃	149
(c) PH ₂ , NH ₂	150
(d) PF ₂ , NF ₂	151
(e) PCl ₂	153
(f) PF ₄ ⁺ , PF ₄ ⁻	154
(g) PF ₄	155
(h) PCl ₄	157
(j) PO ₂ , PO ₃ ²⁻	158
(k) PO ₃ , PO ₄ ²⁻	159
(m) HPO ₂ ⁻	160
(n) FPO ₂ ⁻	161
(o) Phosphorins	162
(p) Phospholes	163
4. <u>Q-Values</u>	164
5. <u>CNDO Programme</u>	169
6. <u>Conclusions</u>	174

1. Radicals from Phospholes and Phosphole Oxides

In this section, the radicals resulting from the room temperature alkali metal reductions of phospholes are discussed first; the evidence here strongly suggests that these do not contain phosphorus. The

mechanism of the alkali metal reductions is then discussed with respect to ring openings, followed by a discussion of the structures of the radical anions. The problem of the phosphorus Q-values for these systems is then treated.

(a) Anomalous Radicals

The first report of the 15-line spectrum identified here as signal A was made by Bøddeker and Schindewolf¹¹⁴ in the reaction of benzene with Na-K alloy in DME-THF mixed solvent. The 7-line $C_6H_6^-$ spectrum was present below -20° , but on warming to above 0° , the colour changed from deep green to yellow-brown, and the 15-line spectrum appeared. This spectrum was ascribed to the benzene anion in which interaction with the metal ions has removed the degeneracy of the two degenerate antibonding orbitals, the electron going into the symmetric (E_{2u}) state. Wormington and Bolton,¹¹⁶ however, succeeded in resolving each of the 15 lines into at least 12 components at low microwave power levels; this structure was analysed by computer simulation, giving the assignments shown in Table XXVII, along with the temperature variation. This complex structure showed that the radical could not be the simple benzene anion, and the authors suggested that the radical resulted from some sort of coupling reaction. (At about the same time, Jones et al.¹⁵⁹ showed that in the solid state at $4.2^\circ K$, the 7-line $C_6H_6^-$ spectrum changed to a 5-line spectrum, which was interpreted as the unpaired electron in the antisymmetric antibonding orbital).

TABLE XXVII

$a_H(G)$

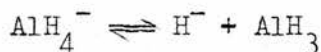
T°C	2H	4H	1H	2H	4H
-63	6.505	1.774	.407	.234	.119
-3	6.252	1.774	.349	.232	.117
+22	6.116	1.758	.326	.231	.115

Splitting constants and temperature variation, ex.
Wormington and Bolton (ref. 116).

Two further papers^{115,117} showed that this radical was only produced if the solvent had been dried over $LiAlH_4$; solvents dried over Na-K alloy gave only the 7-line spectrum. Bøddeker *et al.*¹¹⁷ found that solvent dried over Na-K did not give the 15-line spectrum if LiCl was added; thus ion-pairing was not responsible for this spectrum. Addition of LiCl to samples prepared from solvent dried over $LiAlH_4$ facilitated production of the 15-line spectrum, even at temperatures below 0°; this would appear to be a catalytic effect.

A comparison of the g -values of $C_6H_6^-$ and the unknown by Kelm and Möbius¹¹⁸ showed conclusively that these radicals were not the same. These authors also suggested that the relatively large g factor of the unknown (2.002829 at 20°) compared with that of $C_6H_6^-$ (2.002787 at 20°) showed that metal ion pairing with $C_6H_6^-$ was not occurring, as the g -value should then be smaller. This argument is not valid, however, since in the reference quoted¹⁶⁰ the reduction in g -value only occurred on ion-pairing with the heavy alkali metals, caesium and rubidium; no change was found with the lighter metals. The radical

was assumed to arise from reaction of $C_6H_6^-$ with the solvent, assisted by the presence of $LiAlH_4$. This could result from AlH_3 having distilled over with the ether since, in ethereal solvents, the equilibrium



is set up.¹⁶¹ In fact, AlH_3 was found in the distillate.

To return to the present work, there is little doubt that signal A is the same as that described above. The splitting constants do differ slightly, but the splittings in the DME-THF mixture (Table XXVII) lie between those found here in DME and in THF. The fine structure is seen under the same conditions of low microwave power, and the temperature variation of the main splitting is as above. Radicals B and C must be closely related to A; B has splittings almost identical with those of A, the only noticeable differences being the loss of one proton responsible for the large splitting, and a possible increase in the number of protons responsible for the 1.7G splitting. In C, the two protons responsible for the main splitting have been lost, the number of protons responsible for the 1.7G splitting has increased to 8, and the smallest splitting has approximately doubled to 0.3G. The g-values of all three are 2.0027; although this is close to that of the benzene anion, the more accurate measurements of Kelm et al.¹¹⁸ at various temperatures show that these are not the same species. It would be expected that any major structural differences between A, B, C would significantly change the

values of the splittings and also the g -values.

Signal E from the reaction of PPPL with potassium must also be related to these radicals, despite the unusually large doublet splitting of 12.65G, which is of the magnitude expected from a phosphorus nucleus. The 6.36G and the 1.75G splittings, together with the g -value of 2.0027, would seem to preclude the possibility of a radical of a totally different structure.

The phenyl cleavage reaction (equation 30) provides the necessary phenyl moiety for the formation of these radicals. This is confirmed by the absence of signals A, B, C on reaction with K of MeDPPL and ViTPPL, where there is no phenyl group attached to the phosphorus. The work on the benzene system would indicate that the next step is formation of the benzene anion; however, no signal from this species was seen at all in this work. This could be due to the anion undergoing rapid reaction before an observable steady-state concentration is reached. This is precisely what Bøddeker¹¹⁷ observed when LiCl was added to the reaction mixture; the 15-line spectrum was obtained immediately, even at low temperatures.

Other precursors, such as the phenyl radical or benzyne, may be ruled out. If the phenyl radical were formed, dimerisation to give biphenyl would occur to some extent; in none of the reactions with K was a signal attributable to the biphenyl anion apparent. The reaction of benzene with alkali metals to give benzyne has been observed previously;¹⁶² in this reaction, performed in HMPA solvent, substantial

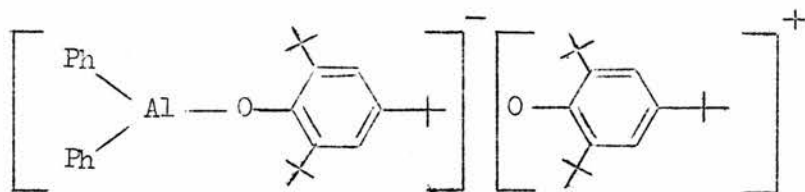
amounts of biphenylene were formed. No signal from the anion of this species was observed in this work, and it is not possible to assign the observed splittings to any form of polymer of this.

It is difficult to speculate on the further reaction mechanism and on the structures of A, B, C on the evidence available. Assuming that the benzene anion is a precursor, this can give either A, B or C as the initial radical. If A or B is formed first, it is not possible to predict which radical will follow, but if C is formed first, no conversion to A or B is possible. Since C is also usually the ultimate radical, it would appear that this is also the least reactive (or most stable) radical. Although in most cases contact with K was apparently necessary for interconversion, the two exceptions noted in Chapter II, Section 2A, suggest that this is not the case. However, in view of the apparent similarity of the structures of A, B, C, the disproportionation and electron transfer reactions postulated in this section would seem unlikely; it also seems likely that, in these reactions, potassium is present, either as a fine suspension or in solution.

The observation¹¹⁷ that AlH_3 is present in the reaction mixtures agrees with the observation that the first few samples prepared using a new solvent batch give A, B, C more readily, and also with the observation that samples prepared in batches give the same radical sequence. This could well arise from AlH_3 being distilled over with the solvent. However, the suggestion by the same authors that the

radicals result from reaction of the benzene anion with the solvent molecules is not supported by this work. If this did occur, significantly different radicals should result from reaction in each solvent. In fact, the same radicals resulted in both DME and THF solutions. The solvent may well play a rôle, but it seems likely that this is limited to either solvation or as a proton source.

Although the large number of hyperfine lines for each of the signals indicates radicals formed by some sort of polymerisation of $C_6H_6^-$ catalysed by AlH_3 , it is likely that such species would have already been observed in ESR work. There is therefore a possibility that the Al nucleus ($I = 5/2$) is responsible for some of the smaller splittings; no evidence exists here for a sextet splitting, but the presence of comparable proton splittings could prevent observation of this. Few attempts have been made to prepare Al-containing radicals in solution; Kochi and Krusic¹⁰⁸ attempted to produce radicals from trialkylaluminiums by reaction with photochemically produced t-butyl radicals, but observed only alkyl radicals in large quantities. However, some time ago Müller et al.¹⁶³ observed an unusual radical on reaction of triphenylaluminium with the 2,4,6-tritertiarybutylphenoxy radical, and assigned to it the structure



The ESR spectrum consisted of a septet split into an octet, the splitting constants (not quoted) being estimated from the published spectrum as 1.8G and 0.4G. Deuteration experiments showed the septet to arise from the ortho-, para-protons on the two phenyl rings, and the octet to arise from the aluminium splitting and the meta-splitting from the attached phenyl ring. The general appearance of the fine structure was similar to that observed in the radicals A, B, C.

This work does show, then, that it is possible to obtain Al-containing radicals with an Al splitting of the correct order of magnitude; if this is occurring in the present work, the question is what is the structure of A, B, C. It is possible that $C_6H_6^-$ could react with AlH_3 to give the series $C_6H_6AlH_2$, $(C_6H_6)_2AlH$, $(C_6H_6)_3Al$. The latter is known to be stable, and the diphenyl derivative is known to be moderately stable.¹⁶⁴ Anions derived from these would explain the large 6.2G splitting in A, B, C: this could arise from the protons attached to Al, the monophenyl compound giving the triplet in A, the diphenyl giving the doublet in B, and the triphenyl with no large proton splitting, as in C. Further splittings would then arise from the phenyl protons and from the Al nucleus. However, it is not possible convincingly to simulate the spectra with these assignment, and it is very probable that the actual situation is more complex, since this scheme does not suggest a possible structure for the radical giving signal E.

It would be unwise to predict the structures of these radicals

on the evidence available so far. Before any definite suggestions can be made, these systems must be subjected to detailed product analysis. Since this thesis is concerned primarily with radicals containing phosphorus, no further attempts were made at elucidation of these structures.

(b) Phosphole Anions

(i) Reaction mechanism

The type D signal from MeDPPL on reaction with K must arise from opening of the phosphole ring and subsequent anion formation. The use of the reaction of 1-phenylphospholes with K as a preparative technique shows that the predominant reaction here initially is phenyl cleavage. The present work supports this, since at room temperature A, B, C never appear after development of D. The similarity of D to the signal from MeDPPL shows that this results from a ring cleavage occurring after phenyl cleavage, and not from the sort of anion obtained from PBP. However, the spectra are much too poorly resolved to present any sort of analysis.

The cleavage reactions with Na do not occur to nearly the same extent as with K. The broad D-type signal produced from TPPL with Na (Fig. 11) is relatively weak; the form of the resolution obtained on this signal indicates some distinct difference from D. This could be due to an ion-pairing effect or, more likely, the effect of the

extra phenyl ring on the phosphorus, which is very probably not cleaved off in the Na reactions, as can be seen from the absence of signals A, B, C. In only one reaction with Na did either of the 1-phenylphospholes give a biphenyl anion signal. If this arose via cleavage of this phenyl group, the signal would also be expected in the reactions with K. The absence of the signal in the K reactions suggests the possibility of some biphenyl impurity, or some impurity giving rise to biphenyl.

It is interesting to note that ViTPPL, together with giving an unexpectedly low anion concentration, does not give any D-type cleavage signals, despite the appearance of the usual intense red colour. This would indicate that ring cleavage is occurring, but not addition of an electron to the product. However, it is not possible to speculate on the reasons for this, since the structure of the product is unknown.

(ii) Structure of anions

The higher yields of the anions of MeDPPL, TPPL and PPPL with Na can be attributed to the lack of competitive reactions such as phenyl or ring cleavage (see previous section). No attempt was made to measure the anion concentrations and yields, but the signal strengths indicated very high yields. The very low yield from ViTPPL is puzzling; although reaction via the vinyl group ring reduces the radical concentration, the strong blue colour indicates a reasonably high radical yield. (However, this colour could be simply due to the

ethereal solution of potassium.) It is also difficult to see why the phospholes with the groups $-\text{CH}_2\text{CO}_2\text{H}$, $-\text{CH}_2\text{Cl}$ and $-(\text{CH}_2)_3\text{Br}$ attached to phosphorus give no signals at all, from either anions or ring cleavage products. One possible explanation here is reaction of the alkali metal with the attached group.

The ESR results and spin density calculations in this work predict geometries which are expected from steric considerations. The low phenyl splittings from the MeDPPL anion suggest that the phenyl rings are pushed out of the plane of the phosphole ring. This is as expected; models show that steric crowding does occur, and twisting of the phenyl rings is the only way to relieve this. The ring twist of 30° suggested by the McLachlan calculations is a reasonable value.

It would be expected that steric crowding in the TPPL anion may be relieved most easily by the central phenyl ring being twisted out of the plane of the phosphole ring, leaving the other two rings planar and increasing the extent of the delocalised π system. The experimental evidence supports this, the splittings from the central ring not being observable. However, the insensitivity of the McLachlan calculations to this ring twist parameter does not permit any estimation of the twist angle. The high value of the ring twist parameter of 1.2 for the other two rings, although inexplicable on the $\cos\theta$ law, suggests the possibility of near-planar rings.

The extra phenyl rings in PPPL must increase the steric crowding, which can only be relieved by all five rings twisting to some extent.

This is supported by the increased a_p value of 31.3G, compared with 26.5G in TPPL; the electron is more localised in the phosphole ring, despite the two extra phenyl rings. Lack of comparative experimental data prevented support of this by McLachlan calculations.

The little ESR evidence available prevents speculation on the geometry of the ViTPPL anion, but the a_p value of 27.6G suggests that ring twisting occurs to a lesser extent than in PPPL. This is as expected, as the vinyl group is less bulky than phenyl.

One problem of great interest is that of the configuration about phosphorus in the neutral phospholes and in the anions. By analogy with tertiary phosphines, it would be expected that the neutral molecule should be pyramidal. However, if evidence was available for aromatic character in these compounds, a planar configuration would be expected to allow fuller participation of the phosphorus in the conjugated system. NMR measurements by Mislow¹⁶⁵ on a 1-isopropylphosphole showed that this molecule is pyramidal, with a very low inversion barrier of about 16 kcal./mole. Mislow ascribed this low barrier to increased delocalisation (i.e. aromaticity) in the planar transition state, in which the phosphorus 3pz orbitals can overlap effectively with the carbon 2pz orbitals. The bulk of the experimental evidence available at present^{61, 166} suggests that the phospholes do possess some degree of aromatic character. Mislow warns that the spectroscopic data available refers to the ground state, and that the chemical reactivity evidence refers to the planar

transition state; great care must therefore be taken in interpreting such data.

In the work presented here, it is not possible to argue for or against a pyramidal or planar configuration in the neutral molecules, but only in the anions. The phosphorus splittings in the anions of MeDPPL, TPPL and PPPL of 23.5G, 26.5G and 31.3G respectively are higher than most of the phosphorus splittings observed previously in organic π systems, including the phosphine anions. This latter point clearly suggests that the electronic structures of the phospholes and the phosphines are significantly different. The phosphole splittings are, in fact, very similar in magnitude to the splittings in the phosphorin radical ions. The stability of the phosphorin ring to oxidation and reduction suggests an aromatic system, although other experimental data is strangely lacking. This would therefore suggest that the phospholes do possess some aromatic character, the phosphorus 3pz orbital donating 2 electrons to the aromatic system. The value of the methyl proton splittings in the MeDPPL anion also suggests that this is attached to a "normal" aromatic system. If a Q_{PP}^P value of about 25G is assumed (Section (iii) *infra*), the phosphorus splitting of 23.5G gives a phosphorus π spin density of about 0.1; the methyl splitting of 2.48G then suggests a $Q_{PCH_3}^H$ value of about 25G. The corresponding $Q_{CCH_3}^H$ values¹⁶⁷ lie in the range 18-38G, and the corresponding $Q_{NCH_3}^H$ value of 24.5G calculated from the 10-methyl-phenothiazine cation¹⁶⁸ is very close.

The CNDO calculations on PH_3^- suggest that this should have exactly the same pyramidal geometry as PH_3 . However, the calculations on PF_3^- predict this to be planar, although PF_3 is pyramidal. It would appear, then, that there is no simple way of predicting the geometries of the anions. It would be of great interest to perform ab initio calculations on these species, since such calculations on the related species CH_3 , CH_3^- , CF_3 , CF_3^- show that the species should become more pyramidal when an electron is added. For instance, CH_3 is predicted to be planar and CH_3^- to be pyramidal.¹⁶⁹ Calculations on CF_3 and CF_3^- ¹⁷⁰ predicted both to be pyramidal, but the latter to be more so.

As outlined in Chapter II, the peculiar line-width effects observed in the spectra of the MeDPPL anion with K in THF suggest the possibility of ion-pairing involving close association of the metal ion with the phosphorus d-orbitals, and the further possibility that the complexity of these spectra could be partly explained by assuming a pyramidal configuration. This evidence is, however, extremely tenuous and cannot be considered too seriously.

The McLachlan spin densities are, in general, in very good agreement with the experimental spin densities, despite the number of parameters that needed to be varied; however, the agreement is with the incorrect ion (see below). The McLachlan λ parameter was also varied, but the results for given h and k values did not improve significantly. Although full optimisation of all the parameters,

including λ , may well have improved the agreement, it was considered that the improvement would not justify the effort. (Recently¹⁷¹ stress has been laid on the better results obtained with hydrocarbon systems using an optimised λ .) This superficially supports the idea of a normal planar π system. However, the agreement of the experimental anion spin densities with the calculated cation spin densities is very difficult to rationalise. For no parameter combination tested was there a reversal of the orbitals to give the expected order. Although the most obvious reason would be an incorrect ordering of nearly degenerate levels, the magnitude of the gap between the cation and anion energy levels of over 0.9 β would seem to preclude this. The same effect was also found in calculations performed on the phosphines studied by Cowley and Hnoosh, using the parameters of these authors.

As outlined in Chapter III, the McLachlan method is only strictly applicable to alternant hydrocarbons, and several approximations are based on this assumption. If a breakdown of the theory was occurring with particular combinations of parameter values, it would be expected that this would also occur with other systems. This has not been recorded previously, and was not found in this work in the calculations on phosphorins.

If these calculations are reliable, and the agreement with the experimental spin densities is very good, then it would appear that the phospholes and phosphines are behaving as if the π system had

2 electrons fewer than expected. This would arise if the phosphorus nucleus was not contributing 2 electrons to the π system. This seems unlikely in view of the large phosphorus splitting, but it must be remembered that the McLachlan calculations predict an abnormally low spin density on the phosphorus, and, in the TPPL anion, in the attached phenyl ring.

The contrasting behaviour of TPPL and TPP on reaction with alkali metals does suggest some distinct difference in the electronic structures of these species. The former forms perfectly stable anions at low temperatures, whereas the latter loses a phenyl group at any temperature.⁹⁸ This provides some evidence that the phosphole anion is a much more stable species, the increase in stability arising from an aromatic phosphole ring. The behaviour of PBP⁹⁹ would appear to be anomalous, since although the structure can be regarded as that of a dibenzophosphole, the cleavage reaction is that of a tertiary phosphine. (Some thermochemical evidence does suggest that conjugation of phosphorus with the rest of the molecule is small.)¹⁷²

Little can be said about the structures of the anions of the phosphole oxides. As expected, the phosphorus splittings are lower than in the corresponding phospholes, owing to delocalisation of the unpaired electron on to the oxygen. The configuration of these compounds about phosphorus must be tetrahedral, but the ESR evidence was insufficient to provide any further information, and it was not possible to perform any meaningful McLachlan calculations.

The occurrence of gegenion pairing in these radicals is shown very clearly in the general form of the spectra. Perhaps the most interesting aspect of this is the distinct, steady decrease in the phosphorus splitting as the metal ion changes from K to Na to Li (Table XXVIII). This marked change must indicate that the metal ion is very closely associated with the phosphorus nucleus. This could occur by close association with the d-orbitals, in the same way as postulated for MeDPPL with K in THF. Alternatively, close association with the oxygen could affect the phosphorus spin densities. Unfortunately the poor resolution of the spectra does not permit observation of any changes of the proton splittings.

TABLE XXVIII

	$a_P(G)$	
metal	TPPLO	DPPL0
K	16.22	16.40
Na	15.75	16.11
Li	14.95	15.25

TPPLO reacts with all three metals in both DME and THF to give the same monoanion, the only differences in the spectra arising through ion-pairing effects. This is in direct contrast to the complex situation with TPPO, in which a number of signals have been reported (Chapter I). The more recent work of Cowley and Hnoosh⁵⁴ suggested a different radical in each solvent: $(C_6H_5)_3PO^{\cdot-}$ in THF (28-line spectrum)

and $(C_6H_5)_2PO^{\cdot-}$ in DME (10-line spectrum). Kabachnik⁹³ reported a 12-line spectrum in THF, which may be a poorly-resolved version of Cowley's signal, and Hofmann and Tesch⁹¹ reported biphenyl anion signals on reaction with Li and Na in DME; an unidentified 11-line signal was obtained with K. Clearly, TPPO undergoes phenyl cleavage much more easily than TPPL, and this reaction is apparently highly metal- and solvent-dependent. This difference is analogous to that found between TPPL and TPP, and can again be ascribed to increased stability of the anion arising from increased conjugation over the phosphole ring.

The failure to prepare cations from any of the phospholes is not too surprising. The only phosphine cations prepared and characterised so far¹⁰⁵ have had electron-donating amino and methoxy substituents present, giving the compounds lower oxidation potentials. No such substituents were present in any of the phospholes used, and it was not possible to obtain any such phospholes.

Unfortunately, it is not possible to compare the spin distributions in these anions with those of the corresponding pyrroles, since no ESR data is available on the simpler pyrroles. The only data available on radicals containing a pyrrole ring is on the dianions of carbazole and 4,5-iminophenanthrene.¹⁷³ No comparison is possible with proton splittings, but the former has zero nitrogen splittings and the latter a 0.6G splitting. This is in good agreement with McLachlan calculations, which predict near-zero nitrogen spin densities.

Thus, as in the phospholes, very small heteroatom spin densities are predicted, but the low nitrogen splitting is in direct contrast to the high phosphorus splitting.

(iii) Q-values

The phosphorus splittings and calculated phosphorus spin densities for the phospholes studied here and the phosphines studied by Cowley are presented in Table XXIX, along with the effective phosphorus Q-values calculated from this data using a one-parameter equation. (The phosphole spin densities were calculated by the McLachlan method, the phosphine spin densities by the Hückel method.)

TABLE XXIX

	a_P	$\rho_P(\text{calc})$	$ Q^P(\text{eff})^- $
MeDPPL	23.5	-.035	671.4
TPPL	26.5	-.034	779.4
Phosphine A	7.8	.22	35.5
Phosphine B	5.25	.21	25.0
Phosphine C	7.9	.285	27.7
Phosphine D	8.75	.421	20.8
Phosphine E	7.2	.233	30.9
Phosphine F	5.7	.194	29.4

As expected, the low phosphole spin densities predict Q-values which must be regarded as erroneous. Even taking into account the relatively high spin densities of 0.2-0.3 on the adjacent carbon atoms

will not lower this anomalously high value sufficiently.

The only possible estimation of Q-values must therefore be made from the phosphines. As may be seen from the table, quite consistent effective Q-values are obtained, the average of the values in the range 20.8G-35.5G being 28.2G. As can be seen from Table II (page 87 supra), the adjacent carbon spin densities are low, and will not affect these Q-values significantly. (However, the Q_{CP}^P terms cannot be estimated.) In phosphines C, D and E, the spin densities on the oxygen and nitrogen are quite high, and could have some influence on the phosphorus splittings. However, it is not possible to estimate the terms Q_{OP}^P and Q_{NP}^P , and it is likely that even if these terms were taken into account the revised Q(eff) values would still fall in the above range. These Q-values will be discussed in more detail in Section 4.

2. Radicals from Phosphorins

(a) Structure

The most striking feature of these radicals is the great ease of preparation compared with other phosphorus systems. No special precautions such as low temperature, very high vacuum or very clean metal mirrors were necessary; some of the cations were prepared at pressures of 10^{-2} - 10^{-3} torr. The anions were stable at room

temperature out of contact with potassium; on further reaction, TPPN went through the dianion to the trianion, DTBPPN stopped at the dianion (probably), and TTBN stopped at the monoanion. The cations, kept in contact with $\text{Pb}(\text{OAc})_4$ eventually gave a yellowish precipitate, but only after about 48 hours. This stability is typical of a system with extensive π delocalisation; coupled with the large phosphorus splitting, this suggests that the phosphorin ring can be regarded as a true aromatic system.

The cations are notable for their extremely narrow lines which, in the case of DTBPPN and TTBN, gave resolution which was at the limits of the spectrometer detection system. No attempt was made here to completely resolve these spectra using the superheterodyne detection system, since this would only have resolved the incomplete overlap of the smallest splittings. The high line-widths of the anions prevented any estimation of most of the proton splittings, and probably arose from electron exchange between the anion and the neutral molecule.

The calculated Q-value for the ortho t-butyl groups in TTBN of 0.85G is in good agreement with that of 0.84G found from the 2,4,6-tritertiarybutylphenoxy radical. The ortho Q-value from DTBPPN of 0.75G is also in good agreement. The para Q-value of 2.0G is rather high; some of this could be due to inaccurate spin densities or estimated splitting constants, but it is possible that, as in the corresponding phenoxy radical, some interaction with the ortho groups

is occurring. This could possibly happen by overlap with the phosphorus d-orbitals, which would be sufficiently diffuse to allow this.

Trapp et al.,¹⁴³ using the C-Y-Z hyperconjugative model, estimated a t-butyl Q-value from the equation

$$a(\text{Bu}^t) = \frac{1}{8} Q_{tZ} \quad . . . (65)$$

The work on monosubstituted semiquinones suggested Q_{tZ} values of about 44G. The present work, using the same parameters, gives values of 33G for the ortho groups in both phosphorins, and 90G for the para group in DTBPPN. This would suggest that the ortho results are, in fact, correct, and that the para results are anomalous. Therefore, although the phosphorus d-orbitals may still be involved, it does appear that the high para Q-values must result largely from inaccurate spin densities or an incorrect assignment; the former seems the more likely.

Both theoretical models for the t-butyl groups in the McLachlan calculations appear reasonable. On account of its greater simplicity, the inductive model would seem to be of most value in calculating ring spin distributions, but if an estimation of the π spin density in the t-butyl group is needed, the hyperconjugative model is useful.

The phosphorus splitting constants in the cations and anions are presented in Table XXX, together with the calculated spin densities. (The spin densities presented for TPPN are set 1 as in Table VIII, page 95 supra, the set 2 cation results being in brackets. For

DTBPPN and TTBPn the inductive model results in Tables IV and VI, pages 91 and 92 supra, are used.) Neither the splittings nor the McLachlan spin densities show any simple variation with the structures. The anion splittings show a decrease as the number of phenyl rings decreases, but this is not paralleled by the McLachlan spin densities. However, analysis of these splittings, discussed in the next section, suggests that the spin densities on the adjacent carbon atoms have a significant effect.

TABLE XXX

Phosphorin	Cation		Anion	
	a_P	r_P	a_P	r_P
TPPN	24.21	.127(.221)	32.90	1.063
DTBPPN	24.14	.228	30.40	.779
TTBPn	26.70	.329	26.91	1.067

It is difficult to give an interpretation of the ring twist parameters of greater than 1 in TPPN and DTBPPN. As mentioned previously this parameter, which may indicate a high degree of conjugation, cannot be explained by a short C-C bond. Since a similar bond parameter is also necessary to explain the spectra of the phosphole anions, this may be a peculiarity of these phosphorus heterocycles. Although this may be a result of d-orbital participation, there is no direct evidence for this, and it seems likely that this parameter represents the limitations of the simple McLachlan theory. It is, however, significant that the cation and anion calculations do give the expected agreement with the

spectra of the cations and anions. Thus the peculiar situation found in the phosphole calculations, where agreement with the "wrong" orbital is found, is not typical of all phosphorus systems. Certainly, there is little doubt that the phosphorins, at least, are true aromatic compounds.

TABLE XXXI

Atom	(a)	(b)	(c)	(d)
3	2.40	1.75	1.68	1.99
8	2.40	1.75	2.10	1.47
9	.70	.64	.84	.63
10	2.40	1.75	2.52	1.70
14	.70	.70	1.26	1.05
15	.50	.37	.42	.42
16	.70	.70	1.26	1.05

It is interesting to compare (Table XXXI) the proton splitting constants in the TPPN cation (a) with those in the radicals 2,4,6-triphenylphenoxy (b),¹²² 2,4,6-triphenylpyryl (c)¹⁷⁴ and 2,4,6-triphenylthiapyryl (d).¹⁷⁵ Although the radicals are not strictly analogous, since (b), (c) and (d) are all neutral, the table does show that the spin distributions in all four radicals are similar. The magnitudes of the splittings are somewhat different in (a) and (b), but both radicals have very little spin density in the 2,6-phenyl rings; the ring twist found here for (a) of 45° is very close to that of 46° found for (b). The higher phenyl ring spin densities in (c) and (d) are interesting since the McLachlan calculations predict twists of 42° for both of these. The 4-phenyl ring twists for (b), (c) and (d) are

found to be 0° , 28° , 31° respectively. In this respect, (a) and (b) are again comparable. It is interesting to note that McLachlan calculations using Longuet-Higgins' d-orbital model for sulphur¹⁷⁶ were performed on (d), and that no improvement was found over the ordinary p-orbital model.

Unfortunately, no pyridine radical ions of comparable structures have been prepared. The simplest pyridine anions studied so far have nitrogen spin densities of about 0.2-0.3, and near-zero spin densities at 3,5. The spin distributions would therefore appear to be somewhat different in the phosphorin anions.

(b) Q-Values

The effective phosphorus Q-values, calculated using a single parameter equation, are shown in Table XXXII. (The figures in brackets have the same significance as those in Table XXX.) The cation Q-values are consistently larger than the anion Q-values, but the values in each set are spread over a wide range.

TABLE XXXII

	$ Q^P(\text{eff})^+ $	$ Q^P(\text{eff})^- $
TPPN	190.6(109.5)	30.8
DTBPPN	105.9	39.0
TTBPN	81.2	25.3

The calculation of the Q_{PP}^P , Q_{CP}^P values from a two-parameter equation was more tricky. Ideally, the best method would have been to perform a least-squares analysis of the 3 equations referring to the cations

and the 3 equations referring to the anions. In this way Q-values typical of the cations and typical of the anions would be obtained. This would give some information on the effect of charge on the Q-values, and also provide a comparison with the Q-values calculated from the single-parameter equation. Unfortunately, the equations in each set were almost dependent, and values found were subject to such large errors as to make them meaningless. It was therefore only possible to solve the equations in pairs for each phosphorin, neglecting possible charge effects. The results are presented in Table XXXIII. The values are fairly consistent within the limits of the accuracy of the calculations, and suggest a substantial adjacent atom effect.

TABLE XXXIII

	$ Q_{PP}^P $	$ Q_{CP}^P $
TPPN	40.8(40.0)	34.7(31.9)
DTBPPN	46.9	23.9
TTBPN	29.8	27.3

3. CNDO Calculations

The calculations on the individual species are discussed here. A more general discussion is left to Section 5.

(a) PH, PN, PO

PH: The optimised length of 1.51 is rather higher than the experimental length and the length found from the more accurate calculations, but is still encouragingly close. An interesting point is the high charge density predicted on the proton. The highest orbital is predicted to be

non-bonding, the electrons located in the phosphorus px and py orbitals.

PN: This divergence may well be an artifact of the SCF procedure, but changing the programme to single precision may also contribute to this.

PO: The divergence problems have prevented a good optimisation. The charge shifts are much more exaggerated than those calculated by Boyd and Lipscomb. Calculations with these authors' bond length of 1.44 still gave much larger shifts. The phosphorus 3p s.d. of 0.835 would give a splitting of about 80G assuming a Q_{PP}^P of about 100G (see below). It is unlikely that the s.d. of 0.059 in the 3d orbitals would have any effect at all on the splittings.

(b) PH₃, PF₃

PH₃: The closeness of the charge densities and dipole moment to those calculated by Pople are sufficient to vindicate the use of single precision in this programme. The differences in the charge densities predicted in the two ab initio calculations makes comparison with the CNDO calculations difficult. However, the higher d-orbital population in the latter suggests that the d-orbital exponent may be incorrect, exaggerating the influence of these orbitals. (The more extensive basis set of Lehn and Munsch, together with the geometry optimisation, suggest that this should be the more accurate.) Geometry optimisations performed on the unknown radicals PH_3^+ , PH_3^- suggested that the

former should have a bond angle of 110° , the latter the neutral molecule bond angle of 92° . The latter result is of particular interest since it predicts that the phosphole anions should be pyramidal about the phosphorus (see Section 1(b)(ii)).

PF₃: Comparison of these results with Pople's results again vindicates the use of single precision. These results again show exaggerated d-orbital charge densities compared with the ab initio results. The calculations on PF_3^- , predicting a planar geometry, are in contrast to the predicted pyramidal geometry for PH_3^- (Section 1(b)(ii)).

(c) PH₂, NH₂

The optimised angles are in excellent agreement with experiment. The optimised NH bond length is significantly better than the PH length; this may be expected since no attempt has been made to optimise parameters for the second-row elements (Section 5). An interesting point is the high charge density of 1.09 on the protons in PH_2 , compared with the lower value of 0.92 for NH_2 , despite the higher 3s population in PH_2 .

The unit s.d. in the px orbital, together with the experimental splittings⁷⁷ of $a_P = 80\text{G}$, $a_H = 18\text{G}$, gives the Q-values

$$Q_{PP}^P = 80\text{G}, \quad Q_{PH}^H = 18\text{G}$$

The value of Q_{PP}^P is significantly higher than calculated from the

phosphorins and phosphines, but some difference may be expected, since this radical is neutral, and the phosphorus is in a very different environment. This may be seen in the NH_2 case; the splittings¹⁷⁷ of $a_{\text{N}} = 10.3\text{G}$, $a_{\text{H}} = 23.9\text{G}$ give $Q_{\text{NN}}^{\text{N}} = 10.3\text{G}$, $Q_{\text{NH}}^{\text{H}} = 23.9\text{G}$. Although the latter value is close to the values of 27-33G found previously from the spectra of heterocyclic nitrogen anions, the Q_{NN}^{N} value is much lower than that of 27G found in these systems.

IBMOL ab initio calculations have also been performed on NH_2 .¹⁷⁸ Using an optimised angle of 100° , and NH length of 1.02, the calculations predicted a charge density of 7.105 on N, and 0.948 on H. (The larger value on N is due to inclusion of the 1s electrons.) Considering the approximate nature of the CNDO theory, these results are in quite good agreement.

(d) PF_2 , NF_2

The optimised PF bond length of 1.73 is significantly higher than the experimental bond length in PF_2H ,¹⁷⁹ for example. However, this length is exactly the same as found experimentally in $\text{HPF}_6 \cdot 6\text{H}_2\text{O}$ and $\text{NaPF}_6 \cdot \text{H}_2\text{O}$.¹⁵¹ The NF bond length of 1.23 is well below that found spectroscopically (1.37), but the bond angles are in good agreement. As would be expected, the F atoms in PF_2 carry a high charge; this charge shift is significantly greater than that in NF_2 .

Comparison with experimental splittings of $a_{\text{P}} = 36\text{G}$, $a_{\text{F}} = 60.5\text{G}$ ⁷⁴ and $a_{\text{P}} = 47\text{G}$, $a_{\text{F}} = 65\text{G}$,⁷⁵ indicates that, if only the high

phosphorus 3p spin density is considered, the Q_{PP}^F value would be about 38G, which is much smaller than that found from PH_2 . However, a very recent reinvestigation of the PF_2 radical by Gordy et al.¹⁸⁰ puts the previous experimental splittings in doubt. These authors observed the isotropic spectrum of PF_2 produced by γ -irradiation of PF_3 in a xenon matrix, and found the splittings $a_P = 84.6G$, $a_F = 32.5G$. These are very different from the previous values and, again considering only the phosphorus 3p spin density, lead to $Q_{PP}^F = 90.3G$, which is very close to that found for PH_2 . The fluorine 2p spin density leads to a Q_{FF}^F of 1195G, which is almost certainly too high, since the high phosphorus 3p spin density must contribute to the fluorine splitting. Assuming a Q_{FF}^F value¹⁸¹ of +146G, this leads to $Q_{PF}^F = +30.5G$.

The NF_2 spin densities, together with the experimental splittings¹⁸² $a_N = 16.3G$, $a_F = 60G$, lead to $Q_{NN}^N = 19.9G$ (neglecting the fluorine s.d.), quite close to the values found from heterocyclic anions. Again using a Q_{FF}^F value of +146G, Q_{NF}^F is found to be +57G.

The spin densities calculated here are in good qualitative agreement with those calculated by Wei⁷⁵ in an extended Hückel calculation, and also presented in Table XIV (page 110 supra). (These authors found the results to be insensitive to the geometries, and used the experimental geometries.) Although the Hückel calculations predict lower phosphorus spin densities than calculated here, both calculations agree that the phosphorus s.d. in PF_2 is higher than the

nitrogen s.d. in NF_2 , despite the greater electronegativity difference between F and P than between F and N. Thus, the bonding electrons are shifted more to F (giving a higher charge density on F), but the unpaired electron is more localised on the central atom.

(e) PCl_2

Although the energy minimisation was poor, the calculated spin densities were fairly insensitive to geometry variation. The optimised PCl length of 1.95 is quite close to the 2.04 length found in PCl_3 , and the average PCl length of 1.98 estimated by Corbridge.¹⁵¹ The s.d. in the phosphorus 3px orbital, when compared with the experimental splittings⁷⁶ of $a_P = 70\text{G}$, $a_{\text{Cl}} = 5\text{G}$, suggests $Q_{\text{PP}}^{\text{P}} = 97.5\text{G}$. This is in remarkably good agreement with the values found from PH_2 and PF_2 . The phosphorus d-orbital spin density of -0.03G will have little effect on the phosphorus splitting, but the chlorine d-orbital spin density of 0.03 may contribute to the chlorine splitting. However, no separate estimation of the d and p polarizations is possible. The effective $Q_{\text{ClCl}}^{\text{Cl}}$ value is then 33G , but this should be modified to allow for the phosphorus spin density.

The energy improvement as the bond angle decreases must be ascribed to the limitations of the theory. This is not very surprising since all three atoms have d-orbitals, and any errors resulting from the inclusion of these orbitals will be magnified.

An interesting point is that the calculated total charge densities

are almost exactly the same as for the separate atoms, and are totally insensitive to geometry variation. The only charge shifts to occur are between the different orbitals on the same atom: on phosphorus, the main shift is $p \rightarrow d$, on chlorine $s \rightarrow d$.

(f) PF^+ , PF^-

Taking the series PF^+ , PF_2 , PF^- the optimised bond lengths of 1.69, 1.73, 1.76 are in the order expected for a system in which electrons are being added to antibonding orbitals. However, it is not possible to correlate the calculated spin densities with the experimental splittings (697G, 168G) for either species. Since both radicals are predicted to be π radicals, correlation would lead to abnormally high Q-values, whichever splitting is assigned to each atom. For instance, assigning the 697G splitting to F would give effective Q-values of about 35,000 for F, and about 172 for P. Although the true Q_{FF}^F value may well be different owing to neglect of the phosphorus s.d., both of these values are much too high. The alternative assignment also gives high values. These calculations therefore support Fessenden's findings⁷³ that the spectrum cannot be assigned to either of these species. An interesting point is that on adding 2 electrons to PF^+ to give PF^- , only 0.25 of the electrons go on to the fluorine atom; the rest go mainly into the phosphorus 3p orbitals.

(g) $\underline{\text{PF}}_4$

(Fessenden and Schuler⁷¹ found splittings of $a_P = 1330\text{G}$, $a_{F(1)} = 282\text{G}(2\text{F})$, $a_{F(2)} = 59\text{G}(2\text{F})$. More recent work by Gordy¹⁸⁰ on PF_4 produced on β -radiolysis of PF_3 gave the values $a_P = 1391\text{G}$, $a_{F1} = 380\text{G}$, $a_{F2} \leq 45\text{G}$.)

Assuming an observed phosphorus splitting of 1330G , the $3s$ orbital spin density is then $1330/3628.6 = 0.367$. This value is in excellent agreement with that found in these calculations, using a PF_2 bond length of 1.73 , and was fairly insensitive to the bond angles. However, the fluorine splittings are not predicted well. For all the bond angles tested, the ratio of the s -orbital spin densities between the two sets of two equivalent fluorines never exceeded 2, and this ratio was only reached when the values of the spin densities were almost zero. Bond lengths of 1.57 and 1.73 were tried, but neither gave an improved ratio. (The bond length of 1.57 was as used by Higuchi,¹⁵⁸ and gave phosphorus spin densities that were much too high.) The poor agreement is puzzling, since the simpler treatments of Higuchi produced fairly good agreement; here, valence bond and extended Hückel calculations were performed, and the optimum bond angles were found in both to be about 174 and 109 , the larger angle being that between the fluorines with the larger splitting. These angles were optimised by comparing the calculated splitting constants (as found from the s -orbital densities) with the experimental phosphorus splitting and the larger fluorine splitting. The smaller fluorine splitting was

assumed to arise via spin polarization by the phosphorus spin density, and was estimated to be between 0 and 55G by comparison with the fluorine splitting in PF_2 . The more recent splittings of Gordy also fitted in with Higuchi's calculations, suggesting angles of 180 and 102. Although the estimated contribution to the splittings from adjacent atom spin densities may be in error (owing to the more recent results on PF_2), these calculations are successful in predicting the large difference between the two pairs of fluorines.

The poor agreement with the CNDO calculations may be due to the use of an incorrect 3d exponent or other parameterisation errors, but if this were the case, a poor phosphorus 3s spin density would also be expected. Even if it is assumed that the fluorine 2p spin densities contribute significantly to the splittings, the similarity of these spin densities (although those on F_1, F_2 are slightly higher than those on F_3, F_4) still does not give the desired ratio of splittings. Another possible contribution to the fluorine splittings can arise from spin polarization by the spin density on the phosphorus. However, this should be the same for all 4 fluorines.

Inaccuracies introduced by rewriting the programme in single precision may provide an explanation for the poor agreement. Since the spin density matrix is formed by taking the difference of the alpha and beta bond order matrices, an error in the third decimal

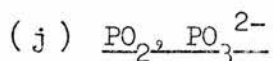
place in each of these matrices could easily cause a serious error in the low spin densities calculated for the fluorines. Although it is unlikely that this alone would wholly explain the poor spin densities, this coupled with the above considerations could explain the poor agreement.

(h) PCl₄

The experimental splittings⁷⁶ of $a_P = 1206G$, $a_{Cl(1)} = 62G$ ($2Cl$), $a_{Cl(2)} = 7G$ ($2Cl$) suggest a phosphorus 3s spin density of $1206/3628.6 = 0.332$. The calculated spin density of 0.268 is slightly lower than this, although the 3p spin density of 0.186 may contribute to the splitting. By analogy with the variation of the 3s spin density and the PF bond length in PF_4 , this may indicate that the bond length of 1.95 is slightly low. As with PF_4 , the calculations do not predict the high ratio between the 3s spin densities on the two sets of chlorines. Moreover, the highest chlorine 3s spin density calculated for any geometry was 0.002, which is too low by a factor of 20 to give the 62G splitting.

In view of the poor convergence encountered, and the inclusion of 3d orbitals on all five atoms, it is perhaps to be expected that the agreement with experiment will be poorer than with PF_4 . It is again puzzling why the phosphorus 3s spin density is reasonable and the chlorine densities are poor. One contributing factor here may be the effect of the chlorine 3p densities; for all geometries, the

3p spin density on Cl_1 , Cl_2 was about 0.2, and that on Cl_3 , Cl_4 about 0.02 to 0.05. This difference is much greater than that in the fluorine 2p orbitals in PF_4 . Again, polarization of the chlorine 3s orbitals by the phosphorus spin densities should be the same for all four atoms. However, the factor of 20 difference between theory and experiment is difficult to explain even if all the above considerations are taken into account.

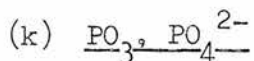


The PO_2 radical was postulated⁶ as a possible, but unlikely, alternative to PO_3^{2-} . Although the bond length used for PO_2 is not the optimised length, the phosphorus 3s spin density of 0.186 is comparable to that calculated from the splittings in the spectrum tentatively assigned to PO_3^{2-} ; the experimental splitting⁶³ of 593G gives a value of 0.163. Therefore these CNDO calculations indicate that, judging by the isotropic splittings alone, the radical could indeed be PO_3^{2-} . However, Symons and Atkins consider it unlikely that this radical would be formed; the anisotropic splittings and g-tensor bear a great resemblance to those found for ClO_3 produced in irradiated perchlorates.¹⁸³

The 3s spin density of 0.205 calculated for PO_3^{2-} is also in good agreement with the experimental value of 0.163. The contributions from spin polarization by the phosphorus p and d spin densities

and the oxygen p spin densities must be small compared with the large direct s spin density.

One very unusual result is that the calculations predict a planar molecule, whereas from consideration of Walsh's rules¹⁸⁴ a pyramidal molecule would be expected. Even more unusual is the increase of s-orbital spin density as the molecule becomes more planar. This may indicate a breakdown of Walsh's rules by inclusion of the d-orbitals; this possibility has been discussed previously.¹⁸⁵



The PO_3 radical was postulated as a possible alternative to PO_4^{2-} , since the phosphorus splitting of the latter varied considerably depending on the irradiated matrix. The average experimental splitting of 30G gives a 3s density of 0.008. This is very close to the calculated value of 0.0075, but the accuracy of this low value must be in some doubt. (The relatively high phosphorus p and d spin densities and oxygen p densities may also have some significant effect via spin polarization.) This calculation alone, therefore, suggests that PO_3 may well be an alternative to PO_4^{2-} . As with PO_3^{2-} , these calculations predict a planar molecule with decreasing s spin densities as the molecule becomes pyramidal.

Symons¹⁸⁶ has recently rationalised the available data on the PO_4^{2-} splittings and has found the splitting for the undistorted PO_4^{2-}

radical to be 30G. The 3s spin density of 0.008 found from this is not in good agreement with the calculated spin density of -0.04, but, as described in Chapter III, the calculated results must be regarded as doubtful. The convergence was close but not complete and the resulting charge and spin densities on the oxygens were totally asymmetric. A variation of the results with the axes chosen was also found, but this may be due to the incomplete convergence. An interesting point is that all the calculations performed predicted a negative 3s spin density on phosphorus.

The multiplicity of splittings reported for this radical were rationalised by Symons as arising from PO_4^{2-} , various distorted forms of this or from other species such as HOPO_3^- , $(\text{OH})_2\text{PO}_2$, $\text{P}_2\text{O}_7^{2-}$ etc. In view of this confusion it is not possible to draw any further conclusions from these calculations.

(m) HPO_2^-

The experimental splittings^{64,67} of $a_P = 500\text{G}$, $a_H = 82.5\text{G}$ give a phosphorus 3s spin density of $500/3628.6 = 0.138$, and a proton 1s spin density of $82.5/508 = 0.162$. The calculated spin densities are both higher than these; the phosphorus s.d. is close, but the proton s.d. is too high. However, the calculations do predict the unusually high proton splitting. An interesting feature is the relatively high phosphorus d-orbital spin density; this may have

some effect on the splitting constants. Although the calculations predicted the expected pyramidal geometry, the s-orbital spin density again increases as the molecule becomes more planar, as with PO_3 and PO_3^{2-} . Again, this could represent a breakdown of Walsh's rules by inclusion of d-orbitals. No evidence was found here for a "weak" PH bond, as discussed by Symons and Atkins.⁶ The values of the overlap integrals (which can give a rough description of bond strength) and of the bond orders between P and H were quite normal.

(n) FPO_2^-

This radical was originally thought to be PF^+ or PF^- , but work by Fessenden⁷³ suggested this structure. The experimental splittings deduced by Fessenden are $a_P = 698.5\text{G}$, $a_F = 168.6\text{G}$, suggesting s-orbital densities of $698.5/3628.6 = 0.193$ for phosphorus and $168.6/17200 \approx 0.01$ for fluorine. The calculated values of 0.152 and 0.008 are in very good agreement. The p and d spin densities on phosphorus and fluorine are unlikely to affect the splittings significantly, but the high oxygen 2p densities may affect the phosphorus splittings. However, these results do support Fessenden's reassignment. As in HPO_2^- , there is a relatively high spin density in the phosphorus d-orbitals. These calculations also predict an increase in the s-orbital spin densities as the radical approaches planarity.

(o) Phosphorine

The calculated spin densities for both the 2,4,6-trimethylphosphorin (2) and the 4-phenylphosphorin (3) models are in very poor agreement with experiment. The change in spin distribution on going from the phosphorin (1) anion to the anion of (2) is very small, and it is therefore unlikely that calculations on the t-butyl derivative would give a very different spin distribution. Similarly, it is unlikely that introducing the t-butyl groups into (3) would improve the spin densities.

In the cation of (2), the calculated s.d. at 3 is far too small; this is also the case for both the cation and anion of (3). The spin densities in (3) show none of the equalities needed to explain the experimental spectra. The only agreement at all, in fact, is in the magnitude of the phosphorus spin densities. Although the anion spin densities of about 0.6 are less than the unusually high McLachlan densities, both types of calculation agree that the cation spin densities should be considerably less, by a factor of 3 in the McLachlan calculations and a factor of 2 in the CNDO calculations. To some extent this does confirm the suspiciously high McLachlan spin densities. An interesting point is the near-zero phosphorus 3p spin density calculated for the trianion of (1), as no obvious phosphorus splitting is observable in the trianion of TPPN. In fact, the relatively high 3d spin density of 0.19, if also present in the TPPN

anion, could give rise to an observable splitting by d-s spin polarization. (The 3d densities calculated for the other radical ions are all small compared with the 3p densities.)

Twisting the rings in (3) makes very little difference to the phosphorin ring spin densities, and only changes the phenyl ring spin densities. It is difficult to explain why the energy minimum at 0° twist is so much better than at 30° twist, unless this is due to neglect of some crucial integrals. This situation is similar to that found with PCl_2 .

The poor agreement with experiment cannot be ascribed wholly to errors arising from the CNDO approximations accumulating in the calculations on these relatively large molecules, since test calculations on the pyridine cation and several polynuclear hydrocarbons gave excellent agreement with other, more accurate calculations and with experiment. The errors would then appear to arise from either inclusion of the d-orbitals (Section 5) or from the use of incorrect geometries. Although the geometries were taken from X-ray work, the properly optimised geometries may be very different from these. This may be seen in the calculations on the smaller radicals, the bond lengths in particular being in some error.

(p) Phospholes

All the calculations predict that the highest filled orbital in the

neutral molecule and anion is a π orbital, and that the lowest empty orbital is a σ orbital. This must be the result of the calculations producing incorrect eigenvalues, with consequent incorrect ordering of the orbitals. This has been found before in CNDO calculations; for instance, the ordering of levels $\dots(\pi)^2(\sigma)^0$ in borazine predicted¹⁸⁷ by ab initio calculations is predicted by CNDO calculations to be $\dots(\sigma)^2(\pi)^0$. Del Bene and Jaffé¹⁸⁸ have suggested a scheme involving different parameterisation for σ and π orbitals to overcome this problem.

Incorrect ordering of this sort may therefore be ascribed to the limitations of the theory. It is unlikely that it is due to incorrect geometries, even though these were only guesses, since the two very different geometries used did not give large changes in the eigenvalues (Table XXXIV).

TABLE XXXIV: Eigenvalues for Neutral Phospholes

Geometry	Highest filled	Lowest empty
(i)	-.3647	-.0085
(ii)	-.3423	.0105

4. Q-Values

As outlined in Chapter I, the phosphorus Q-value question presents several difficulties not encountered with nitrogen. One problem is

whether spin-polarization by d-orbital spin densities can contribute to the splittings, as well as spin-polarization by the p-orbital spin densities. There is also the problem of whether the L-shell orbitals can be disregarded; in this respect, the 2s orbital is particularly important, since spin polarization of electrons in this orbital would contribute a large amount to the splittings. In the calculations performed in this work, no information can be obtained directly on the effect of this inner shell.

The McLachlan calculations cannot give directly any information on possible participation of the phosphorus d-orbitals, since no model has been proposed for a phosphorus atom with d-orbitals as has been done for sulphur.¹⁷⁶ The work of Vilceanu in this respect must be treated with some reserve. Of the two models found consistent with experimental results, the Fukui model is the same as the normal Hückel model used here, with slightly different parameter values; this will therefore give no further information. The Dewar model probably does not provide a realistic picture of a system with trico-ordinated phosphorus. Therefore, the only indication of d-orbital participation can come from anomalous results. Although some results could be explained by the effect of d-orbitals (such as the spectra from MeDDPL/K/THF, ion-pairing with the phosphole oxides and the t-butyl Q-values in the phosphorin cations) the evidence was very tenuous, and most of the results in this work could be explained without recourse to this.

The d-orbital spin densities calculated by the CNDO method are, in general, small compared with the s and p spin densities. Although no figures are available, it may be expected that spin polarization by an electron in a d-orbital will be less important than by an electron in a p-orbital. In σ -radicals, where there is a direct s-orbital density, this effect will be negligible. (One exception here may be the PO_3 radical - Table XX - where the s-orbital density is very small and the d-orbital density relatively high.) To a first approximation, therefore, the d-orbitals may be disregarded in the Q estimations.

The radicals PH_2 , PF_2 , PCl_2 give Q_{PP}^{P} values of 80G, 90G and 98G respectively. Since the spin densities in these smaller radicals should be subject to only small errors, these may be regarded as accurate to within about 20% or less. It is not clear if the increase of Q_{PP}^{P} as the atom X changes is significant. The value of Q_{PH}^{H} of 18G may also be regarded as fairly accurate.

The estimation of other Q_{PX}^{X} values is open to error, owing to conflicting values of Q_{XX}^{X} . The value of Q_{FF}^{F} is open to some doubt, but the value of 146G found for neutral radicals should not be too much in error; the Q_{PF}^{F} value so calculated from the data on PF_2 is 30.5G. Unfortunately, no data is yet available for the estimation of $Q_{\text{ClCl}}^{\text{Cl}}$ values. The chlorine splitting of 5G in PCl_2 is extremely small, and gives a Q(eff) of 4G; it is not possible to judge how

much of this arises from the high phosphorus s.d. The radicals PF^+ , PF^- are the only other radicals predicted to be π radicals, and, as shown previously, the experimental spectrum must be assigned to FPO_2^- . Since all the other radicals are of the σ -type, it is not possible to separate the direct s spin density contribution from that arising via spin polarization mechanisms.

The $Q(\text{eff})$ values calculated from the phosphine anion spectra are remarkably consistent. The effect of the spin density on the oxygen and nitrogen atoms in C, D and E can probably be neglected, since the $Q(\text{eff})$ values calculated are of the same magnitude as those calculated from A, B and F; in the latter radicals, the low adjacent carbon spin densities means that these $Q(\text{eff})$ values are, in effect, Q_{PP}^{P} values.

The $Q(\text{eff})$ values of the phosphorin anions (average value 29.5G) are in very good agreement with those of the phosphine anions (average value 28.2G). However, although the $Q(\text{eff})$ values of the cations (average value 121.8G) are all significantly larger, the wide spread here indicates that the calculated spin densities may be suspect. The higher values of $Q(\text{eff})^+$ are analogous to the higher values for the cations of fluorinated systems,⁴⁴ where $(Q_{\text{FF}}^{\text{F}})^+$ is double that of $(Q_{\text{FF}}^{\text{F}})^-$. Although no conclusive calculations have been made, it seems likely that, for the fluorine case, the difference arises from an excess charge effect. It is possible that the same situation

holds in the phosphorus case; the increased positive charge would have the effect of contracting the orbitals. This may, in fact, contract the d-orbitals to such an extent that they are able to contribute to the bonding in the molecule.⁵³ However, as is the case with so much work on second-row systems, this is pure speculation, and there is no direct evidence in these systems for this phenomenon. This variation with charge, if real, is not found to the same extent with nitrogen. In the 1,3,6,8-tetraazapyrene system,⁴⁸ the $Q(\text{eff})$ values are $Q(\text{eff})^+ = 15\text{G}$, $Q(\text{eff})^- = 27\text{G}$. These values are calculated from spin densities that can not be regarded as accurate, but certainly the higher value of $Q(\text{eff})^+$ found for phosphorus and fluorine is not found here.

It is unfortunate that this charge effect cannot be checked by using a two-parameter equation. The values $Q_{\text{PP}}^{\text{P}} = 39\text{G}$, $Q_{\text{CP}}^{\text{P}} = 28.6\text{G}$ must be regarded as mean values between the cations and the anions. However, these values do indicate that there is a substantial contribution from the adjacent atoms. This relatively important term is much larger than the near-zero Q_{CN}^{N} values found experimentally and calculated theoretically. Although the magnitude of Q_{CP}^{P} is comparable to that of the analogous term for ^{13}C , it is interesting to note that the sign is the same as that of Q_{PP}^{P} , the opposite being found for ^{13}C .

The differences between the Q_{PP}^{P} values found for the organic

radicals and for the inorganic radicals may be partly explained by the fact that the latter are all neutral radicals. In fact, the Q_{PP}^P values for these radicals lie between the $Q(\text{eff})$ values for the organic cations and anions. The very different structures may also account for this; the local environment of the phosphorus may be very important.

Unfortunately, direct calculation of phosphorus Q -values is, at the present time, out of the question. The models used in the calculation of nitrogen Q -values are approximate models, and do not give very good quantitative agreement with experiment. As has been stressed by Henning,⁴⁰ these calculations can only indicate the probable relative importance of the various excitations. In the case of phosphorus, the addition of a third shell increases the number of possible excitations enormously. A full treatment would also need to consider the possibility of excitations involving d -orbitals, and it is unlikely that the necessary integrals are available.

5. The CNDO Theory

The CNDO calculations presented in this thesis are the first of their kind to be performed on radicals containing second-row elements. Although the main reasons for performing the calculations on the small

radicals were to check the results before continuing on to larger radicals, and also to obtain some information on hyperfine splittings, Q-factors and geometries, it is now possible to comment on the suitability of this theory for these calculations.

The calculations on PH_2 and PF_2 give reasonable geometries and spin densities. In the case of PCl_2 , the peculiar geometry predicted must be ascribed to the limitations of the theory; the poor optimisation otherwise could result from the use of single precision. However, the calculated spin densities do seem reasonable. The calculations on PF_4^+ , PF_4^- involved no problems, but the failure of the calculation on PF_4 is disturbing. Owing to the poor minimisation, geometries other than the optimised geometry were tested, but no agreement with the fluorine splittings could be found. The good value for the phosphorus 3s spin density indicates that the theory has not broken down, but it is difficult to understand the poor fluorine spin densities in view of the reasonable values obtained from the simpler extended Hückel theory. The failure of the calculations on PCl_4 is less surprising; any errors in the parameterisation of the d-functions (see below) will be magnified with 5 second-row atoms present.

One of the most interesting aspects of these calculations is the apparent breakdown of Walsh's rules in the radicals PO_3 , PO_3^{2-} , HPO_2^- , FPO_2^- . It would be interesting to see if this breakdown is in fact a result of the inclusion of d-orbitals, as Walsh himself indicated

may happen. An attempt was made to modify the integral section of the programme to exclude the d-orbitals, but this was not found possible in the time available. Further work on this should prove interesting.

In general, therefore, the programme proved very useful in most of the calculations on small radicals. The tendency to mix together σ and π levels, as found in the phospholes, could possibly be reduced by introducing the type of parameterisation used by Del Bene and Jaffé.¹⁸⁸ This was done by using different β^0 values for σ orbitals and for π orbitals, with $\beta^\sigma = K\beta^\pi$. The parameter K was found empirically by comparison with spectroscopic data, and this modification proved very useful in interpreting such data. Jug¹⁴⁶ has taken this one step further and suggests separate evaluation of integrals involving σ and π orbitals.

The failure to predict good spin distributions in the phosphorins is not surprising, since no attempt was made to optimise any of the parameters β^0 , I or A. This programme used the original parameterisation of Santry and Segal.¹²⁸ This was later modified by Santry,¹²⁸ who corrected these parameters by reference to ab initio calculations on neutral molecules. Ideally, however, the parameterisation for radicals and for ions should be carried out by reference to accurate calculations on these systems, and may differ considerably from the above parameterisation for the neutral molecules. Although this

procedure must inevitably be time-consuming, it is imperative that this be done in order to produce meaningful results.

Perhaps potentially more serious than inaccurate parameterisation is the use of an incorrect d-orbital exponent. Santry and Segal compared the results using an sp basis, an spd basis (as used in the present work) and an spd' basis, in which the 3d-orbitals were given a lower exponent than the 3s and 3p orbitals, making the d-orbitals more diffuse. The results for the small molecules studied showed that the spd' basis was significantly better. It would be convenient, therefore, if the programme would allow variation of the d-exponents in order to study the agreement with experiment over a range of values. Unfortunately, usage of a d-exponent different from s and p exponents involves modifications to the calculations involving the coulomb integrals and the nuclear attraction integrals V_{AB} ; this was not possible in the programme used here. Coulson⁵³ has lucidly described the effect of charge on the radial part of the d-orbitals, and it is clear that allowance for variation of d-exponents would be of particular importance in calculations on charged species. For example, a more realistic calculation on phosphorins would use a higher d-exponent for the cation than for the anion.

One of the main premises of the CNDO theory is that the calculated results should be invariant to various transformations; the two simplest are axis rotation and hybridisation of orbitals on the

same centre. On inclusion of d-orbitals, the hybridisation invariance no longer holds. Jug¹⁴⁶ regards this as a serious drawback, and suggests that the results would be very unreliable. However, Jaffé¹⁴⁷ does not regard this as serious, but concludes that invariance to axis rotation is necessary. In several of the calculations presented here, a variation of the calculated results, such as total energy, charge and spin densities, has been found. Although this at first sight would indicate a breakdown of rotational invariance, this variation is found to be most serious in the larger radicals where, in general, the calculated spin densities are poor and the convergence is slow and oscillatory (e.g. PO_4^{2-}). This could well be due to numerical inconsistencies in the programme, possibly arising from the use of single precision. In fact, in many calculations extreme sensitivity to the input co-ordinates was found, which had to be quoted to more decimal places than the experimental values. This situation has also been found in at least one other SCF programme.¹⁵⁴ Before drawing any conclusions about rotational invariance, therefore, these calculations should be checked using the double precision programme with input co-ordinates of maximum accuracy.

6. Conclusions

The reaction of alkali metals with phospholes and phosphole oxides has been investigated. At low temperatures, the phospholes give stable monoanions, characterised by a large phosphorus splitting. The oxides give stable monoanions at room temperature. Comparison with previous work on phosphines and phosphine oxides shows the phosphole systems to be more stable. At room temperature, cleavage reactions occur, and an attempt has been made to characterise a closely related series of radicals so produced. Complete characterisation was not possible, but the radicals appear to result from the reaction of the benzene anion with AlH_3 impurity. Estimation of phosphorus Q -values was not possible from the phosphole spectra, but analysis of the phosphine spectra using a single-parameter equation gave a mean $Q(\text{eff})^-$ of 28.2G.

The cations and anions of three representative phosphorins have also been prepared, and most of the spectra analysed. McLachlan calculations gave excellent agreement with experiment. Analysis using a single-parameter equation gave Q -values of $Q(\text{eff})^+ = 121.8\text{G}$, $Q(\text{eff})^- = 29.5\text{G}$. Although these values are subject to large errors, they do suggest an excess charge effect. Corresponding analysis of each set of cations and anions using a two-parameter equation was not possible, but analysis of the cation and anion of each phosphorin gave mean values $Q_{\text{PP}}^{\text{P}} = 39\text{G}$, $Q_{\text{CP}}^{\text{P}} = 28.6\text{G}$.

The experimental and theoretical results suggest that both types of phosphorus heterocycle are aromatic, although the calculations on the phospholes produced some unusual results. No direct evidence for d-orbital participation in the bonding was found.

Calculations were performed on a large number of phosphorus radicals using a largely untried CNDO programme. Attempts were made to correlate experimental and theoretical spin densities, and also to compare calculated geometries with experimental geometries. For most of the radicals, the calculations were quite successful, but for a number of radicals such as PO_4^{2-} and PCl_4 the correlation was much poorer. Analysis of the series PH_2 , PF_2 and PCl_2 gave Q_{PP}^{P} values of 80G, 90G and 98G respectively. The calculations also supported the reassignment to FPO_2^- of the spectrum originally assigned to PF^+ or PF^- . Although it was not possible to perform the calculations without d-orbitals, the results did suggest that d-orbitals should have little effect on the ESR spectra. The calculations on the radicals PO_3 , PO_3^{2-} , HPO_2^- , FPO_2^- showed spin density variation with geometry not explicable by Walsh's rules, and this has been ascribed to the effect of the d-orbitals.

CNDO calculations on the anions of model phosphole systems predicted these to be σ -radicals, and calculations on model phosphorin cations and anions, although correctly predicting these to be π radicals, gave very poor spin distributions.

Attempts have been made to show that poor results may be due to inaccurate parameterisation in the CNDO programme, and it is suggested that parameterisation for radicals and ions should be made by comparison with accurate ab initio calculations. It is also suggested that the problem of the values to be used for the d-orbital exponent should be examined more closely.

It is apparent that much more work may still be done on the radicals described here, together with other related radicals. More ESR information on small (2-3 atom) phosphorus radicals would be interesting, together with accurate calculations on these species. Less substituted phospholes and phosphorins would provide better systems for radical ion formation, giving simpler spectra and providing better systems for performing calculations. The parameterisation of the CNDO programme needs to be carefully examined, particularly with regard to the best values to be used for the d-orbital exponents.

REFERENCES

1. D.E. Ingram, Free Radicals as Studied by Electron Spin Resonance (Butterworth's Scientific Publications, 1958).
2. P.B. Ayscough, Electron Spin Resonance in Chemistry (Methuen and Co., 1967).
3. A. Carrington and A.D. McLachlan, Introduction to Magnetic Resonance (Harper and Row, 1967).
4. E.T. Kaiser and L. Kevan (editors), Radical Ions (Interscience, 1968).
5. A. Carrington, Quart. Rev. 17, 67 (1963).
6. P.W. Atkins and M.C.R. Symons, The Structure of Inorganic Radicals (Elsevier, 1967).
7. E. Fermi, Z.Physik 60, 320 (1930).
8. S.I. Weissman, J.Chem.Phys. 22, 1378 (1954).
9. M.C.R. Symons, J.Chem.Soc., 2276 (1965).
10. C. Thomson and R.M. Paton, unpublished work.
11. S.I. Weissman, J. Townsend, D.E. Paul and G.E. Pake, J.Chem.Phys. 21, 2227 (1953).
12. H.M. McConnell, J.Chem.Phys. 24, 632, 764 (1956).
13. S.I. Weissman, J.Chem.Phys. 25, 890 (1956).
14. A.D. McLachlan, H.H. Dearman and R. Lefebvre, J.Chem.Phys. 33, 65 (1960).
15. M. Karplus and G.K. Fraenkel, J.Chem.Phys. 35, 1312 (1961).
16. J.C.M. Henning, J.Chem.Phys. 44, 2139 (1966).
17. T. Yonezawa, T. Kawamura and H. Kato, J.Chem.Phys. 50, 3482 (1969).
18. R.G. Parr, Quantum Theory of Molecular Electronic Structure (W.A. Benjamin, Inc., 1963).
19. A. Streitwieser, Molecular Orbital Theory for Organic Chemists (John Wiley and Sons, 1962).
20. F.L. Pilar, Elementary Quantum Chemistry (McGraw-Hill, 1968).
21. A.D. McLachlan, Mol.Phys. 3, 233 (1960).
22. J.D. Memory, Quantum Theory of Magnetic Resonance Parameters (McGraw-Hill, 1968).

23. R. Hoffmann, J.Chem.Phys. 39, 1397 (1964); 40, 3247, 2474, 2480 (1964)
24. IBM Research Laboratories, S n José, California, U.S.A.
25. Quantum Chemistry Programme Exchange no. 47.
26. H.S. Jarrett, J.Chem.Phys. 25, 1289 (1956).
27. S.Y. Chang, E.R. Davidson and G. Vincow, J.Chem.Phys. 49, 529 (1968).
28. J.-P. Malrieu, J.Chem.Phys. 46, 1654 (1967).
29. S.Y. Chang, E.R. Davidson and G. Vincow, J.Chem.Phys. 52, 1740 (1969).
30. R.W. Fessenden and R.H. Schuler, J.Chem.Phys. 39, 2147 (1963).
31. J.R. Bolton, J.Chem.Phys. 43, 309 (1965).
32. A.D. McLachlan, Mol.Phys. 2, 271 (1959).
33. J.R. Bolton and G.K. Fraenkel, J.Chem.Phys. 40, 3307 (1964).
34. J.P. Colpa and J.R. Bolton, Mol.Phys. 6, 273 (1963).
35. See ref. 4, page 13.
36. G. Giacometti, P.L. Nordio and M.V. Pavan, Theoret.Chim.Acta 1, 404 (1963).
37. See ref. 4, page 14.
38. R.E. Moss and G.K. Fraenkel, J.Chem.Phys. 50, 252 (1969).
39. C.L. Talcott and R.J. Myers, Mol.Phys. 12, 549 (1967).
40. J.C.M. Henning, Chem.Phys.Let. 1, 678 (1968).
41. M. Broze and Z. Luz, J.Chem.Phys. 51, 738 (1969).
42. (a) D.R. Eaton, A.D. Josey, W.D. Philips and R.E. Benson, Mol. Phys. 5, 407 (1962).
(b) D.R. Eaton, A.D. Josey, R.E. Benson, W.D. Philips and T.R. Cairns, J.Am.Chem.Soc. 84, 4100 (1962).
43. A. Hinchcliffe and J.N. Murrell, Mol.Phys. 14, 147 (1968).
44. C. Thomson and W.J. McCulloch, unpublished work.
45. P.V. Schastnev, G.M. Zhidomirov and N.D. Chuvylkin, Z.Strukt. Chim. 10, 998 (1969).
46. G.A. Russell and E.J. Geels, J.Am.Chem.Soc. 87, 122 (1965).
47. G. Cauquis, M. Genies, H. Lemaire and A. Rassat, J.Chem.Phys. 47, 4642 (1967).

48. F. Gerson, Helv.Chim.Acta 47, 1484 (1964).
49. See ref. 4, Chapter 4.
50. A.L. Allred and L.W. Bush, Tetrahedron 24, 6883 (1968).
51. P.H.H. Fischer and H. Zimmerman, Tetrahedron Let. 10, 797 (1969).
52. P.H.H. Fischer and J.P. Colpa, private communication quoted in ref. 181.
53. C.A. Coulson, Nature 221, 1106 (1969).
54. A.H. Cowley and M.H. Hnoosh, J.Am.Chem.Soc. 88, 2595 (1966).
55. A.H. Cowley, private communication.
56. G. Märkl, Angew.Chem. 78, 907 (1966).
57. K. Dimroth, N. Greif, H. Perst and F.W. Steuber, Angew.Chem.internat.Edit. 6, 85 (1967).
58. K. Dimroth and F.W. Steuber, Angew.Chem.internat.Edit. 6, 445 (1967).
59. K. Dimroth, N. Greif, W. Städe and F.W. Steuber, Angew.Chem.internat.Edit. 6, 711 (1967).
60. E.H. Braye and W. Hübel, Chem. and Ind., 1250 (1959).
61. L.D. Quin, J.G. Bryson and C.G. Moreland, J.Am.Chem.Soc. 91, 3308 (1969).
62. L.D. Quin and J.G. Bryson, J.Am.Chem.Soc. 89, 5984 (1967).
63. A. Horsfield, J.R. Morton and D.H. Whiffen, Mol.Phys. 4, 475 (1961).
64. N. Keen, Ph.D. thesis (Leicester, 1963).
65. M. Hanna and L. Altman, J.Chem.Phys. 36, 1788 (1962).
66. S. Schlick, B.L. Silver and Z. Luz, J.Chem.Phys. 52, 1232 (1970).
67. J.R. Morton, Mol.Phys. 5, 217 (1962).
68. (a) F. Jeffers, P.F. Wigen and J.A. Cowen, Bull.Am.Phys.Soc. 6, 118 (1961).
(b) E. Hughes and W.G. Moulton, J.Chem.Phys. 39, 1359 (1963).
(c) P.W. Atkins, Ph.D. thesis (Leicester, 1964).
69. J.R. Morton, Can.J.Phys. 41, 706 (1963).
70. P.W. Atkins and M.C.R. Symons, J.Chem.Soc., 4363 (1964).
71. R.W. Fessenden and R.H. Schuler, J.Chem.Phys. 45, 1845 (1966).
72. P.W. Atkins, Mol.Phys. 13, 37 (1967).

73. R.W. Fessenden, J.Magn.Resonance 1, 277 (1969).
74. J.K.S. Wan, J.R. Morton and H.J. Bernstein, Can.J.Chem. 44, 1957 (1966).
75. M.S. Wei, J.H. Current and J. Gendill, J.Chem.Phys. 52, 1592 (1970).
76. G.F. Kokoszka and F.E. Brinckmann, Chem.Comm., 349 (1968); J.Am.Chem.Soc. 92, 1199 (1970).
77. R.L. Morehouse, J.J. Christiansen and W. Gordy, J.Chem.Phys. 45, 1747 (1966).
78. (a) U. Schmidt, F. Geiger, A. Müller and K. Markau, Angew.Chem.internat.Edit. 2, 400 (1963).
(b) U. Schmidt, K. Kabitzke, K. Markau and A. Müller, Chem.Ber. 99, 1497 (1966).
79. S. Sugimoto, K. Kuwata, S. Ohnishi and I. Nitta, Nippon Hoshasen Kobunshi Kenkyu Kyokai Nempo 7, 199 (1965).
80. E. Müller, H. Eggersperger and K. Scheffler, Z.Naturforsch. (B) 16, 764 (1961); Annalen 658, 103 (1962).
81. W.M. Gulick and D.H. Geske, J.Am.Chem.Soc. 88, 2928 (1966).
82. B. Allen and A. Bond, J.Phys.Chem. 68, 2439 (1964).
83. E. Müller, H. Eggersperger, A. Rieker, K. Scheffler, H.D. Spanagel, H.B. Stegmann and B. Teissier, Tetrahedron 21, 227 (1965).
84. A. Rieker and H. Kessler, Tetrahedron 24, 5133 (1968).
85. (a) E.A.C. Lucken, Z.Naturforsch. (B) 18, 166 (1963).
(b) E. Müller, H. Eggersperger, B. Teissier and K. Scheffler, Z.Naturforsch. (B) 18, 984 (1963).
(c) E.A.C. Lucken, J.Chem.Soc., 5123 (1963).
(d) E.A.C. Lucken, F. Ramirez, V.P. Catto, D. Rhum and S. Dershowitz, Tetrahedron 22, 637 (1966).
86. (a) E.A.C. Lucken and C. Mazeline, J.Chem.Soc. (A), 1074 (1966); 439 (1967).
(b) E.A.C. Lucken, J.Chem.Soc. (A), 1357 (1966).
87. E.A.C. Lucken, J.Chem.Soc. (A), 1354 (1966).
88. A.R. Metcalfe and W.A. Waters, J.Chem.Soc. (B), 340 (1967).
89. K. Terauchi and H. Sakurai, Bull.Chem.Soc.Jap. 42, 2714 (1969).
90. F. Hein, H. Plust and H. Pohlemann, Z.Anorg.Allgem.Chem. 272, 25 (1953).
91. A.K. Hoffmann and A.G. Tesch, J.Am.Chem.Soc. 81, 5519 (1959).

92. (a) D. Wittenberg and H. Gilman, J.Org.Chem. 23, 1063 (1958).
(b) K. Issleib and H.O. Fröhlich, Z.Naturforsch. (B) 14, 349 (1949).
(c) A.M. Aguair, J. Beisler and A. Mills, J.Org.Chem. 27, 1001 (1962).
93. M.I. Kabachnik, V.V. Voevodskii, T.A. Mastryukova, S.P. Solodnikov and T.A. Melent'eva, Zhur.Obshchii. Khim. 34, 3277 (1964).
94. A.V. Il'yasov, Y.M. Korgin, Y.A. Levin, B.V. Mel'nikov and V.S. Galeev, Bull.Acad.Sci.USSR, 2698 (1968).
95. G. Fraenkel, S.H. Ellis and D.T. Dix, J.Am.Chem.Soc. 87, 1406 (1965).
96. H.-L.J. Chen and M. Bersohn, J.Am.Chem.Soc. 88, 2663 (1966).
97. M.W. Hanna, J.Chem.Phys. 37, 685 (1962).
98. A.D. Britt and E.T. Kaiser, J.Phys.Chem. 69, 2775 (1965).
99. A.D. Britt and E.T. Kaiser, J.Org.Chem. 31, 112 (1966).
100. M.H. Hnoosh, Can.J.Chem. 47, 4679 (1969).
101. K.S.V. Santhanam and A.J. Bard, J.Am.Chem.Soc. 90, 1118 (1968).
102. D. Chapman, S.H. Glarum and A.G. Massey, J.Chem.Soc., 3140 (1963).
103. H.R. Allcock and W.J. Birdsall, J.Am.Chem.Soc. 91, 7541 (1969).
104. N.V. Eliseeva, V.A. Sharpabyi and A.N. Pravednika, Zh.Strukt.Khim. 7, 511 (1966).
105. G. Tomaschewski, J.Prakt.Chem. 33, 168 (1966).
106. W.G. Bentrude, Ann.Rev.Phys.Chem. 18, 283 (1967).
107. M. Bersohn, private communication quoted in ref. 106.
108. P.J. Krusic and J.K. Kochi, J.Am.Chem.Soc. 91, 3944 (1969).
109. K. Dimroth and W. Städe, Angew.Chem.internat.Edit. 7, 881 (1968).
110. K. Dimroth, A. Hettche, W. Städe and F.W. Steuber, Angew.Chem.internat.Edit. 8, 770 (1969).
111. G.L. Davis, D.H. Hey and G.H. Williams, J.Chem.Soc., 4397 (1956).
112. C.E. Castro, L.J. Andrews and R.M. Keefer, J.Am.Chem.Soc. 80, 2322 (1958).
113. E.H. Braye, private communication.
114. W. Köhnlein, K.W. Böddiker and U. Schindewolf, Angew.Chem.internat.Edit. 6, 360 (1967).
115. G.L. Malinoski and W.H. Bruning, Angew.Chem.internat.Edit. 7, 953 (1968).

116. P. Wormington and J.R. Bolton, Angew.Chem.internat.Edit. 7, 954 (1968).
117. K.W. Böddeker, G. Lang and U. Schindewolf, Angew.Chem.internat.Edit. 9, 954 (1968).
118. J. Kelm and K. Mobius, Angew.Chem.internat.Edit. 9, 73 (1970).
119. H. Nishiguchi, Y. Nakai, K. Nakamura, K. Ishizu, Y. Deguchi and H. Takaki, J.Chem.Phys. 40, 241 (1964).
120. E.G. Janzen and J.B. Pickett, J.Am.Chem.Soc. 89, 3649 (1967).
121. D.L. Allara, B.C. Gilbert and R.O.C. Norman, Chem.Comm., 319 (1965).
122. K. Dimroth, A. Berndt, F. Bar, A. Schweig and R. Volland, Angew.Chem.internat.Edit. 6, 34 (1967).
123. K. Mukai, Y. Deguchi, N. Nishiguchi, H. Takaki and K. Ishizu, Bull.Chem.Soc.Jap. 40, 2731 (1967).
124. A. Streitwieser, Molecular Orbital Theory for Organic Chemists (John Wiley and Sons, 1962).
125. F.L. Pilar, Elementary Quantum Chemistry (McGraw-Hill, 1968).
126. A.D. McLachlan, Mol.Phys. 3, 233 (1960).
127. J.D. Memory, Quantum Theory of Magnetic Resonance Parameters (McGraw-Hill, 1968).
128. (a) J.A. Pople and G.A. Segal, J.Chem.Phys. 43, S129 (1965); 43, S136 (1965); 44, 3289 (1966).
(b) D.P. Santry and G.A. Segal, J.Chem.Phys. 47, 158 (1967).
(c) D.P. Santry, J.Am.Chem.Soc. 90, 3309 (1968).
129. J.A. Pople and D.L. Beveridge, Approximate Molecular Orbital Theory (McGraw-Hill, 1970).
130. C.C.J. Roothaan, Rev.Mod.Phys. 23, 69 (1951).
131. M.E. Anderson, P.J. Zandstra and T.R. Tuttle, J.Chem.Phys. 33, 1951 (1960).
132. P.-O. Löwdin, Phys.Rev. 97, 1509 (1955).
133. R. Pariser and R.G. Parr, J.Chem.Phys. 41, 466, 767 (1953).
134. C.A. Coulson and H.C. Longuet-Higgins, Proc.Roy.Soc.A 191, 39 (1947).
135. D.H. Levy, Ph.D. thesis (California, 1965).
136. D.A. Brown, J.Chem.Soc., 929 (1962).
137. R. Vilceanu, A. Balint and Z. Simon, Rev.Roumaine Chim. 13, 533 (1968).

138. K. Fukui, K. Morokuma and C. Nagata, Bull.Chem.Soc.Jap. 33, 1214 (1961).
139. D.P. Craig and N.L. Paddock, J.Chem.Soc., 4118 (1962).
140. S.F. Mason, Nature 205, 495 (1965).
141. M.J.S. Dewar, E.A.C. Lucken and M.A. Whitehead, J.Chem.Soc., 2423 (1960).
142. R. Vilceanu, A. Balint, Z. Simon, C. Rentia and G. Unterweger, Rev.Roumaine Chim. 13, 1623 (1968).
143. C. Trapp, C.A. Tyson and G. Giacometti, J.Am.Chem.Soc. 90, 1394 (1968).
144. J.C.J. Bart and J.J. Daly, Angew.Chem.internat.Edit. 7, 811 (1968).
145. D.R. Lide, Tetrahedron 17, 125 (1962).
146. K. Jug, Internat.J.Quantum Chem. 111S, 241 (1969).
147. H.H. Jaffé, Accounts of Chemical Research 2, 136 (1969).
148. J.A. Pople, D.L. Beveridge and P.A. Dobosh, J.Chem.Phys. 47, 2026 (1967).
149. Quantum Chemistry Programme Exchange no. 141.
150. G. Herzberg, Spectra of Diatomic Molecules (Van Nostrand, 1950); Electronic Spectra of Polyatomic Molecules (Van Nostrand, 1966).
151. D.E. Corbridge in Topics in Phosphorus Chemistry, Vol. 3 (Interscience, 1966).
152. Quantum Chemistry Programme Exchange no. 136.
153. (a) P.E. Cade and W.M. Huo, J.Chem.Phys. 47, 649 (1967).
(b) P.E. Cade, R.F.W. Bader, W.H. Henneker and I. Keaveney, J.Chem.Phys. 50, 5313 (1969).
154. D.B. Boyd and W.N. Lipscomb, J.Chem.Phys. 46, 910 (1967).
155. C.A. Burrus, A. Jacke and W. Gordy, Phys.Rev. 95, 700 (1954).
156. J.M. Lehn and B. Munsch, Chem.Comm., 1327 (1969).
157. I.H. Hillier and V.R. Saunders, Chem.Comm., 316 (1970).
158. J. Higuchi, J.Chem.Phys. 50, 1001 (1969).
159. M.T. Jones, R.D. Rataiczak and I.M. Brown, Chem.Phys.Lett. 2, 493 (1968).
160. C.L. Dodson and A.H. Reddoch, J.Chem.Phys. 48, 3226 (1968).
161. N.L. Paddock, Nature 167, 1070 (1951).

162. D. Dubois and C. Dodin, Tet.Lett., 2325 (1969).
163. E. Müller, P. Ziemek and A. Rieker, Tet.Lett., 207 (1964).
164. J.J. Eisch and W.C. Kaska, J.Am.Chem.Soc. 88, 2976 (1966).
165. K. Mislow, J.Am.Chem.Soc. 92, 1442 (1970).
166. A.N. Hughes and C. Srivnavit, J.Heterocyclic Chem. 7, 1 (1970).
167. See ref. 4, p. 20.
168. P.D. Sullivan and J.R. Bolton, J.Magn.Resonance 1, 356 (1969).
169. P. Millie and G. Berthier, Int.J.Quantum Chem., IIS, 67 (1968).
170. C. Thomson, unpublished work.
171. J. Nowakowski, Chem.Phys.Lett. 2, 289 (1968).
172. See ref. 166, p. 13.
173. E.G. Janzen, J.G. Pacifico and J.L. Gerlock, J.Phys.Chem. 70, 3021 (1966).
174. I. Degani, L. Lunazzi and G.F. Pedulli, Mol.Phys. 14, 217 (1968).
175. I. Degani, L. Lunazzi, G.F. Pedulli, C. Vincenzi and A. Mangani, Mol.Phys. 18, 613 (1970).
176. H.C. Longuet-Higgins, Trans.Faraday Soc. 45, 173 (1949).
177. S.N. Foner, E.L. Cochran, V.A. Bowers and C.K. Jen, Phys.Rev. Letters, 1, 91 (1958).
178. C. Thomson, unpublished work.
179. R.L. Kuczkowski, J.Am.Chem.Soc. 90, 1705 (1968).
180. W. Nelson, G. Jackel and W. Gordy, J.Chem.Phys. 52, 4572 (1970).
181. W.J. McCulloch, Ph.D. thesis (St. Andrews, 1969), p. 36.
182. P.H. Kasai and E.B. Whipple, Mol.Phys. 9, 497 (1965).
183. (a) T. Cole, J.Chem.Phys. 35, 1169 (1961).
(b) P.W. Atkins, J.A. Brivati, N. Keen, M.C.R. Symons and P.A. Trevalion, J.Chem.Soc., 4785 (1962).
184. A.D. Walsh, J.Chem.Soc., 2266 (1953).
185. A.D. Walsh, Discussions Faraday Soc. 35, 218 (1963).
186. S. Subramanian, M.C.R. Symons and H.W. Wardale, J.Chem.Soc.(A), 1239 (1970).
187. D.R. Armstrong and D.T. Clark, Chem.Comm., 99 (1970).
188. J. Del Bene and H.H. Jaffé, J.Chem.Phys. 48, 1807, 4050 (1968).